

Electronic Thesis and Dissertation Repository

4-18-2016 12:00 AM

Treatment of Landfill Waste, Leachate and Landfill Gas: Modelling/Simulation and Experimental Studies

Hecham M. Omar
The University of Western Ontario

Supervisor
Sohrab Rohani
The University of Western Ontario

Graduate Program in Chemical and Biochemical Engineering
A thesis submitted in partial fulfillment of the requirements for the degree in Master of
Engineering Science
© Hecham M. Omar 2016

Follow this and additional works at: <https://ir.lib.uwo.ca/etd>

 Part of the [Other Chemical Engineering Commons](#)

Recommended Citation

Omar, Hecham M., "Treatment of Landfill Waste, Leachate and Landfill Gas: Modelling/Simulation and Experimental Studies" (2016). *Electronic Thesis and Dissertation Repository*. 3731.
<https://ir.lib.uwo.ca/etd/3731>

This Dissertation/Thesis is brought to you for free and open access by Scholarship@Western. It has been accepted for inclusion in Electronic Thesis and Dissertation Repository by an authorized administrator of Scholarship@Western. For more information, please contact wlsadmin@uwo.ca.

Abstract

Landfilling has been relegated to containing waste and hoping for minimal environmental impact. However, landfills produce harmful leachate and landfill gas that require treatment. To speed up the landfill biodegradation process, aerating the landfill to promote aerobic biodegradation has been implemented successfully. However, the conversion from a traditional anaerobic landfill to an aerobic landfill is to this point, not well researched. A 3-dimensional dynamic mathematical model was developed that depicts the conversion of a landfill from an anaerobic to an aerobic operation. The results of the model (CO₂ volume fraction and temperature), agreed with data from published work. The model solved for the liquid and gaseous pressures/velocities, gas composition, anaerobic/aerobic biomass concentrations and temperature; all were solved with respect to space and time. Landfill leachate requires treatment before release and landfill gas requires purification (removal of CO₂) before it can be used as a fuel. A hybrid sorption (absorption and adsorption/ion exchange) system was developed to treat leachate and purify landfill gas in the same column. The absorption results showed that leachate could remove more carbon dioxide from the landfill gas than pure water, due to its slight basicity. The adsorption/ion exchange results showed that lead could be removed from model leachate but not below Ontario discharge guidelines with the length of the column used (50-55 cm zeolite bed height).

Keywords

Anaerobic landfill, aerobic landfill, landfill gas, leachate, bioreactor landfill, finite element method, mathematical model, absorption, adsorption

Co-Authorship Statement

Chapter 2

Article Title: Treatment of landfill waste, leachate and landfill gas: A review
Authors: Hecham Omar, Sohrab Rohani
Article Status: Published in Front. Chem. Sci. Eng.
Hecham Omar conducted the literature review and wrote the manuscript. The work was supervised by Prof. Sohrab Rohani. The draft of the manuscript was reviewed by Prof. Rohani.
Hecham Omar, Sohrab Rohani, "Treatment of landfill waste, leachate and landfill gas: A review". Front Chem Sci Eng, 9(1), 2015, 15-32.

Chapter 3

Article Title: The mathematical model of the conversion of a landfill operation from anaerobic to aerobic
Authors: Hecham Omar, Sohrab Rohani
Article Status: Submitted to Appl. Math. Model.
Hecham Omar developed the model, ran the simulations and wrote the manuscript. The work was supervised by Prof. Sohrab Rohani. The draft of the manuscript was reviewed by Prof. Rohani

Appendix B

Article Title: Transport phenomena in the conversion of an anaerobic landfill into an aerobic landfill
Authors: Hecham Omar, Sohrab Rohani
Article Status: Published in Proceedings of COMSOL Conference 2015 Boston
Hecham Omar developed the model, ran the simulations and wrote the manuscript. The work was supervised by Prof. Sohrab Rohani. The draft of the manuscript was reviewed by Prof. Rohani.
Hecham Omar, Sohrab Rohani, "Transport phenomena in the conversion of an anaerobic landfill into an aerobic landfill". Proceedings of the COMSOL Conference 2015 Boston, 2015.

Appendix C

Article Title: Microwave assisted zeolitization of coal fly ash using landfill leachate as the solvent
Authors: Syed Salman Bukhari, Hecham Omar, Sohrab Rohani

Article Status: Submitted to Journal of Hazardous Materials

Syed Bukhari and Hecham Omar performed the experiments. The majority of the data analysis and manuscript writing was performed by Syed Bukhari. Hecham Omar helped with data analysis and writing of the manuscript. The work was supervised by Prof. Sohrab Rohani. The draft of the manuscript was reviewed by Prof. Rohani.

Acknowledgments

I would like to acknowledge the guidance provided by Professor Sohrab Rohani. Professor Rohani provided valuable advice and knowledge. His constant encouragement allowed me to exceed my own expectations.

I would like to acknowledge all of my colleagues and members from my lab, for their advice and help when needed. I would specifically like to show appreciation to Dr. Ali Alizadeh and Dr. Hossein Kazemian who worked closely with me and provided valuable advice. I would like to thank Chris Piccolo, Mahshid Attari and the various laboratory technicians for performing some of the characterization tests used in my work.

I would also like to acknowledge my parents, Mohamed and Feyrouz Omar for pushing me towards pursuing my Master's Degree, for never losing faith and for their unbounded support.

Table of Contents

Abstract.....	i
Co-Authorship Statement.....	ii
Acknowledgments.....	iv
Table of Contents.....	v
List of Tables.....	xi
List of Figures.....	xii
List of Abbreviations.....	xv
List of Appendices.....	xvii
Chapter 1.....	1
1 Introduction.....	1
1.1 Background.....	2
1.1.1 Landfill waste treatment.....	2
1.1.2 Leachate treatment.....	3
1.1.3 Landfill gas treatments.....	4
1.2 Modelling methodology.....	5
1.2.1 Methodology.....	5
1.2.2 Finite element method.....	6
1.3 Sorption.....	7
1.4 Objectives.....	8
1.5 Motivation.....	8
1.6 Thesis outline.....	9
1.7 References.....	10
Chapter 2.....	14
2 Treatment of landfill waste, leachate and landfill gas: A review.....	14

2.1	Introduction.....	14
2.2	Landfill treatments	16
2.2.1	Dry-tomb landfill	16
2.2.2	Anaerobic bioreactor landfill	17
2.2.3	Aerobic bioreactor landfill.....	19
2.2.4	Semi-aerobic bioreactor landfill	23
2.2.5	Landfill operations and measurements/control.....	24
2.2.5.1	Operations.....	24
2.2.5.2	Measurement/Control	27
2.3	Leachate treatment	28
2.3.1	Anaerobic treatment.....	30
2.3.2	Aerobic treatment.....	31
2.3.3	Anammox.....	35
2.3.4	Adsorption.....	36
2.3.5	Chemical oxidation	38
2.3.6	Coagulation/flocculation.....	39
2.3.7	Membrane processes.....	41
2.4	Landfill gas treatment/use.....	43
2.4.1	Quality of LFG.....	43
2.4.2	LFG recovery	44
2.4.3	Use of LFG	44
2.4.4	Flaring	45
2.4.5	Adsorption.....	45
2.4.6	Absorption.....	46
2.4.7	Permeation	47

2.4.8	Cryogenic treatments	47
2.5	Conclusions.....	47
2.6	References.....	49
Chapter 3	65
3	The mathematical model of the conversion of a landfill operation from anaerobic to aerobic	65
3.1	Introduction.....	65
3.2	Theory and computation technique.....	67
3.2.1	Momentum balance.....	69
3.2.2	Mass balance	71
3.2.3	Energy balance.....	78
3.2.4	Model assumptions	80
3.3	Results and discussion	81
3.3.1	Geometry and meshing	81
3.3.2	Anaerobic-aerobic conversion	83
3.3.2.1	Parameter estimation	83
3.3.2.2	Growth of aerobic bacteria	86
3.3.2.3	Oxygen consumption.....	89
3.3.2.4	Carbon dioxide production.....	91
3.3.2.5	Methane production.....	92
3.3.3	Higher aerobic biomass concentration.....	92
3.3.3.1	Full scale landfill aerobic biomass concentration	93
3.3.3.2	High aerobic biomass concentration	93
3.3.4	Temperature control.....	96
3.4	Conclusions and summary	98
3.5	References.....	100

Chapter 4.....	106
4 Removal of CO ₂ from landfill gas and Pb ²⁺ from leachate using a hybrid sorption process.....	106
4.1 Introduction.....	107
4.2 Economic incentive for the landfill gas purification.....	109
4.3 Materials and methods	111
4.3.1 Zeolite preparation	111
4.3.2 Leachate preparation	111
4.3.3 Model leachate solution preparation.....	111
4.3.4 Characterization techniques	112
4.3.5 Experimental setup and procedure.....	113
4.3.5.1 Experimental setup	113
4.3.5.2 Absorption column experimental procedure	114
4.3.5.3 Batch adsorption/ion exchange experimental procedure.....	115
4.3.5.4 Adsorption/ion exchange column experimental procedure	115
4.4 Results and discussion	116
4.4.1 Adsorbent characterization	116
4.4.1.1 Chemical composition	116
4.4.1.2 Phase purity (crystallinity) and morphology	117
4.4.1.3 Thermal analysis.....	118
4.4.1.4 Surface area	119
4.4.1.5 Cation exchange capacity	120
4.4.2 Absorption.....	120
4.4.2.1 Agreement between the experimental and simulated results of absorption	120

4.4.2.2	Comparison of the performance of different packings and absorbents	121
4.4.2.3	Simulation results at higher pressures	123
4.4.2.4	Multipass leachate absorption	124
4.4.3	Adsorption/ion exchange	127
4.4.3.1	Batch adsorption/ion exchange test; pH in the batch tests	127
4.4.3.2	Continuous adsorption/ion exchange column test	130
4.5	Conclusions	131
4.6	References	133
Chapter 5	138
5	Conclusions and recommendations	138
5.1	Conclusions	138
5.2	Recommendations	140
Appendices	141
Appendix A	Preliminary adsorption/ion exchange column results	141
A.1	Ammonium assay calibration curve	141
A.2	Absorption equilibrium time determination	142
A.3	Adsorption equilibrium time determination	143
Appendix B	Transport Phenomena in the Conversion of an Anaerobic Landfill into an Aerobic Landfill	145
B.1	Introduction	145
B.2	Governing equations	146
B.2.1	Gas flow equation	146
B.2.2	Gas transport equations	147
B.2.3	Biokinetic equations	148
B.2.4	Species consumption/production equations	150

B.2.5	Energy balance equations	152
B.3	Use of COMSOL Multiphysics	153
B.4	Analysis conditions	154
B.5	Results.....	154
B.6	Conclusions.....	157
B.7	References.....	158
Appendix C	Microwave assisted zeolitization of coal fly ash using landfill leachate as the solvent	160
C.1	Introduction.....	160
C.2	Materials and methods	163
C.2.1	Materials	163
C.2.2	Experimental procedure	163
C.2.3	Characterization	164
C.3	Results and discussion	165
C.3.1	Inductively coupled plasma atomic emission spectroscopy (ICP-AES). 165	
C.3.2	X-ray analysis (XRF and XRD).....	166
C.3.3	Scanning electron microscope (SEM)	173
C.3.4	Thermogravimetric analysis (TGA).....	176
C.3.5	Cation exchange capacity (CEC).....	177
C.4	Conclusions.....	180
C.5	References.....	182
Curriculum Vitae	187

List of Tables

Table 2-1 Advantages and disadvantages of anaerobic bioreactor landfill	17
Table 2-2 Advantages and disadvantages of aerobic bioreactor landfill	22
Table 2-3 Advantages and disadvantages of semi-aerobic bioreactor landfill	23
Table 2-4 Biological treatment removal efficiencies	34
Table 2-5 Comparison of coagulation/flocculation studies	40
Table 3-1 Fickian diffusion estimation parameters	73
Table 3-2 Model equation parameters	79
Table 3-3 Initial conditions	80
Table 4-1 Typical anaerobic landfill gas composition.....	107
Table 4-2 Ontario natural gas prices	109
Table 4-3 Chemical composition of the zeolite sample by XRF technique	116
Table B-1 Physical properties of waste	151
Table B-2 Biokinetic parameters	151
Table B-3 Heat parameters	152
Table C-1 Cation concentrations (mg/L) and pH of leachate	165
Table C-2 XRF analysis of chemical composition of CFA	166
Table C-3 Relative characteristic XRD Peak Intensity for fine-filtered, coarse filtered and unfiltered synthesis after 30 minutes of microwave irradiation.....	171

List of Figures

Figure 1-1 Conservation of property Y.....	5
Figure 2-1 Schematic diagram of: (a) anaerobic bioreactor landfill; (b) aerobic bioreactor landfill; (c) semi-aerobic bioreactor landfill – all with leachate circulation.....	26
Figure 3-1 Flowchart showing model formulation steps	68
Figure 3-2 Model geometry: (a) schematic view; (b) isometric view with symmetric slice shown; (c) symmetric slice with overlain mesh.....	82
Figure 3-3 Mesh refinement study	83
Figure 3-4 Parameter estimation plot: (a) outlet volume fraction of CO ₂ over time; (b) average temperature over time and (c) maximum temperature over time	84
Figure 3-5 Average and maximum temperature of waste after 24 hours with varying initial aerobic biomass concentration (kg/m ³)	87
Figure 3-6 Temperature (°C), aerobic growth rate (kg/m ³ /s) and oxygen volume fraction after 24 hours with initial aerobic biomass concentration of: (a) 0.01 kg/m ³ ; (b) 0.1 kg/m ³ ; (c) 0.6; kg/m ³ (d) 1 kg/m ³ and (e) 5 kg/m ³	88
Figure 3-7 Temperature (°C) and oxygen consumption rate (kg/m ³ /s): (a) 1 day; (b) 2 days; (c) 3 days and (d) 4 days.....	90
Figure 3-8 Carbon dioxide production rate (kg/m ³ /s): (a) 1 day; (b) 2 days; (c) 3 days and (d) 4 days.....	91
Figure 3-9 Methane production rate (kg/m ³ /s): (a) 4 hrs and (b) 24 hrs.....	92
Figure 3-10 After 24 hours: (a) temperature (°C); (b) aerobic growth rate (kg/m ³ /s) and (c) oxygen volume fraction (-).....	93

Figure 3-11 After 24 hours: (a) temperature (°C); (b) aerobic biomass growth rate (kg/m ³ /s); (c) oxygen volume fraction (-) and (d) rate of methane production (kg/m ³ /s)	95
Figure 3-12 Varying air flowrate: (a) average temperature (°C); (b) maximum temperature (°C); varying leachate flowrate: (c) average temperature (°C); (d) maximum temperature (°C)	98
Figure 4-1 Hybrid sorption system schematic	114
Figure 4-2 XRD Patterns of (A) pure clinoptilolite (simulated XRD pattern) compared with (B) zeolite sample	117
Figure 4-3 SEM micrograph of the zeolite sample	118
Figure 4-4 TGA curve of the zeolite sample (heating rate 10°C/min, under N ₂ atmosphere)	119
Figure 4-5 Experimental results vs. Aspen HYSYS simulation results	121
Figure 4-6 Methane vol% with different packing and absorbents	122
Figure 4-7 Methane vol% simulation results at higher pressures using water	124
Figure 4-8 CH ₄ vol% after multiple leachate reuse	125
Figure 4-9 pH after multiple leachate reuse	126
Figure 4-10 pH before and after zeolite contact	128
Figure 4-11 %Removal at different initial pH values	129
Figure 4-12 Lead concentration divided by initial lead concentration over time (inset is a zoomed in view of the line)	131
Figure A-1 Ammonium concentration calibration curve	142
Figure A-2 Absorption equilibrium time	143

Figure A-3 Adsorption/ion exchange equilibrium time using landfill leachate	144
Figure B-1 Geometry of the landfill cell.....	154
Figure B-2 Temperature after 1 day with varying initial aerobic biomass concentrations – initial temperature = 293K.....	155
Figure B-3 Temperature after 1 day with varying air flowrates – initial temperature = 293K.....	156
Figure B-4 Temperature after 1 day with varying leachate injection rates – initial temperature = 293K	156
Figure C-1 The XRD patterns of zeolitized coal fly ash utilizing: a) fine-filtered leachate b) coarse filtered leachate and c) unfiltered leachate as the reaction solvent	170
Figure C-2 The characteristic XRD peak intensities with respect to microwave irradiation utilizing: a) coarse filtered leachate and b) unfiltered leachate as reaction solvent.....	172
Figure C-3 The SEM images of zeolitized coal fly ash utilizing: a, b) fine-filtered c, d) coarse filtered and e, f) unfiltered leachate as solvent	175
Figure C-4 The TGA of synthesized zeolites using fine-filtered, coarse filtered and unfiltered leachate as solvent	176
Figure C-5 The correlation between the NH_4^+ concentration and peak absorbance intensity.....	178
Figure C-6 The CEC values of fine-filtered, coarse filtered and unfiltered leachate prepared zeolites	179

List of Abbreviations

AMAS	Ammonium acetate saturation
BMP	Biological methane potential
BOD	Biochemical oxygen demand
CEC	Cation exchange capacity
CFA	Coal fly ash
COD	Chemical oxygen demand
DEA	Diethanol amine
FDM	Finite difference method
FEM	Finite element method
FVM	Finite volume method
GHG	Greenhouse gas
HEU	Heulandite
HRT	Hydraulic retention time
ICP-OES	Inductively coupled plasma optical emission spectroscopy
LFG	Landfill gas
LOI	Loss on ignition
MEA	Monoethanol amine
MEK	Methyl ethyl ketone
MF	Microfiltration

MMTCO ₂ e	Million metric tons of CO ₂ equivalent
MRL	Method reporting limit
MSW	Municipal solid waste
NF	Nanofiltration
NMOC	Non-methane organic compound
OLR	Organic loading rate
PAC	Poly aluminum chloride
PDE	Partial differential equation
RBC	Rotating biological contactor
RO	Reverse osmosis
SEM	Scanning electron microscope
SS	Suspended solids
TGA	Thermogravimetric analysis
TOC	Total organic carbon
UF	Ultrafiltration
VFA	Volatile fatty acid
VOC	Volatile organic compound
XRD	X-ray diffraction
XRF	X-ray fluorescence

List of Appendices

Appendix A Preliminary adsorption/ion exchange column results.....	141
A.1 Ammonium assay calibration curve.....	141
A.2 Absorption equilibrium time determination.....	142
A.3 Adsorption equilibrium time determination.....	143
Appendix B Transport Phenomena in the Conversion of an Anaerobic Landfill into an Aerobic Landfill	145
B.1 Introduction.....	145
B.2 Governing equations	146
B.2.1 Gas flow equation	146
B.2.2 Gas transport equations.....	147
B.2.3 Biokinetic equations.....	148
B.2.4 Species consumption/production equations.....	150
B.2.5 Energy balance equations	152
B.3 Use of COMSOL Multiphysics	153
B.4 Analysis conditions.....	154
B.5 Results.....	154
B.6 Conclusions.....	157
B.7 References.....	158
Appendix C Microwave assisted zeolitization of coal fly ash using landfill leachate as the solvent	160
C.1 Introduction.....	160
C.2 Materials and methods	163
C.2.1 Materials	163
C.2.2 Experimental procedure	163

C.2.3	Characterization	164
C.3	Results and discussion	165
C.3.1	Inductively coupled plasma atomic emission spectroscopy (ICP-AES).....	165
C.3.2	X-ray analysis (XRF and XRD).....	166
C.3.3	Scanning electron microscope (SEM)	173
C.3.4	Thermogravimetric analysis (TGA).....	176
C.3.5	Cation exchange capacity (CEC)	177
C.4	Conclusions.....	180
C.5	References.....	182

Chapter 1

1 Introduction

The disposal of solid waste in landfills has led to an unsustainable use of land. Landfilling has been historically limited to the dry-tomb method. This method involves dumping the waste on a large piece of land and once full, entombing the waste. By definition, the more waste, the more land is required. There are more issues than simply the large use of land. As the name suggests, this method is predicated on the municipal solid waste (MSW) in the landfill remaining dry. This is done by covering the waste in a landfill cover or cap. The purpose of the cap is to prevent water infiltration and to contain any gases that are produced. In theory, a perfectly dry landfill, will produce no gas. A dry landfill will have very limited microbial activity, producing little to no landfill gas (LFG). However, the cap is designed assuming that moisture will intrude, causing microbial activity, producing LFG, requiring the cap to contain the LFG. Moisture will penetrate the landfill cover and also produce leachate (made when constituents are leached out of the MSW by the moisture). This leachate can contain harmful constituents depending on what is present in the MSW.

The LFG that is produced in a dry-tomb landfill contains mainly carbon dioxide and methane¹⁻³, two harmful greenhouse gases (GHGs). Due to the slow biodegradation, the LFG will be produced for many decades⁴. Another consequence of the slow biodegradation, is the harmful leachate that is produced for extended periods of time. To try and solve both the LFG and leachate problems, research has led to the development of bioreactor landfills. The traditional paradigm is to disallow moisture from entering to prevent microbial activity. In a bioreactor landfill, moisture is injected into the landfill in the form of leachate; this provides moisture and nutrients to the bacteria⁵. The addition of leachate facilitates the speedy biodegradation of the waste.

There are three types of bioreactor landfills: anaerobic, aerobic and semi-aerobic. Anaerobic bioreactor landfills inject only leachate and use anaerobic bacteria to biodegrade

the waste. Oftentimes, due to the increased production, LFG, which is mainly methane and carbon dioxide, is extracted for use. Eventually, the production will decrease and the extraction is not economically viable. Aerobic bioreactor landfills inject leachate and air. The air promotes the growth of aerobic bacteria. Aerobic LFG does not have fuel value as the major constituent is CO₂, but causes less GHG pollution. Aerobic bioreactor landfills are also characterized by a faster biodegradation rate than anaerobic bioreactor landfills¹. Aerobic bioreactor landfills can be costly due to the energy required to run the air compressors. Semi-aerobic bioreactor landfills do not use compressors to inject air. Instead the air is allowed to enter through the leachate collection system.

1.1 Background

All three phases of the landfill (landfill waste, leachate and landfill gas) are studied in this work. Treating one phase, has consequences on the other phases. For example, biodegrading the waste in shorter time, decreases the volume of harmful leachate present. Also, less gas is produced.

1.1.1 Landfill waste treatment

Anaerobic landfills can be categorized into two categories: dry-tomb landfills and anaerobic bioreactor landfills. Dry-tomb landfills entomb the waste to try and mitigate any environmental hazards and limit biodegradation. However, this approach is deeply flawed because dry-tomb landfills have been known to cause environmental problems⁶ due to the leachate and GHGs produced. The advantage of this approach is the relative low cost compared to other landfilling methods. Anaerobic bioreactor landfills promote biodegradation. Anaerobic biodegradation produces mainly carbon dioxide and methane. The gas is exploited by purification and used as fuel and the waste biodegradation is accelerated.

Aerobic landfills use aerobic bacteria to biodegrade the waste. The bacteria are supplied with oxygen via air injection wells connected to air compressors. Aerobic biodegradation produces carbon dioxide and water as the main products^{7,8}. Anaerobic biodegradation

produces mainly carbon dioxide and methane. Methane is 25 times more potent a GHG than carbon dioxide, trapping 25 times the energy⁹. Aerobic landfills biodegrade waste at a faster rate, allowing more waste containment and in some cases, land reuse¹⁰. However, there is a significant operational cost required to run the air compressors continuously.

Semi-aerobic landfills are somewhere in between anaerobic and aerobic landfills. Aerobic bacteria still biodegrade the waste but instead of air compressors supplying the air, air flows through the leachate collection pipes and diffuses through the waste. This significantly reduces the operational cost associated with the air compressors. Semi-aerobic landfills are not as efficient at biodegradation when compared to aerobic landfills but are much more efficient than anaerobic landfills¹¹.

1.1.2 Leachate treatment

Leachate is the wastewater produced when water (e.g. from rain) infiltrates the landfill and leaches out components from the waste¹². Leachate is a complex mixture made up of various components (e.g. organics, inorganics, heavy metals) which is variable depending on the contents of the waste¹³. The variability and complex nature of leachate is what makes treatment difficult and expensive.

Treatment typically requires multiple steps to remove the various harmful constituents. For example, in young leachate (characterized by high biodegradability) biological treatment can be employed to reduce the organic components. Biological treatment methods include: anaerobic, aerobic and anammox treatments. Once biological treatment is no longer viable (due to low biodegradability), physio-chemical treatment methods must be employed.

The physico-chemical treatment method is specific depending on what is being removed. Physico-chemical treatment methods include: adsorption, chemical oxidation, coagulation/flocculation and membrane processes. Physico-chemical treatments are more expensive when compared to biological treatments and are employed after biological treatments. Physico-chemical treatments are used to remove components that cannot be removed using biodegradation. For example, adsorption is used to remove heavy metals.

Chemical oxidation is used to remove non-biodegradable materials. Coagulation/flocculation is also used to remove non-biodegradable materials. Membrane processes can be used for the removal of particles, microorganisms, organic molecules and other fine pollutants¹¹.

1.1.3 Landfill gas treatments

LFG is the gas produced when bacteria biodegrade components of MSW and produce gas as a byproduct. The composition of the gas depends on the type of bacteria that are biodegrading the waste. Anaerobic bacteria produce mainly carbon dioxide and methane and aerobic bacteria produce mainly carbon dioxide and water. Other trace gases are also produced. These trace gases include volatile organic compounds (VOCs), non-methane organic compounds (NMOCs), hydrogen sulfide and ammonia¹¹.

Anaerobic LFG is typically flared, wasting the energy by burning the methane. Anaerobic LFG can be purified by removing the carbon dioxide and used in many applications such as power generation. It takes years to install and commission an aerobic landfill operation. In that time, the anaerobic LFG can be extracted and used for fuel. The air compressors required in the aerobic system require lots of electricity and some of the cost can be recuperated by using the LFG. Treatment/purification of LFG can be done using adsorption, absorption, membrane processes or cryogenic treatment. The selection of treatment/purification technique depends on the purity of methane required and the flowrate of gas. Treatment methods for LFG include adsorption, absorption, membrane separation and cryogenic separation. For example, pressure swing adsorption produces high purity methane but requires a high operational financial expenditure and is only feasible for large gas flowrates. Absorption (using amines) also produces high purity methane but requires high capital financial expenditure due to all of the units required.

1.2 Modelling methodology

1.2.1 Methodology

The modelling used for the landfill was based on conservation and balance principles. Momentum, mass and energy are conserved during the landfill biodegradation process. Momentum conservation deals with the fluid flow (i.e. leachate, air and LFG flow). Mass conservation deals with the chemical species (i.e. nitrogen, oxygen, carbon dioxide and methane) and the biokinetics of anaerobic/aerobic growth/death. Energy conservation deals with the heat produced during biodegradation and convection during fluid flow. Figure 1-1 illustrates an arbitrary conservation system, with property Y being conserved. Equation (1-1) shows the mathematical description of Figure 1-1.

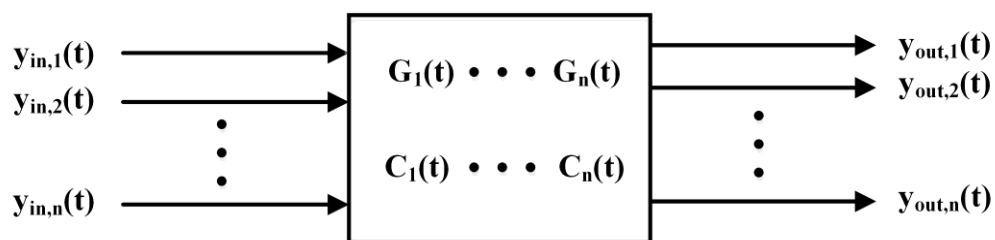


Figure 1-1 Conservation of property Y

$$\frac{dY(t)}{dt} = \sum_1^n y_{in,i}(t) - \sum_1^n y_{out,i}(t) + \sum_1^n G_i(t) - \sum_1^n C_i(t) \quad (1-1)$$

Where y_{in} is the inflow rate of property Y, y_{out} is the outflow rate of property Y, G is the generation of property Y and C is the consumption of property Y.

Once the model equations are developed, a suitable mathematical method to solve the equations is required.

1.2.2 Finite element method

There are numerous methods that are available to solve partial differential equations (PDEs). The three main methods are: finite difference method (FDM), finite volume method (FVM) and finite element method (FEM). Each method has advantages and disadvantages depending on the problem being solved. Various factors have to be taken into consideration before selecting a solution method. For example, a complex geometry eliminates the usage of FDM and favours the usage of FEM or FVM. FEM provides a continuous solution via interpolation whereas the FVM provides a discrete solution¹⁴.

Modelling the landfill conversion requires many different types of physics (fluid dynamics, mass and heat transfer) which favours the use of FEM. FEM has been used for computational fluid dynamics¹⁵⁻¹⁸, mass transfer¹⁹⁻²¹ and heat transfer²²⁻²⁴ applications. FEM produces unambiguous, consistent and accurate approximations of source terms (e.g. mass source, energy source). It also produces valid approximations of second-order partial derivatives, as in the heat conduction equation. FEM also naturally incorporates physical boundary conditions. Finite element modelling consists of six steps²⁵:

1. Restating the PDE system as an integral statement, that is then transformed into a weak statement;
2. Each integral is restated as a sum of integrals in the subdomains (mesh elements);

3. Local coordinates are transformed within each mesh element to calculate each integral;
4. Each function and coordinate is restated as a linear combination of chosen basis functions within each mesh element;
5. A discrete system is produced from the evaluation of each integral;
6. System is solved to determine the computational solution of the original PDE system.

1.3 Sorption

Absorption and adsorption (also ion exchange) are two methods that are used to remove a substance (or substances) from a liquid or gaseous solution/mixture. When both methods are combined, this is referred to as sorption. Absorption is when the constituent to be removed enters a bulk phase (gas, liquid or solid) and is taken in either temporarily or permanently. Adsorption is when the constituent to be removed becomes bonded to the surface of the adsorbent. Ion exchange can be viewed as an extension of adsorption where the constituent trades places with an ion on the surface of an adsorbent.

Carbon dioxide can be dissolved in water removing it from the LFG in an absorption system. This has been done in previous studies^{26,27}. Absorption columns require packing to increase residence time to allow sufficient contact time between the solvent (liquid) and solute (gas to be absorbed) for absorption. Heavy metals have been removed using adsorption/ion exchange using natural zeolites²⁸⁻³¹. Adsorption/ion exchange requires contact between the solution containing the species to be removed and the zeolite (adsorbent). This process is similar to the liquid flow process in an absorption column. Due to the similarity, the proposal is to combine the two processes (absorption and adsorption/ion exchange) and test the efficacy of the process in removing CO₂ from the gas phase (LFG) and heavy metals from the liquid phase (leachate).

1.4 Objectives

The objectives of this thesis work are:

1. To develop a mathematical model that defines the transport phenomena and biokinetics in the conversion of a landfill operation from anaerobic to an aerobic bioreactor.
2. To test the efficacy of a hybrid sorption column which combines both absorption and adsorption/ion exchange, to remove carbon dioxide from landfill gas and heavy metals (lead specifically) from landfill leachate.

1.5 Motivation

An accurate model that portrays the inner workings of the conversion from an anaerobic to aerobic bioreactor landfill can help understand the process which to this point has not been studied extensively. It can give an avenue for further experimental work. The main limitation that holds back research in the field of landfill biodegradation is the long times required for experimentation. Typical experiments last many months/years, testing one set of conditions at a time (making experimental optimization extremely time consuming). A model can help cut down the experiments required and provide information that experimentation cannot provide or would require large costs for the large amount of instrumentation required to collect (e.g. the flow of air/leachate inside the landfill).

Leachate treatment requires a significant cost in the landfilling process. In the case of an aerobic landfill, when compressors are continually blowing in compressed air, energy also becomes a large financial expenditure. Capturing the methane in the LFG can be used as an energy source³² and reduce the cost of energy required to run the compressors. Removal of heavy metals combined with the removal of carbon dioxide from LFG can reduce some of the treatment cost of leachate as well as increase the heating value of the LFG. Combining both the absorption and adsorption/ion exchange processes in a single column, can also decrease the capital cost.

1.6 Thesis outline

Chapter one presents a brief introduction to the techniques used to solve problems outlined in Section 1.4. Chapter one also provides the objectives and motivations of the work presented in this thesis.

Chapter two presents a literature review that covers the treatment of landfill waste, leachate and landfill gas. The chapter is split up into three main sections: (1) the different treatments of landfill waste, (2) the different treatments of leachate and (3) the different treatments of landfill gas.

Chapter three presents a mathematical model that describes transport phenomena occurring during the conversion of an anaerobic landfill into an aerobic bioreactor landfill. The model equations describe the gaseous and leachate flow, the growth and death of anaerobic and aerobic biomass, the movement and consumption/production of chemical species and the energy transformation processes.

Chapter four presents experimental research on a hybrid sorption column which attempts to combine an absorption and an adsorption/ion exchange column to simultaneously treat leachate by removing heavy metals and purifying landfill gas by removing carbon dioxide.

Finally, Chapter five provides conclusions and recommendations of the overall work. Possible directions for future research are also presented.

1.7 References

1. Borglin SE, Hazen TC, Oldenburg CM, Zawislanski PT. Comparison of aerobic and anaerobic biotreatment of municipal solid waste. *J Air Waste Manag Assoc.* 2004;54(7):815–22. Doi: 10.1080/10473289.2004.10470951.
2. Erses AS, Onay TT, Yenigun O. Comparison of aerobic and anaerobic degradation of municipal solid waste in bioreactor landfills. *Bioresour Technol.* 2008;99(13):5418–26. Doi: 10.1016/j.biortech.2007.11.008.
3. Gholamifard S, Eymard R, Duquennoi C. Modeling anaerobic bioreactor landfills in methanogenic phase: Long term and short term behaviors. *Water Res.* 2008;42(20):5061–71. Doi: 10.1016/j.watres.2008.09.040.
4. Méry J, Bayer S. Comparison of external costs between dry tomb and bioreactor landfills: taking intergenerational effects seriously. *Waste Manag Res.* 2005;23(6):514–26. Doi: 10.1177/0734242X05060857.
5. Rendra S, Warith MA, Fernandes L. Degradation of Municipal Solid Waste in Aerobic Bioreactor Landfills. *Environ Technol.* 2007;28(6):609–20. Doi: 10.1080/09593332808618822.
6. Westlake K. Sustainable Landfill—Possibility or Pipe-Dream? *Waste Manag Res.* 1997;15(5):453–61. Doi: 10.1177/0734242X9701500502.
7. Berge ND, Reinhart DR, Townsend TG. The fate of nitrogen in bioreactor landfills. *Crit Rev Environ Sci Technol.* 2005;35(4):365–99. Doi: 10.1080/10643380590945003.
8. Themelis NJ, Kim YH. Material and energy balances in a large-scale aerobic bioconversion cell. *Waste Manag Amp Res J Int Solid Wastes Public Clean Assoc ISWA.* 2002;20(3):234–42. Doi: 10.1177/0734242X0202000304.

9. Huber-Humer M, Kjeldsen P, Spokas KA. Special issue on landfill gas emission and mitigation. *Waste Manag.* 2011;31(5):821–2.
10. Reinhart DR, McCreanor PT, Townsend T. The bioreactor landfill: Its status and future. *Waste Manag Res.* 2002;20(2):172–86. Doi: 10.1177/0734242X0202000209.
11. Omar H, Rohani S. Treatment of landfill waste, leachate and landfill gas: A review. *Front Chem Sci Eng.* 2015;9(1):15–32. Doi: 10.1007/s11705-015-1501-y.
12. Renou S, Givaudan JG, Poulain S, Dirassouyan F, Moulin P. Landfill leachate treatment: Review and opportunity. *J Hazard Mater.* 2008;150(3):468–93. Doi: 10.1016/j.jhazmat.2007.09.077.
13. Senior E. *Microbiology of Landfill Sites*. Second. Boca Raton: Lewis Publishers; 1995.
14. Jeong W, Seong J. Comparison of effects on technical variances of computational fluid dynamics (CFD) software based on finite element and finite volume methods. *Int J Mech Sci.* 2014;78:19–26. Doi: 10.1016/j.ijmecsci.2013.10.017.
15. Baumann CE, Oden JT. A discontinuous hp finite element method for convection—diffusion problems. *Comput Methods Appl Mech Eng.* 1999;175(3–4):311–41. Doi: 10.1016/S0045-7825(98)00359-4.
16. Tobiska L, Verfürth R. Analysis of a Streamline Diffusion Finite Element Method for the Stokes and Navier–Stokes Equations. *SIAM J Numer Anal.* 1996;33(1):107–27. Doi: 10.1137/0733007.
17. Devloo P, Tinsley Oden J, Pattani P. An h-p adaptive finite element method for the numerical simulation of compressible flow. *Comput Methods Appl Mech Eng.* 1988;70(2):203–35. Doi: 10.1016/0045-7825(88)90158-2.

18. Gartling DK, Becker EB. Finite element analysis of viscous, incompressible fluid flow. *Comput Methods Appl Mech Eng.* 1976;8(1):51–60. Doi: 10.1016/0045-7825(76)90052-9.
19. Houston P, Schwab C, Süli E. Discontinuous hp-Finite Element Methods for Advection-Diffusion-Reaction Problems. *SIAM J Numer Anal.* 2002;39(6):2133–63. Doi: 10.1137/S0036142900374111.
20. Omar H, Rohani S. Transport Phenomena in the Conversion of an Anaerobic Landfill Into an Aerobic Landfill. *Proceedings of the 2015 COMSOL Conference in Boston.* Boston; 2015.
21. Ishimori H, Endo K, Ishigaki T, Sakanakura H, Yamada M. Coupled fluid flow and thermal and reactive transport in porous media for simulating waste stabilization phenomena in semi-aerobic landfill. *Proceedings of the 2011 COMSOL Conference in Boston.* Boston; 2011.
22. Reddy JN, Gartling DK. *The Finite Element Method in Heat Transfer and Fluid Dynamics, Third Edition.* CRC Press; 2010.
23. Lewis RW, Morgan K, Thomas HR, Seetharamu K. *The Finite Element Method in Heat Transfer Analysis.* John Wiley & Sons; 1996.
24. Gartling DK. Convective heat transfer analysis by the finite element method. *Comput Methods Appl Mech Eng.* 1977;12(3):365–82. Doi: 10.1016/0045-7825(77)90024-X.
25. Iannelli J. *Characteristics Finite Element Methods in Computational Fluid Dynamics.* Springer Science & Business Media; 2006.
26. Rasi S, Läntelä J, Rintala J. Upgrading landfill gas using a high pressure water absorption process. *Fuel.* 2014;115:539–43. Doi: 10.1016/j.fuel.2013.07.082.

27. Rasi S, Läntelä J, Veijanen A, Rintala J. Landfill gas upgrading with countercurrent water wash. *Waste Manag.* 2008;28(9):1528–34. Doi: 10.1016/j.wasman.2007.03.032.
28. Erdem E, Karapinar N, Donat R. The removal of heavy metal cations by natural zeolites. *J Colloid Interface Sci.* 2004;280(2):309–14. Doi: 10.1016/j.jcis.2004.08.028.
29. Malliou E, Loizidou M, Spyrellis N. Uptake of lead and cadmium by clinoptilolite. *Sci Total Environ.* 1994;149(3):139–44. Doi: 10.1016/0048-9697(94)90174-0.
30. Ouki SK, Kavannagh M. Performance of natural zeolites for the treatment of mixed metal-contaminated effluents. *Waste Manag Res.* 1997;15(4):383–94. Doi: 10.1177/0734242X9701500406.
31. Zamzow MJ, Eichbaum BR, Sandgren KR, Shanks DE. Removal of Heavy Metals and Other Cations from Wastewater Using Zeolites. *Sep Sci Technol.* 1990;25(13-15):1555–69. Doi: 10.1080/01496399008050409.
32. Niskanen A, Värri H, Havukainen J, Uusitalo V, Horttanainen M. Enhancing landfill gas recovery. *J Clean Prod.* 2013;55:67–71. Doi: 10.1016/j.jclepro.2012.05.042.

Chapter 2

2 Treatment of landfill waste, leachate and landfill gas: A review

This review is aimed at the treatment of the entire landfill, including the waste mass and the harmful emissions: leachate and landfill gas. Different landfill treatments (aerobic, anaerobic and semi-aerobic bioreactor landfills; dry-tomb landfills), leachate treatments (anaerobic and aerobic treatments, adsorption, chemical oxidation, coagulation/flocculation and membrane processes) and landfill gas treatments (flaring, adsorption, absorption, permeation and cryogenic treatments) are reviewed. This review is to provide a summary of what information is available and the gaps present in current knowledge. The most significant areas in need of expansion are landfill waste treatments. In recent years this area has begun to grow but there is an opportunity for much more. Another area that needs to be explored is the treatment of LFG. Gas treatment is a very large field but not much effort has been put towards treatment of landfill gas specifically. The aim of this review is to compare treatment methods and give direction to future research.

2.1 Introduction

The increasing human population on Earth has put a strain on the environment. As the population increases, the amount of waste produced will increase. In the United States, generation of municipal solid waste (MSW) has increased from 88.1 million short tons (1 short ton is equivalent to 2,000 lbs) in 1960 to 250.9 million short tons in 2012. This increase in MSW generation is not only due to the increasing population but increased generation per capita. In 1960, 2.68 lbs of waste was generated per person per day and has increased to 4.38 lbs of waste per person per day in 2012¹. In 2006, 28.6% of the generated MSW was recycled, 6.9% was combusted in waste-to-energy plants and 64.5% was landfilled². This trend applies worldwide. This will place a strain on the world's landfills. Landfills need land; the world's land is finite and there will inevitably come a time when

there is no more land for landfills. The vast majority of current landfills do nothing to address the growing requirement for land.

The current state of landfill treatment is limited to the “dry-tomb” method. This treatment method has been used for a long time, is mature and easily applied to a landfill. Methane (CH_4) produced by anaerobic biodegradation of MSW typically makes up greater than 45% of the total landfill gases (LFG)³. Methane is a more powerful greenhouse gas than carbon dioxide (CO_2). The global warming potential over a 100-year span is 25. This is due to its stronger molar absorption coefficient for infrared radiation and longer atmospheric residence time⁴. In 2004 – 2005, anthropogenic greenhouse gas (GHG) emissions from the waste sector totaled 1.4 million metric tons of CO_2 equivalent (MMT CO_2e). The methane made up 90% of the GHG emissions from the waste sector, and 18% of the total global anthropogenic CH_4 emissions⁵. The concentration of methane is more than twice as high as the level from 150 years ago. The increase in methane concentration is indirectly caused by the increasing human population⁶.

Landfills produce leachate and gaseous emissions (LFG) that if not treated can be environmentally harmful. The treatment of landfill and the emissions (leachate and LFG) is a major problem. There has been significant research done on the treatment of leachate, much more than has been done on the treatment of MSW and LFG. The purpose of this review is to show the state of research of landfill, leachate and LFG treatments.

This review paper aims at providing alternatives for treating landfill waste and its harmful byproducts, leachate and LFG. To date, no review paper encompasses all three phases of landfill treatment. It would be impossible to delve into detail of each individual treatment method, however, this paper gives a broad, overall view of the different treatment methods.

It would be impossible to find one perfect solution that treats the waste, leachate and LFG. It takes a combination of different treatment methods to effectively treat all three.

2.2 Landfill treatments

Landfill treatments can be classified into three types: aerobic, anaerobic and semi-aerobic. Historically, landfills were operated in the “dry-tomb” method but landfills have begun to shift towards operating as bioreactors. Operating landfills as bioreactors (aerobic/anaerobic/semi-aerobic) has many advantages over the conventional dry-tomb method (anaerobic) of landfilling. These advantages include: (1) protection to the environment, (2) increased potential for energy production from LFG, (3) in-situ treatment and recirculation of leachate leading to reduced treatment cost, (4) greater stabilization rates allowing more storage due to increased density, (5) increased rate of decomposition shortening post-closure monitoring period and (6) increased sustainability allowing possible reuse of the land⁷⁻⁹. Recirculating leachate turns the dry-tomb landfill into a bioreactor landfill^{10,11}. Higher rates of leachate recirculation accelerate waste biodegradation. A higher rate may leach out large amounts of organic matter, reducing biological methane potential¹². This decreases the time for stabilization. Depending on how permeable (extent of compaction) the waste is, the amount of leachate added is adjusted. In low permeability wastes, less leachate is added to prevent surface seepage problems¹³. This causes a decrease in the biodegradation, meaning if possible waste should not be over-compacted.

2.2.1 Dry-tomb landfill

The dry-tomb approach to landfilling, as the name suggests, is entombing the waste to disallow (as much as possible) any moisture from entering the waste mass. The rationale behind this method is, with no moisture, the waste will remain dry and not decompose, not producing any harmful leachate and LFG¹⁴. However, in reality, a landfill cannot be completely free of moisture infiltration and dry-tomb reactors are not completely dry. This causes very slow biodegradation and harmful leachate and LFG production. Due to this, dry-tomb landfills have aftercare periods of hundreds of years¹⁵. Emissions have to be

tracked for environmental impact; methane emissions remain constant for 100 years and emissions can extend beyond 100 years¹⁶. Aftercare of a landfill typically consists of monitoring of emissions (i.e. leachate and LFG), studying the receiving systems (i.e. groundwater, surface water, soil, and air) and maintenance of the cover, leachate and gas collection systems. The minimum aftercare period depends on regulations. For example, in Europe, many member states require a minimum of 30 years of aftercare, which may be shortened or prolonged on a site-by-site basis¹⁷. This length of aftercare suggests that this method is not effective at mitigating risks to health and the environment.

The dry-tomb approach to landfilling is low cost relative to the bioreactor landfills but is not controlled. Due to the low cost developing countries opt to use these landfills and face environmental problems from leachate contaminated ground water, odor, air pollution and greenhouse gas emissions¹⁸. This technology is fundamentally flawed because it is assumed that leachate and LFG are contained but this is not possible because the cover and liner are not impermeable. This justifies research into finding alternative methods for treating landfills that are both economical and less environmentally detrimental. This has spawned research into bioreactor landfills.

2.2.2 Anaerobic bioreactor landfill

The process by which anaerobic biodegradation occurs is very slow, sometimes spanning decades after landfill closure. This means that leachate emissions can span centuries and LFG emissions can last more than three decades after closure¹⁹. Leachate and LFG emissions have to be monitored to ensure environmental protection. Table 2-1 illustrates consequences, good and bad, of anaerobic bioreactor landfills.

Table 2-1 Advantages and disadvantages of anaerobic bioreactor landfill

Potential Advantages	Potential Disadvantages
<ul style="list-style-type: none"> • LFG has high methane concentration which can be used • Decreased waste stabilization times 	<ul style="list-style-type: none"> • High volatile fatty acid (VFA) concentration can leach harmful constituents • Relatively high levels of ammonia in leachate

- Relatively low cost
 - In-situ treatment of leachate
 - Production of hydrogen sulfide
-

Anaerobic biodegradation can be broken down into two stages. In the first stage, the waste components (e.g. fats, proteins, etc.), are hydrolyzed to their respective subunits (e.g. fatty acids, amino acids, etc.) by a group of facultative and anaerobic bacteria. These products then undergo metabolic processes producing simple organic compounds. These compounds mainly consist of short chain volatile acids (acetic and propionic acid) and alcohols. The second stage takes the products of the first stage and converts them by anaerobic bacteria into gases (mainly CH₄ and CO₂)²⁰. Each of these two stages has sub-stages (e.g. stage 1 – hydrolysis, acidogenesis), but the sub-stages can be grouped into one of the two stages.

Nutrients in the waste (i.e. carbon, nitrogen and phosphorus) significantly affect anaerobic biodegradation of waste. The limiting nutrient has been shown to be phosphorus^{21,22}. With the addition of phosphorus, microbial growth increased up to a concentration of 10 µg of PO₄ phosphorus per litre of water²³. When compared to a control sample, phosphorus addition increased removal efficiency of chemical oxygen demand (COD) and NH₄⁺ nitrogen by 5.1% and 8.1% respectively²¹. Phosphorus can be used to control the growth of bacteria in liquids (e.g. leachate), even liquids with low organic carbon content²⁴. Phosphorus levels can easily be controlled by adding or removing phosphorus to or from the moisture source (i.e. leachate or make up water). Further work can be done with the aim of controlling the degradation rates effectively using phosphorus. This could be useful if for example, the temperature in the waste is getting too high which could cause safety problems or could start killing the microorganisms. Lowering phosphorous levels could slow down the microbial activity to reduce the temperature to a safe level.

Little research has been published on landfill microbiology. Fielding et al. (1998) conducted one such study to identify the predominate species of methanogenic bacteria in traditional landfills. They had 7 (EF1 to EF7) samples and tried to match the samples to known bacteria. Fielding et al. found that isolate EF1 was closely related to *M. formicum*

MF and EF5 was closely related to *M. barkeri* MS. Isolate EF2 was found not to be related to any of the reference bacteria. Isolates EF3, EF4, EF6 and EF7 showed antigenic similarity to *M. bryantii* MoH and *M. bryantii* MoHG. Isolates EF3, EF4, EF6 and EF7 showed differences from the reference bacteria as well as differences among themselves²⁵. Further research needs to be done into learning more about the microorganisms that are present during anaerobic biodegradation. Studying how different nutrients (e.g. adding urea as a nitrogen source to leachate) affect the biodegradation rate could lead to faster stabilization times than are currently possible. Anaerobic landfills attempt to use the gas produced by the biodegradation to produce energy. However, methane is a harmful greenhouse gas. Weighing the benefits of LFG as a fuel compared to the potential environmental hazards becomes a problem. Aerobic bioreactor landfills get rid of this problem by effectively eliminating the methane production, instead producing carbon dioxide and water.

2.2.3 Aerobic bioreactor landfill

Aerobic treatment of landfill waste can be thought of as very large scale composting. Aerobic landfills are different than anaerobic landfills due to air injection into the landfill mass, killing anaerobic bacteria and promoting growth of aerobic bacteria. There are numerous methods used for air injection. These include: intermittent high pressure aeration, low pressure aeration, active aeration with off-gas extraction, active aeration without off-gas extraction, and passive aeration (air venting)²⁶. One benefit/detriment (depends on use of LFG) is that methane production virtually ceases. Air injection reduces methane concentration in LFG from 60% to 10-15% in 7-10 days²⁷. This gives an indication of how fast aerobic bacteria grow and begin degrading the waste. Aerobic biodegradation produces mostly carbon dioxide and water²⁸. The effectiveness of the aerobic biodegradation process is dependent on the oxygen concentration, and along with temperature^{29,30}, moisture content³¹ and pH³², affect all types of biodegradation³³.

Aerobic landfills have many advantages over anaerobic landfills. These advantages include a faster waste stabilization time, lower levels of COD, biological/biochemical oxygen

demand (BOD), total organic carbon (TOC), ammonia (reducing odors), phosphorus and alkali metals and due to higher temperatures evaporating leachate, less leachate requiring treatment. However, injecting compressed air requires a lot of energy.

An aerobic reactor was examined after 374 days having settled 37%. The aerobic reactor was compared to an anaerobic reactor which was operated for 630 days. The anaerobic reactor settled 5%³⁴. The reactor conditions were identical except for air injection into the aerobic reactor. This simple change produced a difference of 32% in settlement. The authors suggested doing more research into aeration rates which has been done by Slezak et al. (2012)³⁵ and extended to where in the waste mass the air should be injected by Wu et al (2014)³⁶.

Aeration rates have a large effect on the degradation of the waste. The greatest degradation rate was found at the high aeration rates and the lowest was found at medium aeration rates. The rate of oxygen assimilation decreased approximately linearly during the 28-day time frame of the experimental study³⁵. A fundamental design factor in an aerobic landfill process is where to inject the air (bottom/middle/surface layer) and the rate of air injection. Aeration at the bottom layer is most effective for decomposition. In terms of how much air is injected, a higher injection rate near the bottom (deepest layer) accelerates the stabilization³⁶.

Aerobic treatment had a two order of magnitude lower leachate ammonia level than anaerobic treatment³⁷. Aerobic bioreactor landfill experiments claim a lack of unpleasant odors and the lower level of ammonia contributes to this. Aerobic landfills treat the leachate and decrease the amount produced significantly and can eliminate production of leachate completely due to high temperatures in the waste³⁸. Aerobic landfills also decrease volatile fatty acid (VFA) levels much more quickly than do anaerobic landfills. Bilgili et al. (2012) conducted a study to find the effect of leachate recirculation and aeration on VFA concentrations in the resultant leachate. They found that total VFA concentrations in the aerobic reactors decreased from 33,930 and 38,270 to 500 and 800 mg L⁻¹, after 120 days of operation. The anaerobic reactors had similar removal but took much longer, decreasing

to 820 mg L^{-1} after 350 days and 786 mg L^{-1} after 450 days³⁹. High VFA concentrations will decrease the pH of the leachate, leaching out more contaminants. A quicker VFA removal time means that less contaminants will be present in the leachate.

The ideal temperature for aerobic biodegradation is in the mesophilic range ($15\text{-}40^\circ\text{C}$)³³. The ideal moisture content is between 50 and 60%⁴⁰. The pH level is not as great a factor in determining effectiveness of aerobic biodegradation as long as the pH is not extremely acidic or basic because of the various bacterial strains present. The optimum pH values are between 6.5 and 8 but can be between 5.5 and 9³³. Air injection into the landfill mass dries out the landfill, minimizing leachate production⁴¹.

Oxygen consumption varies depending on the types and age of waste. A study by Kallel et al. (2003) looked at the oxygen consumption for both fresh and old waste. Fresh waste was made up of bulky waste, incombustible waste and incineration ash; old waste was made up of bulky waste, incombustible waste, incineration ash and sludge. Their findings showed that fresh waste consumed more oxygen than old waste. Bulky waste consumed the most amount of oxygen and incineration ash the least, with the rate of oxygen consumption dropping to zero within weeks⁴². However, these results need to be examined carefully. Waste is a heterogeneous material and all samples are different. For example, COD values for bulky waste and incombustible waste are similar. To compare new and old waste, the composition of the waste has to be as close as possible. This can be done by making “simulated” waste by producing the waste with known proportions to be replicated. If there is a lot of organic material in the old waste, then the results could suggest that old waste uses more oxygen than new waste. Assuming identical waste, old waste is further degraded than new waste and needs less oxygen. Using only four samples may not be enough. To get rid of the error associated with heterogeneity, doing a relatively large number of samples will provide more defined trends.

Shredding wastes increases biodegradation rates^{43,44}. This is true of all types of landfill bioreactors but is especially helpful in aerobic landfills. Shredding increases homogeneity and surface area, allowing a better distribution of air and better contact with the bacteria

lowering the requirement for aeration. Compaction can also be helpful. It results in a more uniform mass allowing a lower aeration rate. Compaction reduces the potential for channeling. Channeling diverts nutrients, lowering the rate of degradation⁴³. In experimental scales, the waste is usually shredded. This is to homogenize the waste as much as possible. Shredding has been shown to be effective in increasing biodegradation rates. However, in full scale landfills the large amounts of energy required to shred the waste make it unfeasible.

Aerobic biodegradation of landfill waste is a promising alternative to the current anaerobic methods in use. Table 2-2 illustrates the consequences of aerobic bioreactor landfills.

Table 2-2 Advantages and disadvantages of aerobic bioreactor landfill

Potential Advantages	Potential Disadvantages
<ul style="list-style-type: none"> • Decreased waste stabilization times • Little to no methane production decreases GHG emissions • In-situ treatment of leachate • Removal of moisture by air stripping • Little to no ammonia production 	<ul style="list-style-type: none"> • High cost for aeration • Air can cause flammable/explosive mixtures • Unknown gases may be produced

Methane, a very dangerous greenhouse gas, is produced from anaerobic but not aerobic biodegradation. If all landfills were to employ aerobic instead of anaerobic treatment, it would have the same effect as removing at least 761 million metric tons of CO₂ from the atmosphere every year. However, aerobic treatment of waste requires large amounts of air, requiring large amounts of energy. Another concern with air present, is the potential for air and methane to mix resulting in a flammable/explosive mixture. This becomes an optimization problem between environmental benefits and financial expenditure. The semi-aerobic landfill attempts to lessen the conflict between benefits and costs by lowering the energy required.

2.2.4 Semi-aerobic bioreactor landfill

A semi-aerobic landfill is similar to the aerobic landfill in that air is allowed to enter the waste. However, in aerobic landfills, the air is injected continuously whereas in semi-aerobic landfills, air flows naturally through the leachate collecting pipes⁴⁵. Tang et al. (2008) attempted to track the stabilization of semi-aerobic landfills. The authors used three different groups of indicators: leachate characteristics (COD, NH₃-N, TOC, etc.); waste characteristics (biologically degradable matter, VFAs, volatile solids, coarse fiber, humic acid); and external characteristics of the landfill (settlement rate, generation of leachate, temperature). Tang et al. came up with three stages: (1) the instability stage, (2) the relative stability stage and (3) the absolute stability stage⁴⁶. Semi-aerobic landfills provide the benefits of the aerobic landfill but lower the operational costs by removing the cost of air injection. Table 2-3 illustrates the features of semi-aerobic landfills.

Table 2-3 Advantages and disadvantages of semi-aerobic bioreactor landfill

Potential Advantages	Potential Disadvantages
<ul style="list-style-type: none"> • Decreased waste stabilization times • Little methane production decreases GHG emissions • In-situ treatment of leachate • Relatively low cost 	<ul style="list-style-type: none"> • Unknown gases may be produced • Air can cause flammable/explosive mixtures

The gaseous emissions from semi-aerobic landfill systems are similar to aerobic landfills. The composition of the LFG produced in a large-scale simulated semi-aerobic landfill was 19-28 vol% CO₂, 1-8 vol% O₂ and 5-13 vol% CH₄. Huang et al. (2008) showed that leachate and LFG (less CH₄, more CO₂) qualities from semi-aerobic were better than leachate and LFG produced from anaerobic landfills⁴⁷. Leachate was tracked using COD, ammonia, nitrate and pH. Although effective at reducing the methane concentrations, the semi-aerobic landfill did not decrease the concentration as much as the aerobic landfill. In this study, none of the analytic methods for tracking leachate or LFG quality were mentioned. For example, the authors did not mention how gas concentration was measured.

This was true for the leachate analysis as well. The whole purpose of this paper was to track the changes of quality of leachate and LFG. The authors displayed the results without mentioning how they arrived at the results.

Leachate samples from two landfills in Malaysia (one anaerobic and one semi-aerobic) were taken and 20 different parameters were measured⁴⁸. Aziz et al. (2010) compared leachate from one anaerobic landfill and a semi-aerobic landfill which had a pond of leachate that was unaerated and a pond that was intermittently aerated. The leachates were at different stages of maturity. The semi-aerobic landfill is older than the anaerobic landfill, which affects the level of the contaminants in the leachate. A comparison cannot be made if the leachates are at different stages of degradation. A study comparing leachate contaminant levels over time from the 3 different bioreactor landfills is useful. However, if a valid comparison is to be done, the leachates have to start from the same time point. The leachates cannot be at different stages of maturity. Also, leachate contaminant levels have to be relatively similar at the start of the study. To do this, three landfill bioreactors with as similar waste compositions as possible need to be constructed. “Synthetic” leachate needs to be created so that the same composition of leachate goes in to the bioreactors. Results from this can then give an accurate description of the leachate quality dynamics in the different types of bioreactor landfills.

2.2.5 Landfill operations and measurements/control

2.2.5.1 Operations

Bioreactor landfills require closer attention on performance than do dry-tomb landfills. Control and monitoring ensure successful system performance. Biological, chemical and hydrologic processes are monitored and controlled. Once the waste has stabilized, the operational and maintenance programs can be reduced⁴⁹.

The fundamental differences between the traditional anaerobic versus aerobic treatment in regards to operations are the presence of wells that provide sources of oxygen and moisture. There are two types of wells: air injection wells and moisture injection wells. The air

injection wells are used to inject compressed air into the waste. The moisture wells are used to inject leachate into the waste⁵⁰. Figure 2-1 illustrates a schematic representation of anaerobic, aerobic and semi-aerobic bioreactor landfills.

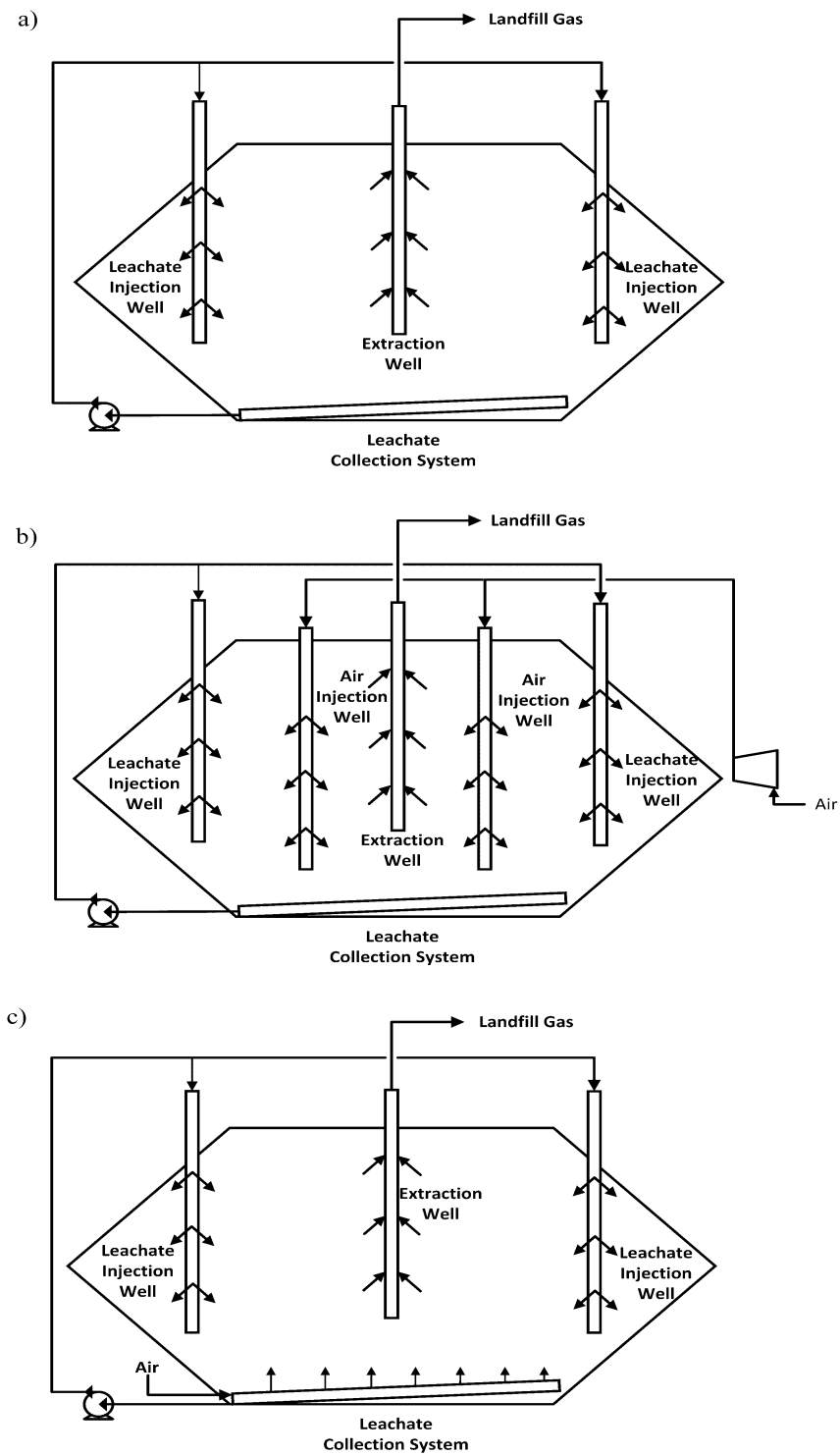


Figure 2-1 Schematic diagram of: (a) anaerobic bioreactor landfill; (b) aerobic bioreactor landfill; (c) semi-aerobic bioreactor landfill – all with leachate circulation

Yazdani et al. (2010) found that rates of oxygen transfer to immobile zones significantly influence the degradation rate. Immobile gas zones occupy between 32 and 92% of the gas filled pore space. Gas tracer tests can determine the size of these zones⁵¹. Knowing the locations of these zones can then help determine locations of gas injection wells to ensure efficient aerobic degradation. Even when sufficient oxygen was supplied, the immobile zones were still present and actually increased as the moisture content of the waste was increased. The most significant finding was that the rate of air transfer from immobile to mobile zones limited aerobic degradation. This is significant because this problem can be solved by choosing appropriate locations for the air injection wells.

2.2.5.2 Measurement/Control

To ensure that conditions are ideal for bioreactor landfill treatment, data collection is essential. The operational parameters need to be monitored. By measuring these parameters, the operators can determine if aerobic or anaerobic biodegradation is dominating. The moisture content should be in the range of 40-70%. The temperature should be in the mesophilic range³³. In an aerobic landfill the oxygen concentration should be above 0% to ensure enough oxygen for aerobic conditions⁵⁰. Once the oxygen (or air) is pumped in, the conditions change from anaerobic to aerobic relatively quickly usually within the first month of injection. In 7 to 10 days, methane concentrations reduced from 60% to 10-15%²⁷. If the concentration of methane in the LFG is less than 10% by volume, this is an indicator of aerobic biodegradation. If the methane concentration is near or above 50%, this is an indicator of anaerobic biodegradation⁵⁰. If an aerobic landfill is left uncontrolled, the landfill will revert back to anaerobic. The oxygen is consumed by the aerobic bacteria and the aerobic bacteria quickly perish.

Rendra, Warith & Fernandes (2007) found that the higher the leachate circulation, the faster the biodegradation. Increasing the leachate circulation rate facilitated the exchange of substrate, nutrients, buffer, and diluted inhibitors. The higher circulation rate also spreads the microorganisms within the waste. In their study, the air was kept at a constant flow rate between samples, so the only variable under consideration was the leachate circulation rate.

To help with nutrient needs Rendra et al. added wastewater sludge to the leachate. However, they found that the leachate circulation rate had a much more pronounced effect on the biodegradation than did the wastewater sludge rate⁵². This was most likely due to the fact that leachate was added at a rate 30 times greater than the wastewater sludge. Rendra et al. looked at leachate recirculation and sludge addition as manipulated variables to see their effects on biodegradation using factorial experimental design. This led to the development of empirical model equations relating the leachate recirculation and sludge addition to biodegradation. Sludge addition was found to be insignificant in increasing biodegradation. Further work can be done to determine an empirical model relating other factors to biodegradation (e.g. air injection and leachate recirculation) using factorial design.

The aerobic biodegradation process is an exothermic process⁵³. This presents two important consequences. The first being that with energy released during the process, the temperature will inevitably increase and require control. The second consequence of the energy release, is the eventual evaporation of water. With the waste being at a moisture content between 40 and 70%, there is moisture that can evaporate. As a result, moisture content needs to be measured and controlled. Leachate generation decreases throughout the degradation process. The evaporation of moisture held in the waste is a reason to the decreasing leachate production.

2.3 Leachate treatment

Leachate is produced from the percolation of precipitation through the waste mass forming a complex liquid. Leachate is a complex variable mixture containing soluble organic, inorganic, bacteriological constituents and suspended solids (SS). Due to the aerobic/anaerobic microbial decomposition, leachates contain intermediate products as well as toxic organics, heavy metals, and other xenobiotic materials⁵⁴. Factors that affect the quality of leachate are age, precipitation, seasonal weather variations, waste type and composition⁵⁵. Hughes et al. (as cited in ⁵⁶) found that leachate quality was highly variable between landfills. This can be attributed to the nature of waste in the landfill. A hazardous

waste disposal site for example, would have much more hazardous leachate than a yard waste disposal site.

The leachate chemistry is highly influenced by the amount of rain⁵⁷. Based on the amount of rainfall, the leachate can be separated into three groups: leachates during severe droughts, leachates of high rainfall periods and leachates of normal rainfall periods. The first group shows the highest mineralization (most concentrated). The second group shows the lowest mineralization and concentration (most diluted)⁵⁷. The composition of leachate also changes with the age of the waste being decomposed. Heavy metal concentrations in leachate from a United Kingdom landfill decreased with time. However, the concentrations of sodium and chlorides increased⁵⁶.

Off-site leachate treatment can be a significant portion of the cost of a landfill. Anaerobic landfill leachate can be acidic, leaching harmful materials from the waste. This toxic leachate left untreated can seep into the groundwater and cause environmental and health problems. Aerobic biodegradation has the advantage of occurring at relatively high temperatures, effectively decreasing the volume of leachate by evaporation. An aerobic landfill was implemented at a landfill near Franklin, Tennessee. Before implementation, the landfill produced 720,000 L of leachate a month, costing US\$0.15 per gallon for treatment and disposal. In this landfill, all of the leachate produced was used onsite as the moisture source. This saved the landfill \$650,000 over two years from off-site leachate treatment. All leachate was consumed onsite and methane production caused by the anaerobic microorganisms decreased by more than 98%³⁸.

Aerobic landfill treatment also treats the leachate, gradually making it less dangerous. At the Columbia County landfill (aerobic treatment), within 5 months, acetone was reduced from 750 ppm to less than 250 ppm; methyl ethyl ketone (MEK) was reduced from 1,800 ppm to 300 ppm, and toluene was reduced from 250 ppm to 50 ppm⁵⁸. At the Columbia County landfill, prior to startup, approximately 453,600 L of leachate was sent for treatment each month. For the first six months of the aerobic treatment, the leachate produced from the entire landfill was utilized in the aerobic landfill (no leachate sent for

treatment). After fourteen months of treatment, 945,000 L was sent for treatment, a reduction of 86%³.

Leachate treatment can be split into two parts: biological treatments and physico-chemical treatments. The main biological treatments are: anaerobic and aerobic treatments and anammox. The main physico-chemical treatments are: adsorption, chemical oxidation, coagulation/flocculation and membrane processes⁵⁹. The treatment methods have to remove biological/chemical pollutants and heavy metals. Heavy metals treatment is common in many industries. The treatment methods used depend on many factors (e.g. type/amount of heavy metals, required final concentration, etc.). Heavy metals include: copper (Cu), silver (Ag), zinc (Zn), cadmium (Cd), gold (Au), mercury (Hg), lead (Pb), chromium (Cr), iron (Fe), nickel (Ni), tin (Sn), arsenic (As), selenium (Se), molybdenum (Mo), cobalt (Co), manganese (Mn), and aluminum (Al)⁶⁰. Physico-chemical treatments are more expensive than biological treatments but when the BOD/COD ratio is low (<0.1), biological processes can be ineffective⁶¹. When the BOD/COD ratio is low, this indicates a low concentration of biodegradable pollutants and physico-chemical treatment methods have to be used.

2.3.1 Anaerobic treatment

Anaerobic systems are successful in treating high chemical oxygen demand (COD) leachates. The resultant effluent however, still has a high COD, requiring additional treatment by aerobic or physico-chemical treatment methods. Anaerobic digestion produces low sludge amounts but experiences low reaction rates⁶². Anaerobic treatment produces methane, in the range of 67-81%⁶³⁻⁶⁵ that can be captured.

Timur and Öztürk found that 83% of the COD removed (the biodegradable portion) from leachate using anaerobic treatment was converted to methane⁶⁶. This is a useful finding if the methane is collected. This allows for a predictive tool if a correlation can be made between COD and methane production to determine the amount of methane that can potentially be captured. However, this study should be repeated with BOD. COD by

definition is all degradable organic compounds, some of which cannot be biodegraded by the anaerobic bacteria. BOD contains only biodegradable organic compounds. COD may be appropriate but the same study should be done using BOD to compare the results. There may be advantages or disadvantages using either COD or BOD but a study comparing the two would be very beneficial. If it provides the same information, it at least provides a second test to validate the results from the COD results. This study did not examine other contaminant data (e.g. BOD, SS, ammonia). These contaminants are important and should be studied.

Anaerobic treatment is unaffected by the presence of metals (alkali, alkali earth and heavy metals) in the leachate. The kinetic mechanism of anaerobic treatment is similar to that of digestion of municipal wastewater sludge. Heavy metal removal efficiencies can be greater than 85% for aluminum, barium, cadmium, mercury, nickel and zinc; 80% for iron; between 40 and 70% for chromium, copper, lead and manganese; 30% for calcium; and less than 10% for magnesium, potassium and sodium⁶⁷. Kheradmand et al. (2010) used an anaerobic digester in series with an activated sludge unit. The anaerobic digester showed excellent heavy metal removal efficiency. The heavy metals that were focused on were Fe, Cu, Mn, Zn and Ni. All the heavy metals except Zn (approximately 50% removal) had removal efficiencies in the range of 88.8-99.9%. However, ammonia decrease did not occur⁶⁸.

2.3.2 Aerobic treatment

In aerobic landfills, leachate is treated as it passes through the waste. The landfill functions as both a waste treatment bioreactor and a leachate treatment bioreactor. Aerobic landfills recycle the leachate. Leachate is treated by the aerobic bacteria. As the waste stabilized using aerobic treatment, metal concentrations were significantly reduced, while no appreciable difference was found when the waste stabilized anaerobically⁶⁹. Kim et al.'s study contained graphs tracking the heavy metal concentrations with respect to time. Nothing was reported on the kinetics of the removal of the heavy metal levels or any kinetic relationships. This should be further explored using experimental design and response

surface methodology to determine empirical relationships between important parameters and the removal of heavy metal levels and related back to the kinetics of the process. This can be further extended to using experimental design to optimize the operational parameters to remove heavy metals as effectively as possible.

Aerobic treatment decreases ammoniacal-N, organic compounds and heavy metals enough to allow discharge. Anaerobic cannot treat ammoniacal-N levels in leachates. A landfill in the United Kingdom (UK) required a treatment method for the stronger leachates that were produced. A sequencing batch reactor using aerobic microorganisms was decided upon for the treatment of the strong leachate. The treatment reduced levels of ammoniacal-N, organic compounds and heavy metal levels low enough that the leachate could safely be discharged into the river⁷⁰.

In an aerobic landfill study, the heavy metal concentrations decreased significantly during the treatment. Ni levels decreased from 88.85 ppb to less than 1 ppb after 510 days and Pb levels decreased from 54.97 ppb to less than 1 ppb after 510 days. Heavy metals may be retained by sorption to the MSW. The levels of heavy metals also may be decreased as a result of the high pH⁷¹. The pH was above 8, which may have caused carbonate precipitation and hydroxide precipitation. These processes are used in offsite wastewater treatment facilities to treat heavy metals. After 250 days of operation, nearly 100% NH_4^+ removal was achieved while NO_3^- levels increased. Most of the removal was due to nitrification, evident by the increased NO_3^- levels. A portion of removal is due to biomass synthesis.

Aerobic treatment of leachate follows the same biological pathways as other aerobic wastewater treatments. Kheradmand, Karimi-Jashni and Sartaj (2010) used a combined anaerobic digester in series with an activated sludge system to treat municipal landfill leachate. They found that in their study the aerobic sludge portion of the treatment showed low removal efficiency. This is due to the high organic loading rate (OLR) in the waste used. This means that leachate containing high amounts of organic material need to be pretreated for more efficient removal⁶⁸. As for the heavy metal present, the anaerobic

digester showed excellent removal efficiency. The heavy metals that were focused on were Fe, Cu, Mn, Zn and Ni. All the heavy metals except Zn (approximately 50% removal) had removal efficiencies in the range of 88.8-99.9%. Biological treatment methods are cost effective compared to other methods (i.e. chemical). However, biological methods produce an overabundance of sludge that requires treatment and disposal⁷². Table 2-4 compares the removal efficiency of COD, BOD and/or TOC using both anaerobic and aerobic treatments.

Table 2-4 Biological treatment removal efficiencies

	Leachate characteristics				Operational conditions			Removal efficiency (%)	Reference
	COD (mg/L)	BOD (mg/L)	BOD/COD	pH	Temperature (°C)	Volume (L)	HRT ^{a)} (days)		
Aerobic reactor (In-situ)	45,000	35,000	0.8	4.5	-	334	-	89 COD 97 BOD	73
	40,500	-	-	4	25-53	250	-	91 COD	74
Aerobic reactor (Ex-situ)	4,298-5,547	913-1,017	0.16-0.24	8.6-9.3	-	3	12	84.4 COD	75
	4,740-28,120	2,840	0.4	7.53	26-30	18	-	60-90 TOC	76
	3,246	-	-	7	25	4	0.33	69-83 COD	77
Anaerobic reactor (In-situ)	62,000	-	-	6.3	-	392	-	98 COD	78
Anaerobic reactor (Ex-situ)	55,351	49,400	0.81	6.31	32 ± 1	150	15	73 COD 77 BOD	68
	16,200-20,000	10,750-11,000	0.54-1.02	7.3-7.8	35 ± 2	1	1.5-10	85 COD	66
	32,562	16,011	0.49	5.1-5.31	34 ± 1	14	20	79.3 COD 97.1 BOD	67
	1,365	276	0.2	7.52	-	4	24	76.8 COD	79
	43,000	-	-	6.4 ± 2	37	2	5	87 COD	80

^{a)} HRT: hydraulic retention time

2.3.3 Anammox

Anammox (anaerobic/anoxic ammonium oxidation) treatment is specifically used for removing nitrogenous compounds in leachates. Anammox is a bacterium-mediated process⁸¹. The exact mechanism that anammox follows is unknown but a few have been proposed⁸². An advantage of anammox treatment is the low sludge production. This is due to the low biomass yield⁸³. However, the low biomass yield is due to the slow growth of anammox bacteria (generation times of 10 to 12 days at 35°C) and limits the anammox process⁸⁴. Anammox is currently limited to high ammonium containing wastewaters.

In a study conducted by Cema et al. (2007), they combined a rotating biological contactor (RBC) with anammox treatment. The RBC contained aerobic and anaerobic ammonium oxidizers. This resulted in autotrophic nitrification and heterotrophic denitrification coupled with the existing anammox treatment. They achieved 3.0 g Nm⁻²d⁻¹ and 3.9 g Nm⁻²d⁻¹ of ammonia and nitrite respectively, maximum removal rates. The maximum removal rate of inorganic nitrogen was 5.8 g Nm⁻²d⁻²⁸⁵.

Recent advances in anammox have been aimed at increasing the activity of the anammox bacteria using external energy such as magnetic fields, electric fields and ultrasound. Liu et al. (2008) demonstrated that a magnetic field could significantly shorten start-up time although the exact physiology change in the bacteria is not well understood. A control reactor was compared to a reactor undergoing a magnetic field. The magnetic reactor start-up time was 3/4 of the start-up time for the control reactor. Short term batch tests were conducted to observe the activity at varying magnetic field strengths. A maximum of 50% increase in activity was found at 75 mT. To monitor long term effects, a magnetic field strength of 60 mT was operated. The results showed a 30% increase in maximum nitrogen removal rate and a 1/4 saving in cultivation time⁸⁶.

A study conducted by Qiao et al. (2014) looked at the effects of electric fields on anammox bacteria. Qiao et al. proposed that the electric fields may alter the redox potential and supply energy for growth. Qiao et al. found that anammox activity increased by 25.6%

above the control experiment in a certain range of electric field strengths. For their particular system this range was between 0 and 2 V/cm, with the optimum value being at 2 V/cm. Above this range, the activity decreased 21.2% below the control experiment levels. Another factor that Qiao et al. considered was the application time. Application time was varied between 5 and 60 minutes while keeping the electric field constant at 2 V/cm. The application time followed the same trend as electric field strength, increasing the activity when compared to the control experiment for a range of 5-40 minutes but decreasing activity compared to the control experiment when applied for 60 minutes. The maximum activity of 25.6% was reached at an application time of 20 minutes⁸⁷.

Another technology that is being used to increase anammox bacteria activity is ultrasound although the exact mechanism of ultrasound effect on bacteria activity is unknown. Duan et al. (2011) determined that total nitrogen removal rate increased by approximately 21% compared to the blank experiment when an ultrasound intensity of 0.3 W/cm² was applied. An ultrasound intensity greater than 0.3 W/cm² decreased the anammox activity. This was done at an exposure time of 5 minutes. Duan et al. then studied the effect of exposure time. Intensity was held constant at 0.3 W/cm² and varied exposure time between 0 and 10 minutes. They found that the optimal exposure time was 4 minutes, which led to an increase of 25.5% over the blank experiment⁸⁸. Due to its slow biomass growth, anammox has been limited in application. However, in the last few years a lot of work has been done on increasing the anammox biomass activity to overcome the slow growth. There is a lot of potential for application of anammox with increasing treatment rates.

2.3.4 Adsorption

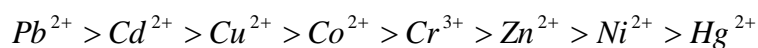
Granular (or powdered) activated carbon is the most common type of adsorbent used in treating leachate. An area of research that is quickly growing is the application of natural zeolites for the treatment of wastewaters. Their relative low cost and ion-exchange properties make them very useful for industrial wastewater (leachate) treatment applications. Adsorption alone cannot be used as the sole treatment method for leachate. Leachate is a complex mixture of numerous contaminants.

Marañón et al. used leachate that had already undergone treatment to test activated carbon as a post treatment method to remove COD. Three different activated carbons were used: Organosorb 10, Organosorb 10MB and Filtracarb CC65/1240. Equilibrium and column data were gathered to see how favourable these three carbons were. The data showed that the equilibrium was unfavourable and adsorption capacities were low⁸⁹. Adsorption using activated carbon to remove COD is not effective. However, where adsorption may provide a solution is in the removal of heavy metals.

Zeolitic materials have been shown to be very effective in treating heavy metals contaminated waste waters (as is the case with leachate) by adsorption/ion exchange. Natural zeolites are also attractive because of their low price compared to other adsorbents. Zeolite particle size significantly affects the metal uptake; the smaller the particle size, the greater the uptake. Metal uptake increases upon increasing temperatures⁹⁰.

Zeolites are tectoaluminosilicates with the tetrahedral structure TO_4 (where the T can be silicon, or aluminum). Zeolites have a negatively charged oxide framework requiring balancing by cations. Typical cations found in natural zeolites are alkali metals (i.e. Na^+ , K^+) and alkali earth metals (i.e. Ca^{2+} , Ba^{2+})⁹¹. Ion exchange using zeolites work by exchanging the alkali/alkali earth metal ions with heavy metal ions.

In 1990, Zamzow et al. found that the ion exchange loading values could range from 1.6 mg/g for Pb^{2+} to 0 mg/g for Cr^{3+} when using the zeolitic material clinoptilolite. Clinoptilolite is commonly studied for heavy metal treatment because of its selectivity to heavy metals. Zamzow et al. also found that the selectivity of the series of heavy metals studied was as follows:



Zamzow et al. used clinoptilolite to treat wastewater from an abandoned copper mine in Nevada. This was done to see how well clinoptilolite performed on multi-ion wastewater. Zamzow et al. found that Al, Fe(III), Cu(II), and Zn were removed to below drinking water

standards. However, Mn(II) and Ni(II) were not⁹². Clinoptilolite is the most abundant natural zeolite in the world and as such is very heavily tested. However, other natural zeolites and maybe even synthetic zeolites should be tested to compare the efficacy of treatment.

2.3.5 Chemical oxidation

Physical and biological treatments are less expensive when compared to chemical treatments. There are however instances when physical and biological treatments are not effective. These instances include for physical: soluble substances; for biological: non-biodegradable and/or toxic substances⁹³. Derco et al. (2010) used chemical oxidation as a pretreatment for leachate with high organic load, high toxicity and low biodegradability. Physical and biological treatments would not have been effective as a sole means of treatment for this leachate so chemical oxidation was used. Fenton's oxidative pretreatment and ozone treatment were both used on both fresh and mature leachates. Fenton's oxidation involves the reaction of organic material using hydrogen peroxide with ferrous acting as a catalyst⁹⁴. Both Fenton's oxidation and ozone treatment resulted in comparable removal of COD. For mature leachate, Fenton's oxidation and ozone treatment resulted in the removal of 88% and 70% of COD, respectively. For fresh leachate, the removals were 46% and 42%, respectively. Derco et al. also fitted the experimental data with zero order, first order and second order models as well as a two component combined reaction kinetic models. The two component combined model consisted of the summation of two first order models, one for easily and one for hard oxidable materials. The Fenton's oxidation best fit the zero and first order models and the ozone treatment best fit the combined model⁹⁴. These kinetic models only represent the experimental conditions used in this study. Further work should be done to find empirical relationships between the rate constants and experimental parameters using response surface methodology. This way, the models can be used to find the reduction in COD at different conditions and can be used for optimization. Other pollutants (e.g. BOD, SS, ammonia, heavy metals) should have been measured to ascertain the effectiveness of removal.

Chemical oxidation has been studied in combination with other treatment methods most often with coagulation-flocculation^{61,95}, to reduce costs associated with using chemical oxidation as a sole means of treatment. Using coagulation-flocculation followed by Fenton process removed greater than 80% of the COD. Reversing the order (i.e. Fenton process followed by coagulation-flocculation) did not increase the removal efficiency⁹⁵.

2.3.6 Coagulation/flocculation

There are numerous coagulants that can be applied to leachate depending on the presence and concentrations of pollutants. Table 2-5 compares different coagulants and the COD removal efficiencies. Coagulation/flocculation is useful as pretreatment for raw (fresh) leachate. Samadi et al. (2010) did an experimental study to find effects of different coagulants, dosage amounts and pH for the removal of COD and total suspended solids. The coagulants used were poly aluminum chloride (PAC), alum and ferrous sulfate. Samadi et al. found that alum could remove the suspended solids and the best coagulant to remove COD was ferrous sulfate. The coagulants were most effective at a pH of 2 and a pH of 12. At other pH values, more coagulant had to be added to increase removal efficiency⁹⁶.

Tatsi et al. looked at using coagulation-flocculation for the treatment of raw and partially stabilized leachates. Raw leachate is characterized by low pH and high concentrations of pollutants. In the study, the organic matter was in the range of 100,000 mg/L COD for raw leachate. Partially stabilized leachate is characterized by higher pH and lower COD, ranging from 700 and 15,000 mg/L. Using ferric or aluminum coagulants to treat the raw leachate reduced the COD between 25-38%. The partially stabilized leachate had a higher removal rate, exceeding 75% reduction⁹⁷. The removal of COD and TOC is usually between 10-25% for raw leachates and between 50-65% with stabilized or biologically pretreated leachates⁹⁸. Consideration has to be taken that the raw leachate had a higher COD at the beginning of the treatment process affecting the treatment efficiency. Another finding of the study was that mixtures of coagulants did not increase the reduction in COD⁹⁷.

Table 2-5 Comparison of coagulation/flocculation studies

Leachate characteristics				Coagulant/Flocculent	Dose (g/L)	Removal efficiency (%)	Reference
COD (mg/L)	BOD (mg/L)	BOD/COD	pH				
700-15,000	50-4,200	0.2	7.9	$\text{Al}_2(\text{SO}_4)_3 \cdot 18\text{H}_2\text{O}$	0.8	31 COD	97
				$\text{FeCl}_3 \cdot 6\text{H}_2\text{O}$	2	80 COD	
44,000-115,000	9,500-80,800	0.38	6.2	$\text{Al}_2(\text{SO}_4)_3 \cdot 18\text{H}_2\text{O}$	1.5	38 COD	
				$\text{FeCl}_3 \cdot 6\text{H}_2\text{O}$	5.2	30 COD	
4,100	200	0.05	8.2	$\text{Al}_2(\text{SO}_4)_3 \cdot 18\text{H}_2\text{O}$	0.035 M	42 COD	98
				$\text{FeCl}_3 \cdot 6\text{H}_2\text{O}$	0.035 M	55 COD	
1,925	-	-	8.4	$\text{Al}_2(\text{SO}_4)_3 \cdot 18\text{H}_2\text{O}$	9.5	62.8 COD	99
				PAC	2	43.1 COD	
5,050	840	0.17	8	$\text{FeCl}_3 \cdot 6\text{H}_2\text{O}$	7 mM	72 COD	100
				PAC	11 mM	62 COD	

2.3.7 Membrane processes

Membrane processes include microfiltration (MF), ultrafiltration (UF), nanofiltration (NF) and reverse osmosis (RO). Membranes are used for the separation of particles, microorganisms, organic molecules and other fine pollutants. Depending on the size of the pollutant requiring separation, different membrane processes (MF, UF, NF, or RO) are chosen. Membranes are more economical when compared to other treatment methods for fine pollutants and provide reliable separation. However, fouling is a problem, which reduces the removal efficiency. Fouling leads to frequent changing of membranes, decreasing the amount of leachate that can be treated. Also, filters accumulate a lot of concentrate that needs to be further treated. Due to fouling, the leachate needs pre-treatment before membranes can be used.

MF has a treatment range of between 0.02 and 10 μm (20 and 10,000 nm)¹⁰¹. UF has a treatment range of 1-20 nm¹⁰². NF rejects particles and molecules smaller than 2 nm. RO only allows solvent to pass through¹⁰³. As the membrane becomes finer, smaller pollutants can be removed. However, as the membrane becomes finer, flux decreases and the operating pressure must increase. This is a problem for RO due to high costs for pre-treatment to prevent fouling and high operating pressure. The mechanism for removal is sieving and once at the nanoscale (NF, RO and potentially UF) steric and/or charge effects also provide a mechanism for removal¹⁰⁴.

Ameen et al. (2011) showed that MF was capable of removing solids from leachate. Leachate was pretreated using a coagulation process before passing the leachate through a membrane with 0.1 μm surface pores. The turbidity, colour, total suspended solids, total dissolved salts and volatile suspended solids decreased by 98.3, 90.3, 99.63, 14.71 and 20%, respectively. Although this was pretreated leachate, COD should have also been tracked. MF removed a high percentage of solids from the leachate making it useful as a post-treatment after biological treatment. Ameen et al. found that the membrane experienced two types of fouling. The first type was due to buildup of particles on the

surface. The second type of fouling was physical deterioration due to either a high pressure stretching the surface pores or due to some substance in the leachate causing change in the membrane structure. The first type of fouling was reversible using backwash. However, the second type of fouling was irreversible¹⁰¹.

Renou et al. (2009) tested two different ultrafilters for removal of COD. The two membranes were a mineral (CARBOSEP® category) membrane and a ceramic (KERASEP™ category) membrane. The exact specifications of the membranes are found in the study. Two CARBOSEP membranes were used, 10 and 50 kDa MWCO. The removal of COD was 48 and 38%, respectively. Three KERASEP membranes were used, 1, 5 and 15 kDa MWCO. The removal of COD was 66, 63 and 47%, respectively¹⁰⁵.

Trebouet et al. (2001) compared the removal efficiency of two different types of nanofilters, MPT-20 and MPT-31 membranes. MPT-20 and MPT-31 had molecular weight cut-offs (MWCO) of 450 Da. The COD, BOD and SS of the leachate were 500, 7.1 and 130 mg/L, respectively. MPT-20 decreased the COD, BOD and SS by 74, 85 and 100%, respectively. The MPT-31 decreased COD and BOD by 80 and 98% respectively¹⁰⁴. Although, the nanofilters had very high removal of COD and BOD, the leachate had relatively low COD and BOD values before treatment. These results show potential for post-treatment when COD and BOD are low.

RO can be used to remove both organic and inorganic compounds. Rejection coefficients of COD and heavy metals higher than 0.98 and 0.99, respectively, have been reported. Chianese et al. (1999) found that increasing the operating pressure from 20 atm to 53 atm increased the COD removal from 96 to 98%. The COD of the incoming leachate was 3,840 mg/L¹⁰⁶. RO is very effective in leachate treatment but needs high operating pressures and pre-treatment, making it a good candidate for post-treatment or polishing.

2.4 Landfill gas treatment/use

As previously stated the vast majority of landfills employ an anaerobic treatment method. This leads to higher levels of methane in the LFG when compared to aerobic treatment. Due to this, treatments that are used with current landfills may not be applicable/feasible to aerobic landfills. Current treatments fall into four categories: adsorption, absorption, permeation, and cryogenic treatments. The central treatments are: physical adsorption, chemical absorption, pressure swing adsorption, membrane separation and cryogenic separation¹⁰⁷. Landfill gas can also be used in applications such as power generation, as a cheap fuel for ovens/furnaces and with treatment, pipeline quality natural gas.

2.4.1 Quality of LFG

The amount of LFG (and methane) produced depends on the waste composition, age of waste and the amount of waste dumped (available)¹⁰⁸. The quality (amount of methane) of LFG varies with time. A study conducted by Staley et al. (2006) determined the majority of methane was produced within the first 150 days¹⁰⁹. This result was found using 8L reactors, meaning there could be differences in full scale operations. However, the key detail is that there was a significant drop in methane production. This means the majority of methane is produced relatively early in the lifetime of the landfill, this is the optimal time to extract LFG for use. About 50 Nm³ of methane was released per ton of typical MSW and 200 Nm³ released per dry ton of organic waste¹¹⁰. The landfills examined only captured 43 Nm³ of the methane. In addition to CO₂ and CH₄ and depending on the composition of the waste, there can be anywhere from 70 to more than 200 non-methane organic compounds (NMOCs)^{111,112}. The significant contributors to the generation of NMOCs are the intermediates of anaerobic biodegradation¹¹³. This means that aerobic conditions would decrease NMOC levels. Zhang et al. (2012) found that aerobically pretreated MSW decreased the amount of NMOCs produced. They compared 4 tests to a control and found that the 4 tests accounted for 15%, 9%, 16% and 15% of NMOC mass compared to that of the control test. The NMOC emissions levels decreased as the aeration rate increased¹¹⁴.

Powell et al. (2006) found that addition of air into the waste had an impact on the composition of LFG in surrounding wells (15 – 17 m away). They found that the CH₄/CO₂ ratio decreased significantly at 9 of the 12 vertical wells. The reasons proposed were dilution by the air, formation of aerobic conditions and the biological oxidation of the methane. The primary goal of this research was finding the effect of air addition on the trace gas compositions (H₂S, CO, N₂O, and volatile organic compounds, VOCs). Powell et al. found that CO increased, while H₂S decreased. The increase in CO was dramatic, raising concerns over the occurrence of incomplete combustion in the waste. There was no evidence of any change of N₂O and VOCs concentrations¹¹⁵.

2.4.2 LFG recovery

The production of LFG is dependent on a number of variables: volume, organic content, moisture content and age of waste. Moisture content increases production of LFG but too much moisture can block pathways for the escaping LFG, reducing collection efficiency¹¹⁶. The need to determine how much LFG (specifically the methane) is produced has led to numerous numerical and mathematical models using zero order, first order and second order kinetics.

Zero order models are not used because of their lack of fit with empirical data. Second order models are not used because the errors in model parameters add too much uncertainty to be useful for prediction¹¹⁷. First order models are most often used, but they do not model all of the complicated processes occurring in landfill degradation. The two most common models used are the EPA model^{118–122}, and the IPCC model^{123–126}. The EPA model can underestimate the production of LFG^{127,128}, making the choice of the parameters in the model critical. The IPCC model can be effective but the model parameters have to be chosen with consideration¹²⁶.

2.4.3 Use of LFG

This category is not a treatment method; it is an alternative to releasing the LFG to the atmosphere. There are numerous uses for LFG including power generation, energy source

for heating, and pipeline quality gas. In the case of power generation from LFG, pretreatment is relatively basic. Treatment is limited to condensate removal and filtration. More extensive cleaning may be required if there are corrosive or harmful trace constituents¹²⁹. Han et al. found that using LFG for power generation in China, lead to a decrease of approximately 25,000 tonnes of CO₂ in 2009, projecting a maximum decrease in CO₂ of nearly 125,000 tonnes of CO₂ in 2019¹³⁰. The LFG extraction process may become economically unfeasible relatively early in the process. Emissions may not be significant but LFG generation continues for decades after closure. The total emissions after decades can be significant and environmentally harmful. Niskanen found that the best utilization of LFG was combined heat and power production with a heat engine. The LFG is used in a heat engine until it is no longer economically feasible at which point the waste is used for incineration. They showed that it provided the greatest GHG removal compared to proposed alternatives. Incineration however, has been widely reported to be harmful. Anaerobic LFG, on average, has a methane concentration of between 45 and 50% and has approximately half the heating value of natural gas¹³¹.

2.4.4 Flaring

Flaring is the combustion of flammable gases (LFG). Flaring converts the methane in the LFG to carbon dioxide via combustion with oxygen. Depending on the composition (H₂S, N₂) of the LFG, very harmful gases can be released upon combustion (SO_x, NO_x, CO)¹³². Flaring has to be carried out at 1200°C or higher. Lower temperatures risk the formation of toxic compounds like dioxins¹³³. Flaring is very common in landfills that do not capture the LFG for use. LFG with little CH₄ (aerobic and semi-aerobic landfills) cannot be flared without adding methane before combustion. Therefore, this “treatment” method is aimed towards anaerobic LFG.

2.4.5 Adsorption

The two primary constituents that need to be separated in LFG are CO₂ and CH₄. All organic (activated carbons) and inorganic (silica gels, aluminas, zeolites) adsorbents,

selectively adsorb CO_2 over CH_4 . This is due to CO_2 having a larger molecular weight and a permanent quadrupole whereas CH_4 is nonpolar¹³⁴. Since CO_2 is the dominant constituent in aerobic LFG, ideally CH_4 would be adsorbed. However, in industry, virtually all CO_2 - CH_4 separations adsorb CO_2 , not CH_4 . In anaerobic LFG, CO_2 and CH_4 are roughly in equal proportions. Therefore, high concentrations of CH_4 can be produced and used for numerous applications.

Shin et al. (2002) used granular activated carbon to assess the removal of trace compounds and measure the change in adsorption capacity with differing moisture contents in the LFG. The breakthrough time and adsorption capacity of benzene, toluene and ethylbenzene decreased when the relative humidity was greater than 60%. As the moisture decreased, the trace compounds were removed effectively¹³⁵. In bioreactor landfills, there is moisture present in the landfill and as a result present in the LFG. If adsorption is to be used to purify or treat LFG, moisture has to be removed prior to treatment. Adsorption is an attractive LFG treatment method because it is a mature technology. However, LFG is a complex mixture of many trace compounds and the adsorbents (activated carbons, zeolites, metal-organic frameworks) have to be selected appropriately.

2.4.6 Absorption

Absorption can be used to remove CO_2 from LFG. With pretreatment to remove toxic trace components commercial natural gas can be made. Gaur et al. (2010) used a combined adsorption-absorption process to clean LFG. They used activated carbon to remove small amounts of toxic compounds and then absorbed the CO_2 using monoethanol amine (MEA) and diethanol amine (DEA). The MEA had a higher absorption rate than the DEA, but the DEA had a better cyclic capacity. After the second and third cycles, the cyclic capacity of MEA decreased nearly 18% and 9%, respectively. The cyclic capacity of DEA decreased by 10% and 6%. Using a mixture of MEA and DEA could exploit the strengths of both absorbents. The methane obtained using a combined adsorption-absorption was of high enough quality to use as residential natural gas¹³⁶.

2.4.7 Permeation

Permeation is used in the last stages of LFG treatment to remove CO₂, leaving CH₄ remaining. Permeation is the use of a membrane to separate gaseous components¹³⁷. With respect to other treatment methods used for LFG, permeation is not used very often and is not a heavily researched area. Permeation is the superior treatment choice in smaller landfills with LFG production of less than 1000 m³ (STP) h⁻¹¹³⁸. Disadvantages associated with membranes include the mass transfer resistance due to the membrane itself, potential fouling of the membrane especially with LFG, and periodic changing of the membranes¹³⁹.

2.4.8 Cryogenic treatments

This method is also not very widely used because of the high costs associated with cooling to cryogenic temperatures. The LFG has to be compressed and isenthalpically expanded repeatedly to cool down, requiring high amounts of energy. Methanol is injected into the gas forming condensate containing the impurities requiring removal. The condensate is removed and water is added, forming a supernatant layer that can be separated, leaving diluted methanol¹⁴⁰.

2.5 Conclusions

There have been a lot of studies done on leachate treatments. This is evident by the numerous review papers available. However, this is not the case with landfill and LFG treatments. Landfills produce harmful gases and these gases need treatment. In most full scale landfills, the landfill gases are flared. However, this is not a suitable treatment method. Other methods need to be investigated and scaled up to large scale landfills for implementation.

The literature available on aerobic treatment of landfill waste is lacking. It presents a very promising alternative to traditional landfill technologies and as of yet very little research has been done in this area. This presents a promising opportunity for further research in a field that is very much in its infancy. The treatment and use of by-products of aerobic

biodegradation also require extensive research. Another significant finding is the lack of research done on the microbiology of both aerobic and anaerobic landfill bioreactors. Little research has been done on characterizing what microorganisms are responsible for decomposing the landfill waste. Greater understanding can lead to optimization of current treatment practices. A lot of the research that has been done on landfill treatment as a whole (waste, leachate and LFG) has been done on lab scales. Some effort needs to be put into scaling the promising areas of research up, so that eventually this research can make an impact.

This review paper provides a glimpse into the world of landfill treatment. As long as there are humans there will be waste; this waste will always need treatment. There will inevitably come a time when landfills will be problematic. Area is finite and bound to eventually exhaust. Another challenge is the environmental problems that come from leachate and LFG. The long-term effects of these two harmful materials will be known in years to come. One treatment cannot solve all the problems that are associated with landfills; it will take a combination of treatments. The best way to treat these problems is preemptive action, by finding solutions for problems before they occur to lessen the impact. This review encompasses all aspects of the landfill. There is definitely a need for expansion of our knowledge in all aspects of landfills and one aim of this review is pave the way for expansion.

2.6 References

1. United States Environmental Protection Agency. *Municipal Solid Waste Generation, Recycling, and Disposal in the United States: Facts and Figures for 2012*. 2014.
2. Arsova L, van Haaren R, Goldstein N, Kaufman SM, Themelis NJ. The state of garbage in America. *Biocycle*. 2008.
3. Hudgins M, Harper S. Operational characteristics of two aerobic landfill systems. *Paper Presented at The Seventh International Waste Management and Landfill Symposium in Sardinia, Italy, on October 4, 1999*. Sardinia, Italy; 1999.
4. Huber-Humer M, Kjeldsen P, Spokas KA. Special issue on landfill gas emission and mitigation. *Waste Manag*. 2011;31(5):821–2.
5. Bogner J, Pipatti R, Hashimoto S, Diaz C, Mareckova K, Diaz L, et al. Mitigation of global greenhouse gas emissions from waste: conclusions and strategies from the Intergovernmental Panel on Climate Change (IPCC) Fourth Assessment Report. Working Group III (Mitigation). *Waste Manag Res*. 2008;26(1):11–32. Doi: 10.1177/0734242X07088433.
6. Rasmussen RA, Khalil MAK. Atmospheric methane in the recent and ancient atmospheres: Concentrations, trends, and interhemispheric gradient. *J Geophys Res Atmospheres*. 1984;89(D7):11599–605. Doi: 10.1029/JD089iD07p11599.
7. Mehta R, Barlaz M, Yazdani R, Augenstein D, Bryars M, Sinderson L. Refuse decomposition in the presence and absence of leachate recirculation. *J Environ Eng*. 2002;128(3):228–36. Doi: 10.1061/(ASCE)0733-9372(2002)128:3(228).
8. Reinhart DR, McCreanor PT, Townsend T. The bioreactor landfill: Its status and future. *Waste Manag Res*. 2002;20(2):172–86. Doi: 10.1177/0734242X0202000209.

9. Reinhart DR, Townsend T. *Landfill Bioreactor Design and Operation*. New York, NY: Lewis Publishers; 1998.
10. Kulkarni HS, Reddy KR. Moisture distribution in bioreactor landfills: A review. *Indian Geotech J*. 2012;42(3):125–49. Doi: 10.1007/s40098-012-0012-8.
11. Reddy K, Hettiarachchi H, Parakalla N, Gangathulasi J, Bogner J, Lagier T. Hydraulic Conductivity of MSW in Landfills. *J Environ Eng*. 2009;135(8):677–83. Doi: 10.1061/(ASCE)EE.1943-7870.0000031.
12. Jiang J, Yang G, Deng Z, Huang Y, Huang Z, Feng X, et al. Pilot-scale experiment on anaerobic bioreactor landfills in China. *Waste Manag*. 2007;27(7):893–901. Doi: 10.1016/j.wasman.2006.07.008.
13. McCreanor P, Reinhart D. Hydrodynamic modeling of leachate recirculating landfills. *Waste Manag Res*. 1999;17(6):465–9.
14. Westlake K. Sustainable Landfill—Possibility or Pipe-Dream? *Waste Manag Res*. 1997;15(5):453–61. Doi: 10.1177/0734242X9701500502.
15. Wang Y, Pelkonen M, Kaila J. Optimization of landfill leachate management in the aftercare period. *Waste Manag Res*. 2012;30(8):789–99. Doi: 10.1177/0734242X12440483.
16. Méry J, Bayer S. Comparison of external costs between dry tomb and bioreactor landfills: taking intergenerational effects seriously. *Waste Manag Res*. 2005;23(6):514–26. Doi: 10.1177/0734242X05060857.
17. Laner D, Crest M, Scharff H, Morris JWF, Barlaz MA. A review of approaches for the long-term management of municipal solid waste landfills. *Waste Manag*. 2012;32(3):498–512. Doi: 10.1016/j.wasman.2011.11.010.

18. Hirata O, Matsufuji Y, Tachifuji A, Yanase R. Waste stabilization mechanism by a recirculatory semi-aerobic landfill with the aeration system. *J Mater Cycles Waste Manag.* 2012;14(1):47–51. Doi: 10.1007/s10163-011-0036-7.
19. Ritzkowski M, Heyer K-U, Stegmann R. Fundamental processes and implications during in situ aeration of old landfills. *Waste Manag.* 2006;26(4):356–72. Doi: 10.1016/j.wasman.2005.11.009.
20. Benefield JC, Randall SJ. *Biological process design for wastewater treatment.* Prentice-Hall; 1980.
21. Dong J, Sheng H, Wen C, Hong M, Jiang H. Effects of phosphorous on the stabilization of solid waste in anaerobic landfill. *Process Saf Environ Prot.* 2013;91(6):483–8. Doi: 10.1016/j.psep.2012.10.009.
22. Jegatheesan V, Kastl G, Fisher I, Chandy J, Angles M. Modeling bacterial growth in drinking water: effect of nutrients. *Am Water Works Assoc J.* 2004;96(5):129.
23. Miettinen IT, Vartiainen T, Martikainen PJ. Phosphorus and bacterial growth in drinking water. *Appl Environ Microbiol.* 1997;63(8):3242–5.
24. Sathasivan A, Ohgaki S, Yamamoto K, Kamiko N. Role of inorganic phosphorus in controlling regrowth in water distribution system. *Water Sci Technol.* 1997;35(8):37–44. Doi: 10.1016/S0273-1223(97)00149-2.
25. Fielding ER, Archer DB, Macario EC de, Macario AJL. Isolation and characterization of methanogenic bacteria from landfills. *Appl Environ Microbiol.* 1988;54(3):835–6.
26. Ritzkowski M, Stegmann R. Landfill aeration worldwide: Concepts, indications and findings. *Waste Manag.* 2012;32(7):1411–9. Doi: 10.1016/j.wasman.2012.02.020.

27. Leikam K, Heyer K-U, Stegmann R. In situ stabilization of completed landfills and old sites. *Proceedings Sardinia 1997, Sixth International Waste Management and Landfill Symposium*. Cagliari, Italy; 1997.
28. Berge ND, Reinhart DR, Townsend TG. The fate of nitrogen in bioreactor landfills. *Crit Rev Environ Sci Technol*. 2005;35(4):365–99. Doi: 10.1080/10643380590945003.
29. Bonany JE, Geel PJV, Gunay HB, Isgor OB. Simulating waste temperatures in an operating landfill in Québec, Canada. *Waste Manag Res*. 2013;31(7):0734242X13485794. Doi: 10.1177/0734242X13485794.
30. Crutcher AJ, Rovers FA, McBean EA. Temperature as an indicator of landfill behavior. *Water Air Soil Pollut*. 1982;17(2):213–23. Doi: 10.1007/BF00283304.
31. Hettiarachchi H, Meegoda J, Hettiaratchi P. Effects of gas and moisture on modeling of bioreactor landfill settlement. *Waste Manag*. 2009;29(3):1018–25. Doi: 10.1016/j.wasman.2008.08.018.
32. Öncü G, Reiser M, Kranert M. Aerobic in situ stabilization of Landfill Konstanz Dorfweiher: Leachate quality after 1 year of operation. *Waste Manag*. 2012;32(12):2374–84. Doi: 10.1016/j.wasman.2012.07.005.
33. Zanetti MC. Aerobic Biostabilization of Old MSW Landfills. *Am J Eng Appl Sci*. 2008;1(4):393–8. Doi: 10.3844/ajeassp.2008.393.398.
34. Erses AS, Onay TT, Yenigun O. Comparison of aerobic and anaerobic degradation of municipal solid waste in bioreactor landfills. *Bioresour Technol*. 2008;99(13):5418–26. Doi: 10.1016/j.biortech.2007.11.008.
35. Slezak R, Krzystek L, Ledakowicz S. Mathematical model of aerobic stabilization of old landfills. *Chem Pap*. 2012;66(6):543–9. Doi: 10.2478/s11696-012-0133-7.

36. Wu C, Shimaoka T, Nakayama H, Komiya T, Chai X, Hao Y. Influence of aeration modes on leachate characteristic of landfills that adopt the aerobic–anaerobic landfill method. *Waste Manag.* 2014;34(1):101–11. Doi: 10.1016/j.wasman.2013.10.015.
37. Borglin SE, Hazen TC, Oldenburg CM, Zawislanski PT. Comparison of aerobic and anaerobic biotreatment of municipal solid waste. *J Air Waste Manag Assoc.* 2004;54(7):815–22. Doi: 10.1080/10473289.2004.10470951.
38. Vitello C. Aerobic degradation: increasing landfill efficiency. *Solid Waste Recycl.* 2001;6(1):25–7.
39. Bilgili MS, Demir A, Varank G. Effect of leachate recirculation and aeration on volatile fatty acid concentrations in aerobic and anaerobic landfill leachate. *Waste Manag Res.* 2012;30(2):0734242X11417983. Doi: 10.1177/0734242X11417983.
40. Zhang X, Matsuto T. Assessment of internal condition of waste in a roofed landfill. *Waste Manag.* 2013;33(1):102–8. Doi: 10.1016/j.wasman.2012.08.008.
41. Bilgili MS, Demir A, Özkaya B. Influence of leachate recirculation on aerobic and anaerobic decomposition of solid wastes. *J Hazard Mater.* 2007;143(1–2):177–83. Doi: 10.1016/j.jhazmat.2006.09.012.
42. Kallel A, Matsuto T, Tanaka N. Determination of oxygen consumption for landfilled municipal solid wastes. *Waste Manag Res.* 2003;21(4):346–55. Doi: 10.1177/0734242X0302100407.
43. El-Fadel M, Fayyad W, Hashisho J. Enhanced solid waste stabilization in aerobic landfills using low aeration rates and high density compaction. *Waste Manag Res.* 2013;31(1):0734242X12457118. Doi: 10.1177/0734242X12457118.
44. Warith M. Bioreactor landfills: experimental and field results. *Waste Manag.* 2002;22(1):7–17. Doi: 10.1016/S0956-053X(01)00014-9.

45. Yang Y, Yue B, Yang Y, Huang Q. Influence of semi-aerobic and anaerobic landfill operation with leachate recirculation on stabilization processes. *Waste Manag Res.* 2012;0734242X11413328. Doi: 10.1177/0734242X11413328.
46. Tang P, Zhao Y, Liu D. A laboratory study on stabilization criteria of semi-aerobic landfill. *Waste Manag Res.* 2008;26(6):566–72. Doi: 10.1177/0734242X08091341.
47. Huang Q, Yang Y, Pang X, Wang Q. Evolution on qualities of leachate and landfill gas in the semi-aerobic landfill. *J Environ Sci.* 2008;20(4):499–504. Doi: 10.1016/S1001-0742(08)62086-0.
48. Aziz SQ, Aziz HA, Yusoff MS, Bashir MJK, Umar M. Leachate characterization in semi-aerobic and anaerobic sanitary landfills: A comparative study. *J Environ Manage.* 2010;91(12):2608–14. Doi: 10.1016/j.jenvman.2010.07.042.
49. Kumar S, Chiemchaisri C, Mudhoo A. Bioreactor landfill technology in municipal solid waste treatment: An overview. *Crit Rev Biotechnol.* 2010;31(1):77–97. Doi: 10.3109/07388551.2010.492206.
50. Green LC. *A method and system for treating biodegradable waste material through aerobic degradation.* Google Patents; 1998.
51. Yazdani R, Mostafid ME, Han B, Imhoff PT, Chiu P, Augenstein D, et al. Quantifying Factors Limiting Aerobic Degradation During Aerobic Bioreactor Landfilling. *Environ Sci Technol.* 2010;44(16):6215–20. Doi: 10.1021/es1022398.
52. Rendra S, Warith MA, Fernandes L. Degradation of Municipal Solid Waste in Aerobic Bioreactor Landfills. *Environ Technol.* 2007;28(6):609–20. Doi: 10.1080/09593332808618822.
53. Wadkar DV, Modak PR, Chavan VS. Aerobic thermophilic composting of municipal solid waste. *Int J Eng Sci Technol.* 2013;5(3):716–8.

54. Senior E. *Microbiology of landfill site*. Second. Boca Raton: Lewis Publishers; 1995.
55. Renou S, Givaudan JG, Poulain S, Dirassouyan F, Moulin P. Landfill leachate treatment: Review and opportunity. *J Hazard Mater*. 2008;150(3):468–93. Doi: 10.1016/j.jhazmat.2007.09.077.
56. Lu JCS, Eichenberger B, Stearns RJ. *Leachate from Municipal Landfills: Production and Management*. Park Ridge, NJ: Noyes Publications; 1985.
57. Vadillo I, Carrasco F, Andreo B, Torres AG de, Bosch C. Chemical composition of landfill leachate in a karst area with a Mediterranean climate (Marbella, southern Spain). *Environ Geol*. 1999;37(4):326–32. Doi: 10.1007/s002540050391.
58. Hudgins MP, March J. In-Situ solid waste composting using an aerobic landfill system. *Oral Presentation to Conference Attendees Composting in the Southeast*. 1998.
59. Wiszniowski J, Robert D, Surmacz-Gorska J, Miksch K, Weber JV. Landfill leachate treatment methods: A review. *Environ Chem Lett*. 2006;4(1):51–61. Doi: 10.1007/s10311-005-0016-z.
60. Dhokpande SR, Kaware JP. Biological methods for heavy metal removal: A review. *Int J Eng Sci Innov Technol*. 2013;2(5):304–9.
61. Rivas FJ, Beltrán F, Carvalho F, Acedo B, Gimeno O. Stabilized leachates: sequential coagulation–flocculation + chemical oxidation process. *J Hazard Mater*. 2004;116(1–2):95–102. Doi: 10.1016/j.jhazmat.2004.07.022.
62. Berrueta J, Castrillón L. Anaerobic treatment of leachates in UASB reactors. *J Chem Technol Biotechnol*. 1992;54(1):33–7. Doi: 10.1002/jctb.280540107.
63. Chang JE. Treatment of landfill leachate with an upflow anaerobic reactor containing a sludge bed and a filter. *Water Sci Technol*. 1989;21:133–43.

64. Henry JG, Prasad D, Young H. Removal of organics from leachates by anaerobic filter. *Water Res.* 1987;21(11):1395–9.
65. Kennedy KJ, Hamoda MF, Guiot SG. Anaerobic treatment of leachate using fixed film and sludge bed filter systems. *J Water Pollut Control Fed.* 1988;60(9):1675–83.
66. Timur H, Öztürk I. Anaerobic sequencing batch reactor treatment of landfill leachate. *Water Res.* 1999;33(15):3225–30. Doi: 10.1016/S0043-1354(99)00048-2.
67. Cameron RD, Koch FA. Trace metals and anaerobic digestion of leachate. *J Water Pollut Control Fed.* 1980;52(2):282–92.
68. Kheradmand S, Karimi-Jashni A, Sartaj M. Treatment of municipal landfill leachate using a combined anaerobic digester and activated sludge system. *Waste Manag.* 2010;30(6):1025–31. Doi: 10.1016/j.wasman.2010.01.021.
69. Kim H, Jang Y-C, Townsend T. The behavior and long-term fate of metals in simulated landfill bioreactors under aerobic and anaerobic conditions. *J Hazard Mater.* 2011;194:369–77. Doi: 10.1016/j.jhazmat.2011.07.119.
70. Robinson HD, Barr MJ. Aerobic biological treatment of landfill leachates. *Waste Manag Res.* 1999;17(6):478–86.
71. Giannis A, Makripodis G, Simantiraki F, Somara M, Gidaracos E. Monitoring operational and leachate characteristics of an aerobic simulated landfill bioreactor. *Waste Manag.* 2008;28(8):1346–54. Doi: 10.1016/j.wasman.2007.06.024.
72. Liu Y. Chemically reduced excess sludge production in the activated sludge process. *Chemosphere.* 2003;50(1):1–7. Doi: 10.1016/S0045-6535(02)00551-9.
73. Bilgili MS, Demir A, Özkaya B. Quality and Quantity of Leachate in Aerobic Pilot-Scale Landfills. *Environ Manage.* 2006;38(2):189–96.

74. Sartaj M, Ahmadifar M, Jashni AK. Assessment of in-situ aerobic treatment of municipal landfill leachate at laboratory scale. *Iran J Sci Technol Trans B Eng.* 2010;34(B1):107–16.
75. Wei Y, Ji M, Li R, Qin F. Organic and nitrogen removal from landfill leachate in aerobic granular sludge sequencing batch reactors. *Waste Manag.* 2012;32(3):448–55.
76. Yahmed AB, Saidi N, Trabelsi I, Murano F, Dhaifallah T, Bousselmi L, et al. Microbial characterization during aerobic biological treatment of landfill leachate (Tunisia). *Desalination.* 2009;246(1-3):378–88.
77. Andrés P, Gutierrez F, Arrabal C, Cortijo M. Aerobic Biological Treatment of Leachates from Municipal Solid Waste Landfill. *J Environ Sci Health Part A.* 2004;39(5):1319–28.
78. Bilgili MS, Demir A, Akkaya E, Özkaya B. COD fractions of leachate from aerobic and anaerobic pilot scale landfill reactors. *J Hazard Mater.* 2008;158(1):157–63.
79. Kamaruddin MA, Yusoff MS, Aziz HA, Basri NK. Removal of COD, ammoniacal nitrogen and colour from stabilized landfill leachate by anaerobic organism. *Appl Water Sci.* 2013;3(2):359–66.
80. Thabet OBD, Bouallagui H, Cayol J, Ollivier B, Fardeau M-L, Hamdi M. Anaerobic degradation of landfill leachate using an upflow anaerobic fixed-bed reactor with microbial sulfate reduction. *J Hazard Mater.* 2009;167(1-3):1133–40.
81. David R. Environmental microbiology: Deciphering anammox. *Nat Rev Microbiol.* 2011;9(12):833. Doi: <http://dx.doi.org.proxy1.lib.uwo.ca/10.1038/nrmicro2699>.
82. Kartal B, Maalcke WJ, de Almeida NM, Cirpus I, Gloerich J, Geerts W, et al. Molecular mechanism of anaerobic ammonium oxidation. *Nature.* 2011;479(7371):127–30. Doi: 10.1038/nature10453.

83. Strous M, Van Gerven E, Zheng P, Kuenen JG, Jetten MSM. Ammonium removal from concentrated waste streams with the anaerobic ammonium oxidation (Anammox) process in different reactor configurations. *Water Res.* 1997;31(8):1955–62. Doi: 10.1016/S0043-1354(97)00055-9.
84. Kartal B, Kuenen JG, Loosdrecht MCM van. Sewage Treatment with Anammox. *Science.* 2010;328(5979):702–3. Doi: 10.1126/science.1185941.
85. Cema G, Wiszniewski J, Żabczyński S, Zabłocka-Godlewska E, Raszka A, Surmacz-Górska J. Biological nitrogen removal from landfill leachate by deammonification assisted by heterotrophic denitrification in a rotating biological contactor (RBC). *Water Sci Technol.* 2007;55(8-9):35–42. Doi: 10.2166/wst.2007.239.
86. Liu S, Yang F, Meng F, Chen H, Gong Z. Enhanced anammox consortium activity for nitrogen removal: Impacts of static magnetic field. *J Biotechnol.* 2008;138(3-4):96–102.
87. Qiao S, Yin X, Zhou J, Furukawa K. Inhibition and recovery of continuous electric field application on the activity of anammox biomass. *Biodegradation.* 2014;25(4):505–13.
88. Duan X, Zhou J, Qiao S, Wei H. Application of low intensity ultrasound to enhance the activity of anammox microbial consortium for nitrogen removal. *Bioresour Technol.* 2011;102(5):4290–3.
89. Marañón E, Castrillón L, Fernández-Nava Y, Fernández-Méndez A, Fernández-Sánchez A. Tertiary treatment of landfill leachates by adsorption. *Waste Manag Res.* 2009;27(5):527–33. Doi: 10.1177/0734242X08096900.
90. Malliou E, Loizidou M, Spyrellis N. Uptake of lead and cadmium by clinoptilolite. *Sci Total Environ.* 1994;149(3):139–44. Doi: 10.1016/0048-9697(94)90174-0.

91. Davis ME, Lobo RF. Zeolite and molecular sieve synthesis. *Chem Mater.* 1992;4(4):756–68. Doi: 10.1021/cm00022a005.
92. Zamzow MJ, Eichbaum BR, Sandgren KR, Shanks DE. Removal of Heavy Metals and Other Cations from Wastewater Using Zeolites. *Sep Sci Technol.* 1990;25(13-15):1555–69. Doi: 10.1080/01496399008050409.
93. Marco A, Esplugas S, Saum G. How and why combine chemical and biological processes for wastewater treatment. *Water Sci Technol.* 1997;35(4):321–7. Doi: 10.1016/S0273-1223(97)00041-3.
94. Derco J. Pretreatment of landfill leachate by chemical oxidation processes. *Chem Pap.* 2010;64(2):237–45.
95. Boumechhour F, Rabah K, Lamine C, Said BM. Treatment of landfill leachate using Fenton process and coagulation/flocculation. *Water Environ J.* 2013;27(1):114–9.
96. Samadi MT, Saghi MH, Rahmani A, Hasanvand J, Rahimi S, Syboney MS. Hamadan landfill leachate treatment by coagulation-flocculation process. *Iran J Environ Health Sci Eng.* 2010;7(3):253–8.
97. Tatsi AA, Zouboulis AI, Matis KA, Samaras P. Coagulation–flocculation pretreatment of sanitary landfill leachates. *Chemosphere.* 2003;53(7):737–44. Doi: 10.1016/S0045-6535(03)00513-7.
98. Amokrane A, Comel C, Veron J. Landfill leachates pretreatment by coagulation-flocculation. *Water Res.* 1997;31(11):2775–82. Doi: 10.1016/S0043-1354(97)00147-4.
99. Ghafari S, Aziz HA, Isa MH, Zinatizadeh AA. Application of response surface methodology (RSM) to optimize coagulation–flocculation treatment of leachate using poly-aluminum chloride (PAC) and alum. *J Hazard Mater.* 2009;163(2–3):650–6. Doi: 10.1016/j.jhazmat.2008.07.090.

100. Ntampou X, Zouboulis AI, Samaras P. Appropriate combination of physico-chemical methods (coagulation/flocculation and ozonation) for the efficient treatment of landfill leachates. *Chemosphere*. 2006;62(5):722–30. Doi: 10.1016/j.chemosphere.2005.04.067.
101. Ameen E, Muyibi S, Abdulkarim M. Microfiltration of pretreated sanitary landfill leachate. *The Environmentalist*. 2011;31(3):208–15. Doi: 10.1007/s10669-011-9322-0.
102. Primo O, Rueda A, Rivero MJ, Ortiz I. An Integrated Process, Fenton Reaction–Ultrafiltration, for the Treatment of Landfill Leachate: Pilot Plant Operation and Analysis. *Ind Eng Chem Res*. 2008;47(3):946–52. Doi: 10.1021/ie071111a.
103. Vandezande P, Gevers LEM, Vankelecom IFJ. Solvent resistant nanofiltration: separating on a molecular level. *Chem Soc Rev*. 2008;37(2):365–405.
104. Trebouet D, Schlumpf JP, Jaouen P, Quemeneur F. Stabilized landfill leachate treatment by combined physicochemical–nanofiltration processes. *Water Res*. 2001;35(12):2935–42. Doi: 10.1016/S0043-1354(01)00005-7.
105. Renou S, Poulain S, Givaudan JG, Moulin P. Amelioration of ultrafiltration process by lime treatment: Case of landfill leachate. *Desalination*. 2009;249(1):72–82. Doi: 10.1016/j.desal.2008.09.007.
106. Chianese A, Ranauro R, Verdone N. Treatment of landfill leachate by reverse osmosis. *Water Res*. 1999;33(3):647–52. Doi: 10.1016/S0043-1354(98)00240-1.
107. Rajaram V, Siddiqui FZ, Khan ME. Landfill gas treatment technologies. *From landfill gas to energy technologies and challenges*. Leiden, The Netherlands: CRC/Balkema; 2012. p. 153–208.

108. Mor S, Ravindra K, De Visscher A, Dahiya RP, Chandra A. Municipal solid waste characterization and its assessment for potential methane generation: A case study. *Sci Total Environ.* 2006;371(1–3):1–10. Doi: 10.1016/j.scitotenv.2006.04.014.
109. Staley BF, Xu F, Cowie SJ, Barlaz MA, Hater GR. Release of Trace Organic Compounds during the Decomposition of Municipal Solid Waste Components. *Environ Sci Technol.* 2006;40(19):5984–91. Doi: 10.1021/es060786m.
110. Themelis NJ, Ulloa PA. Methane generation in landfills. *Renew Energy.* 2007;32(7):1243–57. Doi: 10.1016/j.renene.2006.04.020.
111. Allen MR, Braithwaite A, Hills CC. Trace organic compounds in landfill Gas at seven U.K. waste disposal sites. *Environ Sci Technol.* 1997;31(4):1054–61. Doi: 10.1021/es9605634.
112. Eklund B, Anderson EP, Walker BL, Burrows DB. Characterization of landfill gas composition at the Fresh Kills Municipal Solid-Waste Landfill. *Environ Sci Technol.* 1998;32(15):2233–7. Doi: 10.1021/es980004s.
113. Thomas CL, Barlaz MA. Production of non-methane organic compounds during refuse decomposition in a laboratory-scale landfill. *Waste Manag Res.* 1999;17(3):205–11. Doi: 10.1034/j.1399-3070.1999.00030.x.
114. Zhang Y, Yue D, Liu J, Lu P, Wang Y, Liu J, et al. Release of non-methane organic compounds during simulated landfilling of aerobically pretreated municipal solid waste. *J Environ Manage.* 2012;101:54–8. Doi: 10.1016/j.jenvman.2011.10.018.
115. Powell J, Jain P, Kim H, Townsend T, Reinhart D. Changes in Landfill Gas Quality as a Result of Controlled Air Injection. *Environ Sci Technol.* 2006;40(3):1029–34. Doi: 10.1021/es051114j.

116. Goossens MA. Landfill gas power plants. *Renew Energy*. 1996;9(1–4):1015–8. Doi: 10.1016/0960-1481(96)88452-7.
117. Aguilar-Virgen Q, Taboada-González P, Ojeda-Benítez S. Analysis of the feasibility of the recovery of landfill gas: a case study of Mexico. *J Clean Prod*. 2014;79:53–60. Doi: 10.1016/j.jclepro.2014.05.025.
118. Chiemchaisri C, Juanga JP, Visvanathan C. Municipal solid waste management in Thailand and disposal emission inventory. *Environ Monit Assess*. 2007;135(1-3):13–20. Doi: 10.1007/s10661-007-9707-1.
119. Faour AA, Reinhart DR, You H. First-order kinetic gas generation model parameters for wet landfills. *Waste Manag*. 2007;27(7):946–53. Doi: 10.1016/j.wasman.2006.05.007.
120. Garg A, Achari G, Joshi RC. A model to estimate the methane generation rate constant in sanitary landfills using fuzzy synthetic evaluation. *Waste Manag Res*. 2006;24(4):363–75. Doi: 10.1177/0734242X06065189.
121. Machado SL, Carvalho MF, Gourc J-P, Vilar OM, do Nascimento JCF. Methane generation in tropical landfills: Simplified methods and field results. *Waste Manag*. 2009;29(1):153–61. Doi: 10.1016/j.wasman.2008.02.017.
122. Wanichpongpan W, Gheewala SH. Life cycle assessment as a decision support tool for landfill gas-to energy projects. *J Clean Prod*. 2007;15(18):1819–26. Doi: 10.1016/j.jclepro.2006.06.008.
123. Abushammala MFM, Basri NEA, Basri H, Kadhum AAH, El-Shafie AH. Estimation of methane emission from landfills in Malaysia using the IPCC 2006 FOD model. *J Appl Sci*. 2010;10(15):1603–9. Doi: 10.3923/jas.2010.1603.1609.

124. Börjesson G, Samuelsson J, Chanton J, Adolfsson R, Galle B, Svensson BH. A national landfill methane budget for Sweden based on field measurements, and an evaluation of IPCC models. *Tellus B*. 2009;61(2):424–35. Doi: 10.1111/j.1600-0889.2008.00409.x.
125. Heyer K-U, Hupe K, Stegmann R. Methane emissions from MBT landfills. *Waste Manag*. 2013;33(9):1853–60. Doi: 10.1016/j.wasman.2013.05.012.
126. Penteado R, Cavalli M, Magnano E, Chiampo F. Application of the IPCC model to a Brazilian landfill: First results. *Energy Policy*. 2012;42(1):551–6. Doi: 10.1016/j.enpol.2011.12.023.
127. Amini HR, Reinhart DR, Mackie KR. Determination of first-order landfill gas modeling parameters and uncertainties. *Waste Manag*. 2012;32(2):305–16. Doi: 10.1016/j.wasman.2011.09.021.
128. Tintner J, Kühleitner M, Binner E, Brunner N, Smidt E. Modeling the final phase of landfill gas generation from long-term observations. *Biodegradation*. 2012;23(3):407–14. Doi: 10.1007/s10532-011-9519-4.
129. Brown KA, Maunder DH. Exploitation of landfill gas: A UK perspective. *Water Sci Technol*. 1994;30(12):143–51.
130. Han H, Long J, Li S, Qian G. Comparison of green-house gas emission reductions and landfill gas utilization between a landfill system and an incineration system. *Waste Manag Res*. 2010;28(4):315–21. Doi: 10.1177/0734242X09349761.
131. Jewaskiewitz B. Landfill gas recovery, green energy, and the clean development mechanism. *Civ Eng Mag South Afr Inst Civ Eng*. 2010;18(7):19–23.
132. Solov'yanov AA. Associated petroleum gas flaring: Environmental issues. *Russ J Gen Chem*. 2011;81(12):2531–41. Doi: 10.1134/S1070363211120218.

133. Ménard C, Ramirez AA, Nikiema J, Heitz M. Biofiltration of methane and trace gases from landfills: A review. *Environ Rev.* 2012;20(1):40–53. Doi: 10.1139/a11-022.
134. Sircar S. Separation of methane and carbon dioxide gas mixtures by pressure swing adsorption. *Sep Sci Technol.* 1988;23(6-7):519–29. Doi: 10.1080/01496398808057650.
135. Shin H-C, Park J-W, Park K, Song H-C. Removal characteristics of trace compounds of landfill gas by activated carbon adsorption. *Environ Pollut.* 2002;119(2):227–36. Doi: 10.1016/S0269-7491(01)00331-1.
136. Gaur A, Park J-W, Maken S, Song H-J, Park J-J. Landfill gas (LFG) processing via adsorption and alkanolamine absorption. *Fuel Process Technol.* 2010;91(6):635–40. Doi: 10.1016/j.fuproc.2010.01.010.
137. Koros WJ, Fleming GK. Membrane-based gas separation. *J Membr Sci.* 1993;83(1):1–80. Doi: 10.1016/0376-7388(93)80013-N.
138. Rautenbach R, Welsch K. Treatment of landfill gas by gas permeation — pilot plant results and comparison to alternatives. *J Membr Sci.* 1994;87(1–2):107–18. Doi: 10.1016/0376-7388(93)E0091-Q.
139. Gabelman A, Hwang S-T. Hollow fiber membrane contactors. *J Membr Sci.* 1999;159(1–2):61–106. Doi: 10.1016/S0376-7388(99)00040-X.
140. Markbreiter SJ, Weiss I. Cryogenic treatment of landfill gas to remove troublesome compounds. US5596884 A, 1997.

Chapter 3

3 The mathematical model of the conversion of a landfill operation from anaerobic to aerobic

Transport phenomena equations were applied to develop a dynamic mathematical model that accurately describes the conversion of an anaerobic landfill to an aerobic bioreactor. The model equations were solved using the finite element method with the commercially available software COMSOL Multiphysics®. The initial aerobic bacteria concentration and heat of reaction were fitted with values in the range reported in the literature. The consumption rate of oxygen and production rates of carbon dioxide and methane and growth rate of aerobic biomass were examined at a biomass concentration of 0.6 kg/m^3 , at full scale landfill biomass concentration of 1 kg/m^3 and with a high biomass concentration of 10 kg/m^3 . The bioreactor configuration used in the model showed biodegradation occurred in “plugs”. Varying leachate injection rate was shown to be more effective for temperature control than the rate of air injection. This model provides a framework to determine how other factors such as pH or moisture content affect the conversion from anaerobic to aerobic conditions.

3.1 Introduction

Effective treating of municipal solid waste (MSW) reduces the potential harm from leachate and landfill gas (LFG). In order to increase the rate of biodegradation of the MSW, recirculation of leachate has been shown effective in promoting microbial growth. The biodegradation rate is further increased by aeration of the landfill body, promoting aerobic microbial growth¹. Aerobic bioreactor landfills use aerobic bacteria to biodegrade the landfill waste. Traditional landfills use the “dry-tomb” method, where the landfill is essentially used for waste containment without treating. The dry-tomb method theoretically disallows moisture, inhibiting microbial growth and decomposition². However, dry-tomb landfills cannot prevent moisture from infiltrating the landfill. This causes slow biodegradation, producing harmful leachate and LFG (primarily methane and carbon

dioxide). The bioreactor landfill instead promotes microbial biodegradation by recirculating the leachate produced³.

Bioreactor landfills fall into three categories: aerobic, anaerobic and semi-aerobic. This study is focused on aerobic bioreactor landfills. The procedure and development of the model could be slightly modified to represent anaerobic/semi-aerobic bioreactor landfills. Aerobic bioreactor landfills have many advantages over other landfill types. These advantages include: faster waste stabilization, decrease of CO₂ equivalent release of greenhouse gases (GHGs), decrease in non-methane organic compounds (NMOCs), faster reduction in chemical oxygen demand (COD) of leachate⁴⁻⁶.

Due to the porous nature of the waste, the injection/extraction of gases, the injection of leachate and the exothermic nature of the biodegradation, the transport phenomena occurring inside an aerobic landfill are complex. Many models have been developed on landfills (both dry-tomb and bioreactor landfills). These models represent various aspects of landfills. Models have been reported on anaerobic bioreactor landfills^{7,8} and aerobic bioreactor landfills⁹⁻¹³. Various approaches have also been proposed to model flows through landfills¹⁴⁻¹⁸. Other models describing other phenomena such as landfill settlement¹⁹, pressure distribution due to landfill gas in landfill²⁰ and gas production²¹⁻²³ have also been formulated. Many of these models are formulated using 1 or 2 space dimensions and often only looking at steady-state behaviour.

Once a landfill is closed, there is enough oxygen to sustain aerobic bacteria for a short time. After the oxygen is consumed, the aerobic bacteria gradually perish, giving way to the anaerobic bacteria, which begin to dominate. If the landfill is left isolated, the aerobic bacteria consume the trapped oxygen and die once the oxygen is consumed. The landfill will then become anaerobic.

In this study, a theoretical dynamic 3-dimensional model is developed that represents the conversion of an anaerobic bioreactor landfill into an aerobic bioreactor landfill at the onset of aeration of the landfill. Changing the parameters of an aerobic landfill and measuring

the outcome experimentally can take anywhere from a month to a year whereas changing a parameter on a validated model and studying the outcome can be done in less than a week. These parameters include temperature of the landfill, oxygen injection rate, pH and moisture content of the landfill material⁶. Also, models can provide insight that experimental data cannot provide. For example, the model can be run under conditions that are not physically realizable.

3.2 Theory and computation technique

The model equations were solved using the finite element method (FEM). The equations were solved using the commercially available software COMSOL Multiphysics. Two Darcy's Law interfaces were used for each phase (gas and liquid). The two phases were coupled using a storage model node. A transport of concentrated species interface was used to define the composition of the gaseous components. A heat transfer in porous media interface was used to define the energy balance and temperature of the bioreactor. Finally, the biokinetic equations were not included by default in COMSOL Multiphysics, and user-defined ordinary differential equations were added defining the anaerobic and aerobic biomass growth rate equations. All the parameters used in the model (Table 3-1 and Table 3-2) were defined as global parameters. All the algebraic equations used (e.g. the rates of consumption/production, diffusion coefficients) were defined as component variables. Figure 3-1 shows a flow diagram that outlines the steps used for the model development.

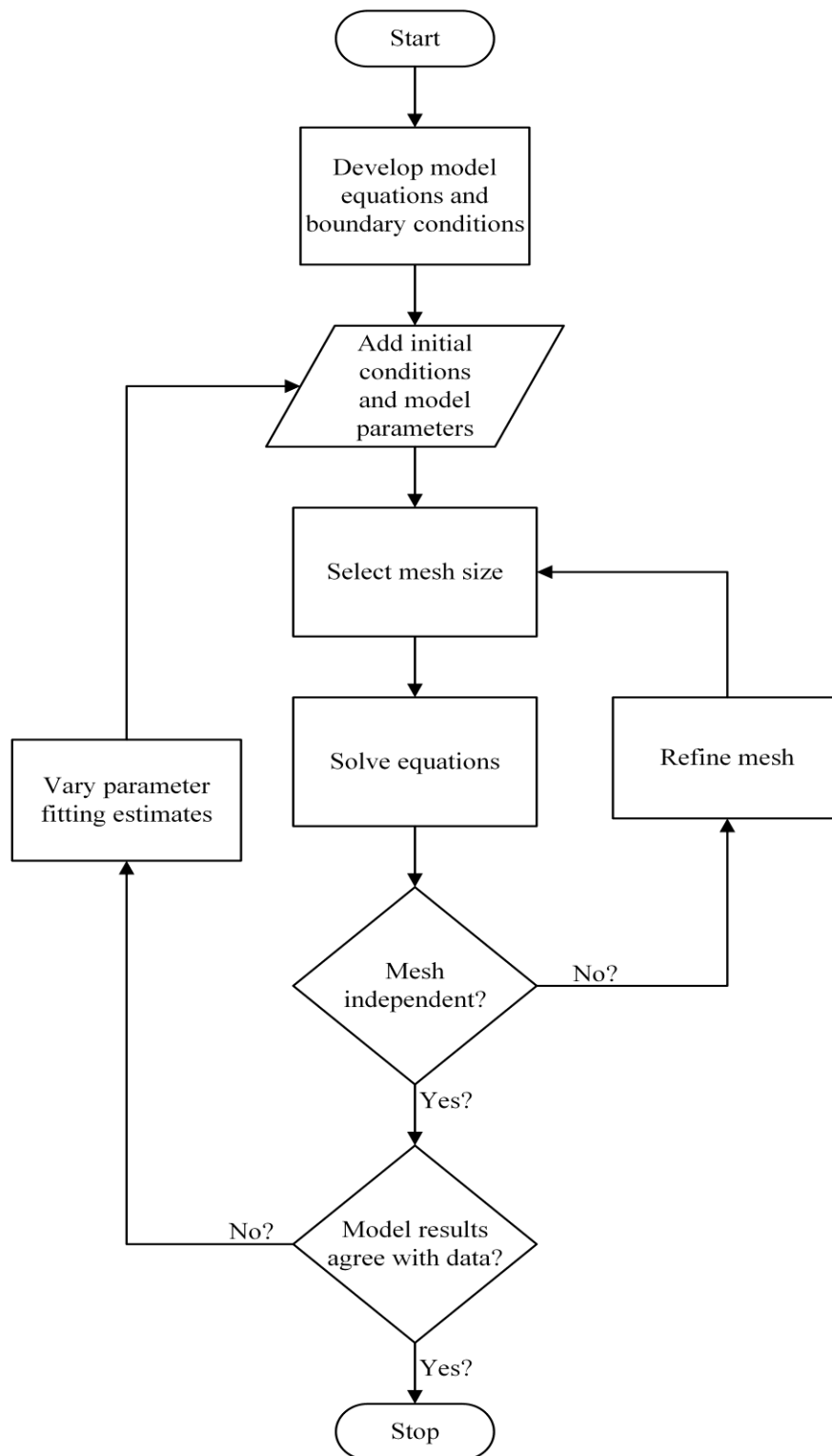


Figure 3-1 Flowchart showing model formulation steps

The following model equations describe the gaseous and leachate flow through the MSW. Air is injected from the bottom of the bioreactor and flows upwards towards the gas exit at the top of the bioreactor. Leachate is injected from the top of the bioreactor and flows downwards towards the leachate collection port at the bottom of the bioreactor. Figure 3-2(a) shows a schematic representation of the bioreactor. Initially, the bioreactor is under anaerobic conditions and as the air is injected, the anaerobic bacteria begin to perish and the aerobic bacteria grow and consume the oxygen, producing carbon dioxide. The composition of the gas changes as it flows through the bioreactor, both spatially and temporally. The aerobic biodegradation is exothermic. The rate of aerobic bacterial growth is coupled with the temperature. The model also describes the changing temperature of the MSW, spatially and temporally.

3.2.1 Momentum balance

Two Darcy's Law equations were formulated to describe the pressure inside of the bioreactor. The Darcy's Law equations were modified to include terms to account for the unsaturated flow (pores are not saturated by either fluid phase) inside the bioreactor^{24,25}.

Darcy's Law for liquid phase:

$$\rho_a S_c \frac{\partial P_a}{\partial t} + \nabla \cdot \rho_a \left[-\frac{\kappa k_{r,a}}{\mu_a} (\nabla P_a + \rho_a g \nabla z) \right] = \rho_a S_c \frac{\partial P_g}{\partial t} \quad (3-1)$$

Darcy's Law for gaseous phase:

$$\rho_g S_c \frac{\partial P_g}{\partial t} + \nabla \cdot \rho_g \left[-\frac{\kappa k_{r,g}}{\mu_g} (\nabla P_g + \rho_g g \nabla z) \right] = \rho_g S_c \frac{\partial P_a}{\partial t} \quad (3-2)$$

Where ρ_a is the density of the aqueous phase [kg/m³], S_c is the specific capacity of the MSW [1/Pa], P_a is the pressure of aqueous phase [Pa], κ is the intrinsic permeability of the MSW [m²], $k_{r,a}$ is the relative permeability of the aqueous phase [-], μ_a is the dynamic

viscosity of the aqueous phase [Pa·s], g is the gravitational acceleration constant [m/s²], z is the coordinate of vertical elevation [m], P_g is the pressure of the gaseous phase [Pa], ρ_g is the density of the gaseous phase [kg/m³], $k_{r,g}$ is the relative permeability of the gaseous phase [-] and μ_g is the dynamic viscosity of the gaseous phase [Pa·s].

$$S_c = (\phi_r - \phi_s) \frac{\partial S_{e,a}}{\partial P_c} \quad (3-3)$$

$$P_c = -\frac{\rho_a g}{\alpha} \left(\left(\frac{1}{S_{e,a}} \right)^{1/\gamma-1} \right)^{1/\beta} \quad (3-4)$$

$$\rho_g = \sum_i \omega_i \rho_i \quad (3-5)$$

$$\mu_g = \sum_i \omega_i \mu_i \quad (3-6)$$

ϕ_r is the residual volume fraction [-], ϕ_s is the total porosity or saturated volume fraction [-], $S_{e,a}$ is the effective saturation of the aqueous phase [-], P_c is capillary pressure [Pa], α [1/m], β [-] and γ [-] are the van Genuchten constants, ω_i is the mass fraction of component i [-], ρ_i is the density of component i [kg/m³] and μ_i is the dynamic viscosity of component i [Pa·s].

$$H_c = \frac{P_c}{\rho_a g} \quad (3-7)$$

Where H_c is the capillary pressure head [m].

$$S_{e,a} = \frac{a_w - a_{wr}}{a_{ws} - a_{wr}} \quad (3-8)$$

$$S_{e,g} = 1 - S_{e,a} \quad (3-9)$$

$S_{e,g}$ is the effective saturation of the gaseous phase [-], a_w is the volume fraction of the aqueous phase [m^3/m^3], a_{wr} is residual saturation of water [m^3/m^3] and a_{ws} is the saturation water content [m^3/m^3]. The numerical values of the parameters used in the previous equations are found in Table 3-2.

For the aqueous phase:

$$k_{r,a} = S_{e,a}^{0.5} (1 - (1 - S_{e,a}^{1/\gamma})^\gamma) \quad (3-10)$$

For the gas phase:

$$k_{r,g} = S_{e,g}^{0.5} (1 - (1 - S_{e,g}^{1/\gamma})^{2\gamma}) \quad (3-11)$$

3.2.2 Mass balance

Equations 3-12, 3-13 and 3-14 are the continuity equation, Darcy's velocity and component mass balance in the gas phase, respectively²⁸. Equations 3-12 and 3-13 are formulated for each phase.

$$\frac{\partial(\phi_s \rho)}{\partial t} + \nabla \cdot (\rho \mathbf{u}) = Q_m \quad (3-12)$$

$$\mathbf{u} = -\frac{\kappa}{\mu} (\nabla P + \rho g \nabla z) \quad (3-13)$$

\mathbf{u} is velocity vector [m/s], Q_m is the source term mass flow rate [$\text{kg}/\text{m}^3/\text{s}$] and P is the pressure [Pa]. Table 3-2 provides the physical properties of the MSW used in the model equations.

$$\rho \frac{\partial \omega_i}{\partial t} + \nabla \cdot \mathbf{j}_i + \rho(\mathbf{u} \cdot \nabla) \omega_i = R_i \quad (3-14)$$

Where \mathbf{j}_i is the mass flux relative to the mass averaged velocity of component i [kg/m²/s] and R_i is the rate of consumption/production of component i [kg/m³/s].

$$\mathbf{j}_i = - \left(\rho D_i^F \nabla \omega_i + \rho \omega_i D_i^F \frac{\nabla M_n}{M_n} \right) \quad (3-15)$$

D_i^F is the Fickian diffusion coefficient of component i [m²/s], M_n is the average molecular weight [kg/mol].

The multicomponent Fickian diffusion coefficients were estimated using the following relationship³⁰:

$$D_i^F = \frac{1 - x_i}{\sum_{j, j \neq i} \frac{x_j}{D_{ij}}} \quad (3-16)$$

D_{ij} is the binary Fickian diffusion coefficient of components i and j [m²/s], x_i is the mole fraction of component i [-] and x_j is the mole fraction of component j [-].

The binary diffusion coefficients can be found using the Chapman-Enskog equation³¹:

$$D_{ij} = \frac{5.953 \times 10^{-4}}{P \sigma_{ij}^2 \Omega_D} \sqrt{\frac{T^3}{M_i} + \frac{T^3}{M_j}} \quad (3-17)$$

σ_{ij} is the average collision diameter of components i and j [m], Ω_D is the collision integral [-], T is the temperature of the MSW [K], M_i is the molecular mass of component i

[kg/mol] and M_j is the molecular mass of component j [kg/mol]. The parameters used in the Chapman-Enskog Equation are found in Table 3-1.

$$\sigma_{ij} = \frac{\sigma_i + \sigma_j}{2} \quad (3-18)$$

σ_i is the collision diameter of component i [m] and σ_j is the collision diameter of components j [m].

$$\Omega_D = \frac{1.060}{T_N^{0.156}} + \frac{0.193}{e^{0.476T_N}} + \frac{1.036}{e^{1.530T_N}} + \frac{1.765}{e^{3.894T_N}} \quad (3-19)$$

T_N is the standardized temperature [-].

$$T_N = \frac{T}{\sqrt{\frac{\varepsilon_i}{k_{b,i}} \sqrt{\frac{\varepsilon_j}{k_{b,j}}}}} \quad (3-20)$$

T is the model temperature, ε_i is the characteristic energy of component i [J], ε_j is the characteristic energy of component j [J], $k_{b,i}$ is the Boltzman's constant of component i [J/K] and $k_{b,j}$ is the Boltzman's constant of component j [J/K].

Table 3-1 Fickian diffusion estimation parameters

	Collision diameter, σ (10^{-10} m)	Characteristic energy, ε/k_b (K)	Reference
oxygen	3.476	106.7	
nitrogen	3.798	71.4	32
carbon dioxide	3.941	195.2	
methane	3.758	148.6	

$$M_n = \left(\sum_i \frac{\omega_i}{M_i} \right)^{-1} \quad (3-21)$$

$$\mathbf{N}_i = \mathbf{j}_i + \rho \mathbf{u} \omega_i \quad (3-22)$$

\mathbf{N}_i is the combined mass flux of component i [$\text{kg}/\text{m}^2/\text{s}$].

Biokinetic equations

Monod-type kinetics have been used to describe the bacteria in landfills by many researchers^{7,8,10,12,17} and was used in this model.

$$R_N = \frac{\partial X_N}{\partial t} = k_{m,N} k_{temp,N} \frac{S}{k_{s,N} + S} X_N - R_{D,N} \quad (3-23)$$

If the substrate concentration is sufficiently high ($S \gg k_{s,N}$), Equation 3-23 reduces to:

$$R_N = \frac{\partial X_N}{\partial t} = k_{m,N} k_{temp,N} X_N - R_{D,N} \quad (3-24)$$

Where R_N is the anaerobic biomass production rate [$\text{kg}/\text{m}^3/\text{day}$], X_N is the concentration of the anaerobic biomass [kg/m^3], $k_{m,N}$ is the maximum anaerobic biodegradation rate constant [day^{-1}], $k_{temp,N}$ is the temperature correction factor for anaerobic biomass [-], S is the available substrate [kg/m^3], $k_{s,N}$ is the substrate half-saturation constant for anaerobic growth [kg/m^3] and $R_{D,N}$ is the anaerobic biomass decay rate [$\text{kg}/\text{m}^3/\text{day}$].

$$R_A = \frac{\partial X_A}{\partial t} = k_{m,A} k_{temp,A} \frac{S}{k_{s,A} + S} \frac{c_{O_2}}{k_{O_2} + c_{O_2}} X_A - R_{D,A} \quad (3-25)$$

If the substrate concentration is sufficiently high ($S \gg k_{s,A}$), Equation 3-25 reduces to:

$$R_A = \frac{\partial X_A}{\partial t} = k_{m,A} k_{temp,A} \frac{c_{O_2}}{k_{O_2} + c_{O_2}} X_A - R_{D,A} \quad (3-26)$$

Where R_A is the aerobic biomass production rate [kg/m³/day], X_A is the concentration of the aerobic biomass [kg/m³], $k_{m,A}$ is the maximum aerobic biodegradation rate constant [day⁻¹], $k_{temp,A}$ is the temperature correction factor for aerobic biomass [-], $k_{s,A}$ is the substrate half-saturation constant for aerobic growth [kg/m³], c_{O_2} is the mass concentration of oxygen [kg/m³], k_{O_2} is the oxygen half-saturation constant [kg/m³] and $R_{D,A}$ is the aerobic biomass decay rate [kg/m³/day].

Kim et al. (2007) assumed that the decay rate for both anaerobic and aerobic species are:

$$R_{D,N} = 0.05k_{m,N}(X_N - X_{N,0}) \quad (3-27)$$

$$R_{D,A} = 0.05k_{m,A}(X_A - X_{A,0}) \quad (3-28)$$

Where $X_{N,0}$ and $X_{A,0}$ are the initial anaerobic and aerobic biomass concentrations [kg/m³], respectively.

When the anaerobic bacteria are exposed to oxygen, there is no growth and Equation 3-24 becomes:

$$R_N = -0.05k_{m,N}(X_N - X_{N,0}) \quad (3-29)$$

When the aerobic bacteria are starved of oxygen in the anaerobic phase of the landfill, there is no growth and Equation 3-26 becomes:

$$R_A = -0.05k_{m,A}(X_A - X_{A,0}) \quad (3-30)$$

The temperature correction factor was proposed by Rosso et al. (1993) to correlate microbial growth with cardinal temperatures³³ and has been used in aerobic biodegradation

models^{12,34}. Equation 3-31 is used in both the anaerobic and aerobic biokinetic equations (Equations 3-23 to 3-26). The cardinal temperatures in the correction factor are changed according to the biomass and are found in Table 3-2.

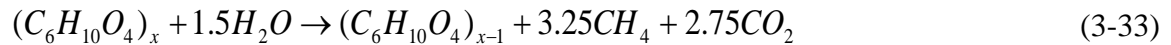
$$k_{temp} = \frac{(T - T_{max})(T - T_{min})^2}{(T_{opt} - T_{min})[(T_{opt} - T_{min})(T - T_{opt}) - (T_{opt} - T_{max})(T_{opt} + T_{min} - 2T)]} \quad (3-31)$$

T is the temperature of the MSW [K], T_{max} is the maximum temperature for microbial growth [K], T_{min} is the minimum temperature for microbial growth [K] and T_{opt} is the optimal temperature for microbial growth [K].

$$x_i = \frac{c_i}{\sum_j c_j} \quad (3-32)$$

Where x_i is the mole fraction of component i [-], c_i is the molar concentration of component i [mol/m³] and c_j is the molar concentration of component j [mol/m³].

Many different chemical formulas have been proposed for use as MSW^{9,10,35} and biochemical reactions for anaerobic biodegradation. In this model the following formula, proposed by Themelis and Kim (2002), was used:



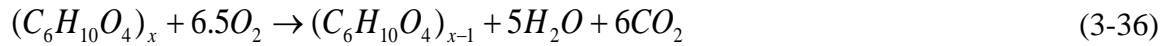
This biochemical formula is used to estimate the methane and carbon dioxide production rate using stoichiometric relationships combined with the anaerobic growth equation (Equation 3-24). The product gases are only produced as the anaerobic bacteria grow, therefore the decay term is not included:

$$\frac{R_{CO_2}}{2.75 \frac{M_{CO_2}}{M_{MSW}}} = \frac{R_N}{Y_{S/B,N}} = \frac{k_{m,N} k_{temp,N} X_N}{Y_{S/B,N}} \quad (3-34)$$

$$\frac{R_{CH_4}}{3.25 \frac{M_{CH_4}}{M_{MSW}}} = \frac{R_N}{Y_{S/B,N}} = \frac{k_{m,N} k_{temp,N} X_N}{Y_{S/B,N}} \quad (3-35)$$

Where R_{CO_2} is the production rate of carbon dioxide [kg/m³/day], R_{CH_4} is the production rate of methane [kg/m³/day] and $Y_{S/B,N}$ is the substrate/anaerobic biomass yield coefficient [kgB/kgs].

Themelis and Kim (2002) proposed the following generalized reaction for the aerobic biodegradation of MSW:



This biochemical formula is used to estimate the oxygen consumption rate and carbon dioxide production rate using stoichiometric relationships combined with the aerobic growth equation (Equation 3-26). The gases are only consumed and produced as the aerobic bacteria grow, therefore the decay term is not included:

$$\frac{R_{O_2}}{-6.5 \frac{M_{O_2}}{M_{MSW}}} = \frac{R_A}{Y_{S/B,A}} = \frac{k_{m,A} k_{temp,A} \frac{x_{O_2}}{k_{O_2} + x_{O_2}} X_A}{Y_{S/B,A}} \quad (3-37)$$

$$\frac{R_{CO_2}}{6 \frac{M_{CO_2}}{M_{MSW}}} = \frac{R_A}{Y_{S/B,A}} = \frac{k_{m,A} k_{temp,A} \frac{x_{O_2}}{k_{O_2} + x_{O_2}} X_A}{Y_{S/B,A}} \quad (3-38)$$

Where R_{O_2} is the consumption rate of oxygen [kg/m³/day] and $Y_{S/B,A}$ is the substrate/aerobic biomass yield coefficient [kg_B/kg_S]. The parameters used in the biokinetic equations are found in Table 3-2.

3.2.3 Energy balance

Equations 3-39 to 3-43 were used for the energy balance²⁸:

$$V(\rho C_p)_{eq} \frac{\partial T}{\partial t} + V\rho_g C_p \mathbf{u} \cdot \nabla T + V\rho_a C_{p,w} \mathbf{u} \cdot \nabla T = \nabla \cdot (k_{eq} \nabla T) + R\Delta H_{reac} - \rho_a F_{L,in} C_{p,w} (T - T_{L,0}) - \rho_g F_{g,in} C_p (T - T_{g,0}) \quad (3-39)$$

Where V is the volume of the MSW [m³], $(\rho C_p)_{eq}$ is the equivalent heat capacity [J/m³/K], k_{eq} is the equivalent thermal conductivity [W/m/K], C_p is the specific heat of the gas [J/kg/K], ΔH_{reac} is the reaction heat [kJ/mol], $F_{L,in}$ is the flowrate of leachate [mL/min], $C_{p,w}$ is the specific heat of water [J/kg/K], $T_{L,0}$ is the initial leachate temperature [K], $F_{g,in}$ is the flowrate of gas [L/min] and $T_{g,0}$ is the initial temperature of the gas [K].

$$(\rho C_P)_{eq} = \theta_{MSW} \rho_{MSW} C_{P,MSW} + (1 - \theta_{MSW}) \rho C_P \quad (3-40)$$

$$C_P = \sum_i \omega_i C_{P_i} \quad (3-41)$$

Where θ_{MSW} is the mass fraction of the MSW [-], ρ_{MSW} is the density of MSW [kg/m^3], $C_{P,MSW}$ is the specific heat of MSW [J/kg/K] and C_{P_i} is the specific heat of component i [J/kg/K].

$$k_{eq} = \theta_{MSW} k_{MSW} + (1 - \theta_{MSW}) k \quad (3-42)$$

k_{MSW} is the thermal conductivity of the MSW [W/m/K] and k is the thermal conductivity of the gas [W/m/K].

$$k = \sum_i \omega_i k_i \quad (3-43)$$

Where k_i is the thermal conductivity of component i [W/m/K]. The parameters used in Section 3.2.3 are found in Table 3-2.

Table 3-2 Model equation parameters

Parameter	Unit	Value	Reference
α	1/m	0.2	12
β	-	5	12
γ	-	0.8	12
a_w	m^3/m^3	0.28	12
a_{wr}	m^3/m^3	0.2	26
a_{ws}	m^3/m^3	0.49	27
ϕ_s	-	0.3	17
ϕ_r	-	0.1	27
K	m^2	10^{-12}	17
ρ_{MSW}	kg/m^3	164	29
$k_{m,N}$	day^{-1}	0.2	10

$k_{m,A}$	day ⁻¹	1.0	10
$Y_{S/B,N}$	kgB/kgS	0.05	10
$Y_{S/B,A}$	kgB/kgS	0.1	36
k_{O_2}	kg/m ³	7x10 ⁻⁶	12,37
$T_{min,N}$	°C	15	38
$T_{opt,N}$	°C	35	38
$T_{max,N}$	°C	70	38
$T_{min,A}$	°C	5	12,34,37
$T_{opt,A}$	°C	58.6	12,34,37
$T_{max,A}$	°C	71.6	12,34,37
$C_{P,MSW}$	MJ/m ³ /K	2.0	39
k_{MSW}	W/m/K	0.0445	40
ΔH_{reac}	kJ/mol	-1,500	Estimated from model
$F_{L,in}$	mL/min	20	29
$F_{g,in}$	L/min	1.9	29

Table 3-3 Initial conditions

Parameter	Unit	Value	Reference
X_N	kg/m ³	0.2	Set equal to X_A
X_A	kg/m ³	0.2	Estimated from model
T	°C	20	29
P	atm	1	Assumed
x_{CH_4}	-	0.542	9
x_{CO_2}	-	0.458	9

3.2.4 Model assumptions

This model has inherent assumptions to decrease the number of equations required:

- Mass of MSW is sufficient to render biokinetic dependence to unity; $S \gg k_{s,N}$ and $S \gg k_{s,A}$
- Biodegradation of MSW is negligible during the model time period (mass of MSW remains constant; $S(t) = S_0$)

- MSW is homogeneous; material properties (e.g. permeability, porosity) are isotropic

3.3 Results and discussion

3.3.1 Geometry and meshing

Figure 3-2(a) gives a schematic view of the bioreactor geometry used. The geometry is based on previous literature (experimental study)²⁹. Due to the symmetry in the x- and y-directions, the geometry was cut in half in the x-direction and again cut in half in the y-direction (Figure 3-2(b) and (c)) and a symmetry boundary condition was enforced on the x- and y-planes. This was done to decrease the computational cost and decrease the time required for solution convergence. The solution was mirrored in the x- and y-directions to give the full bioreactor geometry. The relative tolerance for convergence was set to 10^{-12} due to the small magnitudes of the variables. The initial conditions used in the model are found in Table 3-3.

The dimensions of the bioreactor were 0.71 m in width and 0.55 m in height. However, in the study, the bioreactor had a 0.1 m gravel layer at the bottom. Since the gravel layer is inert and non-biodegradable it was excluded from the model geometry. Therefore, the model was run using a height of 0.45 m. The model begins at the onset of aeration and was solved in 4 hour increments for 7 days, to allow 6 time points in each day.

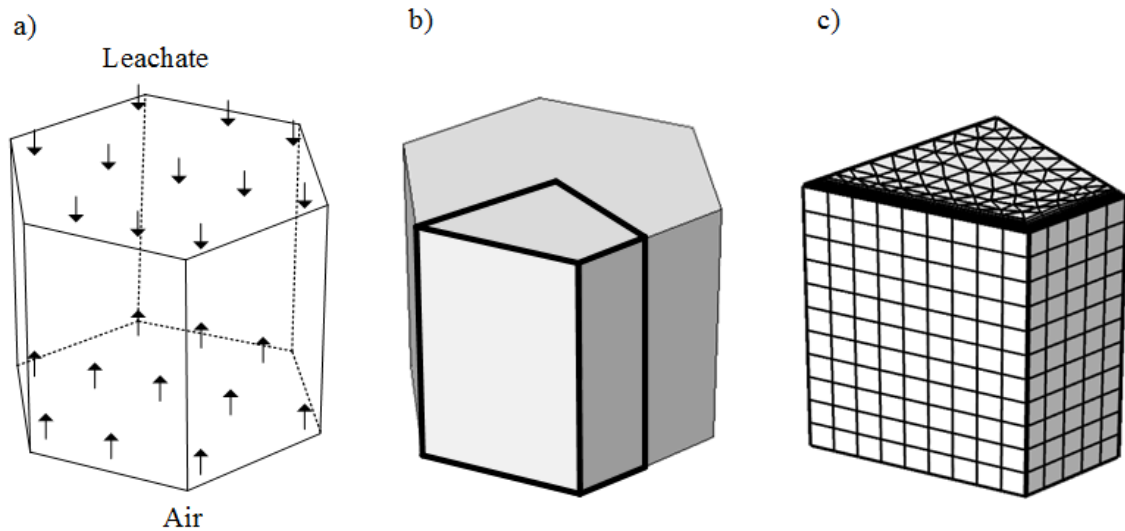


Figure 3-2 Model geometry: (a) schematic view; (b) isometric view with symmetric slice shown; (c) symmetric slice with overlain mesh

The mesh refinement study is shown in Figure 3-3. Multiple variables were tracked and the finest mesh that led to mesh independence was used (<1%). Percent difference (Equation 3-44) was used to track the mesh independence. Triangular mesh elements were used on the top and bottom faces. The mesh was then swept in the z direction. Boundary layer mesh elements were also added to the faces that had gas flow running in parallel (non-symmetry faces).

$$\%Difference = \frac{|mesh_x - finest\ mesh|}{finest\ mesh} \times 100 \quad (3-44)$$

The mole fraction of methane plot showed 0 due to the very small numbers. The finest mesh gave a mole fraction of 0 and due to numerical noise the other mesh values were approximately 10^{-23} . The mesh was sufficiently fine at 42.4 mm based on the %Difference (<1 %) observed in Figure 3-3. All the mesh values were much less than 1% but this mesh size was chosen because it provided minimum error with relatively short convergence time. The refined mesh is shown in Figure 3-2(c).

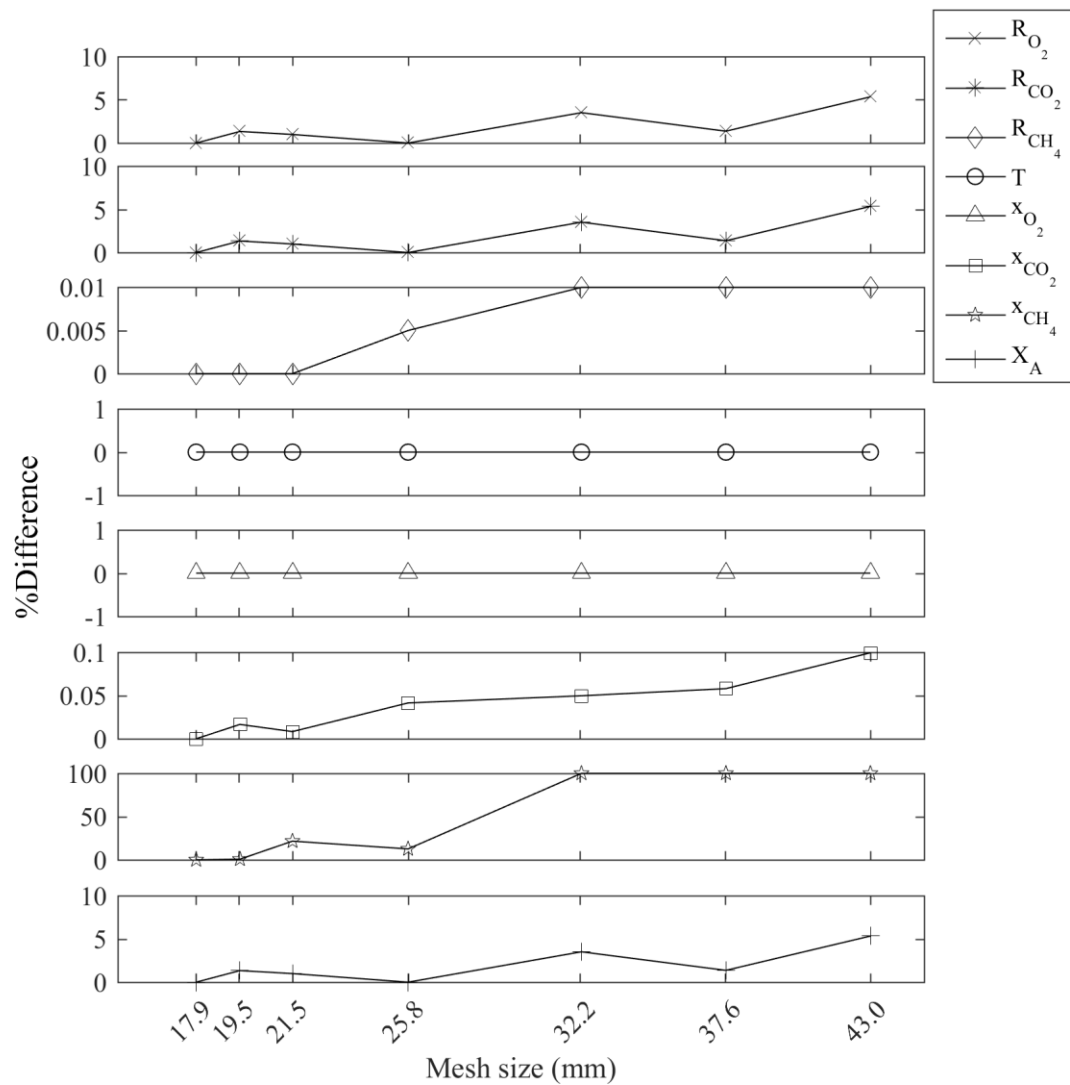


Figure 3-3 Mesh refinement study

3.3.2 Anaerobic-aerobic conversion

3.3.2.1 Parameter estimation

Based on the results of Borglin et al.²⁹, the model was consistent with what was found in the experimental results. Borglin et al. used 200L tanks filled with fresh waste. Leachate was injected from the top of the tank and air injected from the bottom. The outlet gas and

leachate composition, temperature, pressure, moisture content, humidity and flowrates were monitored. The model was run assuming the top face of the tank was not insulated to represent the difficulty that Borglin et al. had maintaining the elevated temperatures. The initial aerobic biomass and heat of reaction were the two parameters that were used to control gas composition and temperature. These parameters were fit by varying the values and observing the outlet composition of the gas and the average temperature. The composition of the outlet gas was between 0-1% carbon dioxide (Figure 3-4(a)) as reported by Borglin et al. The average temperature was 26°C and the maximum temperature was 26.4°C.

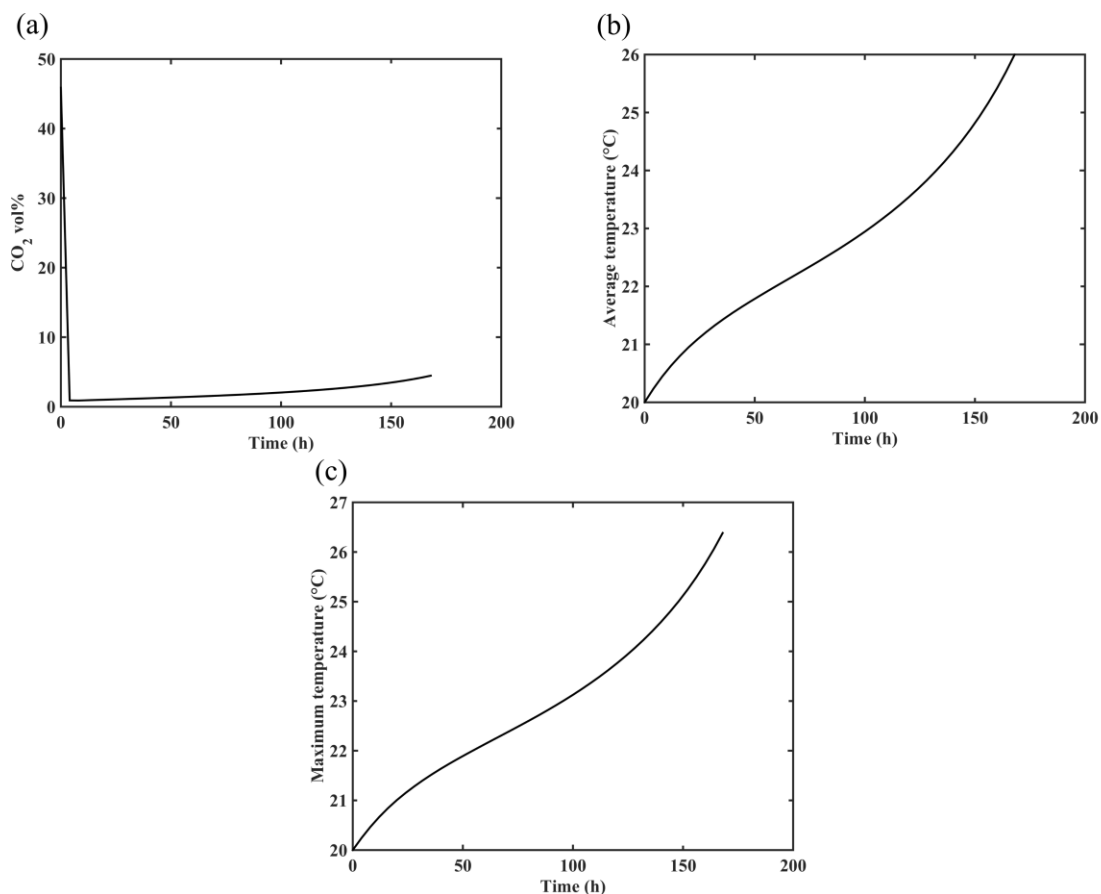


Figure 3-4 Parameter estimation plot: (a) outlet volume fraction of CO₂ over time; (b) average temperature over time and (c) maximum temperature over time

To correspond with 0-1% carbon dioxide, initial aerobic biomass concentration had to be within the range of 0 to 0.6 kg/m³ and the heat of reaction was -1,500 kJ/mol. Because Borglin et al. did not add any initial inoculum, this corresponds to the aerobic biomass present in the waste initially. Generally, aerobic biomass concentrations are higher^{10,12}. However, as evidenced by the low decrease in oxygen when compared to Kim et al. (2007)¹⁰ and Fytanidis and Voudrias (2014)¹², and observed in field conditions⁴², the fitted biomass concentration was logical. The modest increase in temperature also showed this fact. Waste temperature typically increases to 50°C and more⁴²⁻⁴⁴. However, Borglin et al. had trouble keeping temperature in the system, losing heat, further validating the lower aerobic concentration value.

After approximately 1 day, the carbon dioxide concentration increased above 1% and continued to rise (Figure 3-4(a)). The carbon dioxide volume fraction decreased from its initial concentration (due to the initial anaerobic state) to the concentration of carbon dioxide being produced via the aerobic biodegradation. The gas composition did not completely match the 0-1% reported by Borglin et al. and this can be explained by the differing biokinetics. Landfills have different consortiums of bacteria with different biokinetics. Another consideration for the differing concentration is the assumption that substrate concentration was constant. As time progresses, this concentration will decrease and the rate of production of carbon dioxide will also decrease. Running the model for many months or a year in the future would require this assumption be eliminated and substrate concentration be factored into the model.

After 7 days the average bioreactor temperature reached 26°C (Figure 3-4(b)). The maximum temperature in the waste reached approximately 26.4°C (Figure 3-4(c)). Borglin et al. have reported a temperature of 27°C. Giannis et al. (2008) conducted a similar study to Borglin et al. but used a cubic cell instead of a hexagonal prism as their lab scale landfill. Giannis et al. (2008) found during their study that the temperature varied between 20°C and 54°C for the first 70 days of their experiment⁴⁵. The difference can be attributed to the heterogeneous nature of MSW and the varying composition of the MSW. MSW and

therefore the biokinetic/heat values are different from landfill to landfill and can be different from one location to another in the same landfill. The fitted value was in the range of the heat of reaction reported in literature (-460 kJ/mol by Kim et al. (2007) and -616 kcal/mol by Kim et al. (2007)). The results presented in Section 3.3.2 (and its subsections) were simulated using the estimated initial aerobic biomass concentration and heat of reaction values.

Another consequence of the bioreactor not being able to retain heat (due to heat loss), is that the temperature did not reach the optimal temperature (58.6°C). An advantage of using a model is that the model can be run assuming no loss of heat and the effects of retaining the heat (and subsequent increase of temperature) on the growth of aerobic bacteria, consumption of oxygen and production of carbon dioxide and methane can be examined.

3.3.2.2 Growth of aerobic bacteria

An important parameter in the conversion from an anaerobic to aerobic landfill is the initial aerobic biomass concentration. Figure 3-5 shows the effect of initial aerobic biomass concentration on the average and maximum temperatures in the waste after 24 hours. Since the heat produced during anaerobic biodegradation is negligible compared to the heat produced during aerobic biodegradation, temperature can be used as an indicator to determine the efficacy of aerobic biodegradation and subsequently, the conversion from an anaerobic landfill to an aerobic landfill. Looking at Figure 3-5, at low aerobic biomass (0.01 and 0.1 kg/m³) concentration, the temperature was near ambient temperature (assumed to be 20°C). This indicates little aerobic biodegradation. At 5 kg/m³, the opposite behaviour occurred; the temperature increased significantly. This indicates high aerobic biodegradation. Aerobic biomass concentration can be increased physically by the addition of aerobic sludge.

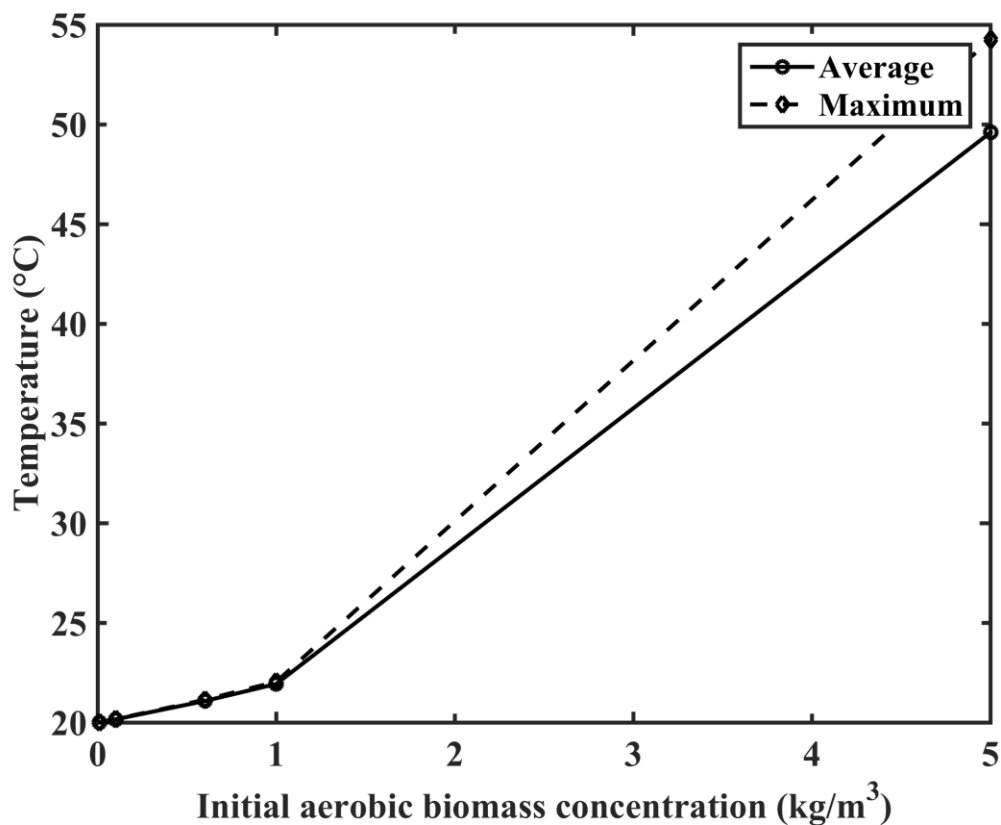


Figure 3-5 Average and maximum temperature of waste after 24 hours with varying initial aerobic biomass concentration (kg/m³)

If the initial aerobic biomass concentration increases, the aerobic bacteria grow faster and as a result will consume oxygen faster. Figure 3-6 shows the growth rate of aerobic biomass concentration with increasing initial aerobic biomass concentration after 24 hours in 3 dimensions. This agrees with Figure 3-5, however a piece of information was not represented in Figure 3-5. Figure 3-6(e) shows a negative growth rate in the top half of the bioreactor. This was due to the lack of oxygen in these areas. The high concentration of aerobic biomass consumed the oxygen before it made its way through the entire volume.

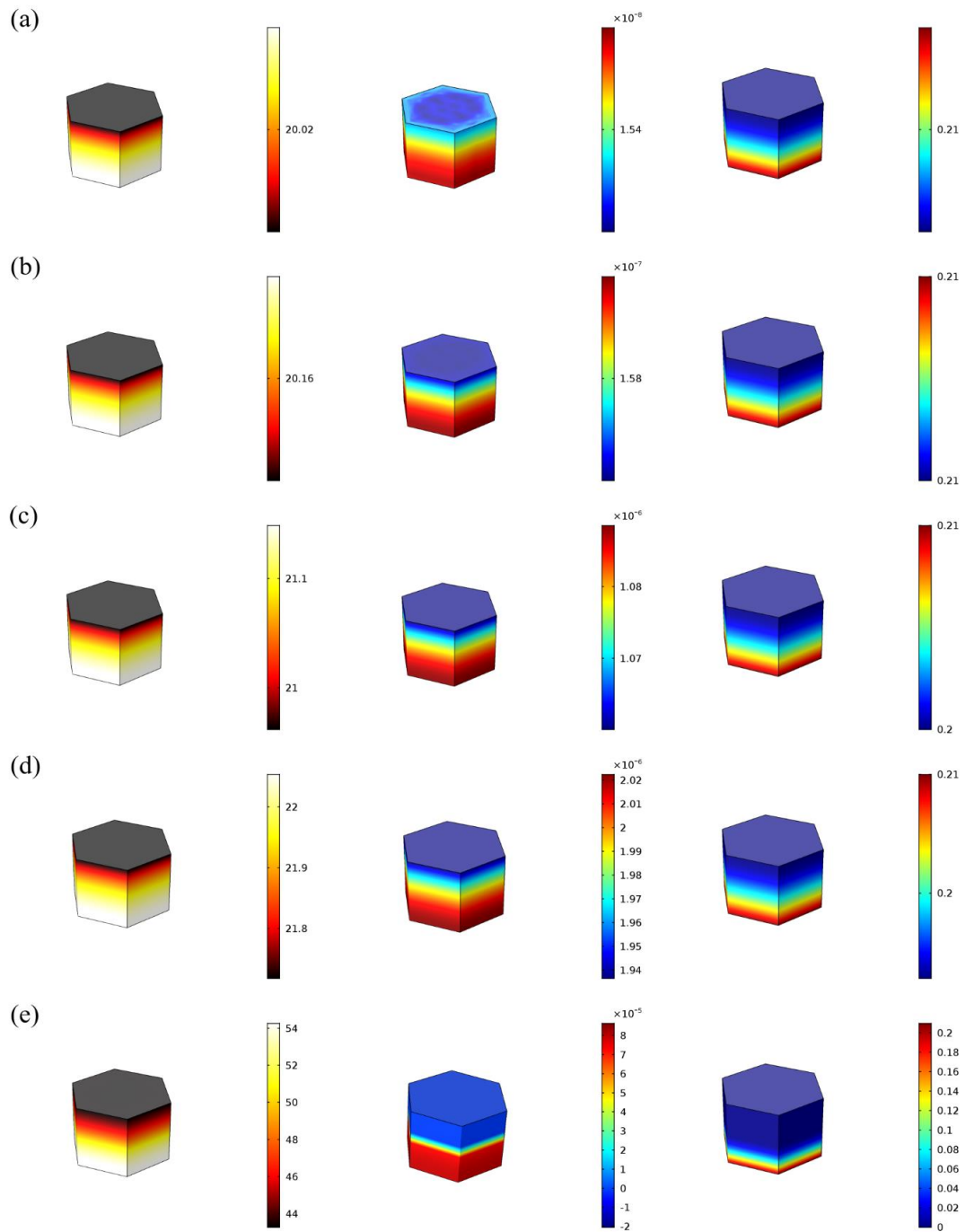


Figure 3-6 Temperature (°C), aerobic growth rate (kg/m³/s) and oxygen volume fraction after 24 hours with initial aerobic biomass concentration of: (a) 0.01 kg/m³; (b) 0.1 kg/m³; (c) 0.6; kg/m³ (d) 1 kg/m³ and (e) 5 kg/m³

3.3.2.3 Oxygen consumption

As time progressed, the aerobic bacteria began to produce heat. The temperature profile inside the bioreactor began to stabilize and the temperature effects on the aerobic bacteria dominated growth rates and subsequently, oxygen consumption rates. The areas that showed the highest oxygen consumption were areas that had a higher temperature (Figure 3-7). A higher oxygen consumption rate directly relates to the biodegradation rate of MSW. The areas with higher concentrations of aerobic bacteria are biodegraded faster. The top of the bioreactor was not insulated and natural convection lead to heat losses from the bioreactor. This removed heat and decreased the temperature at the top of the bioreactor by fractions of a degree when compared to the bottom.

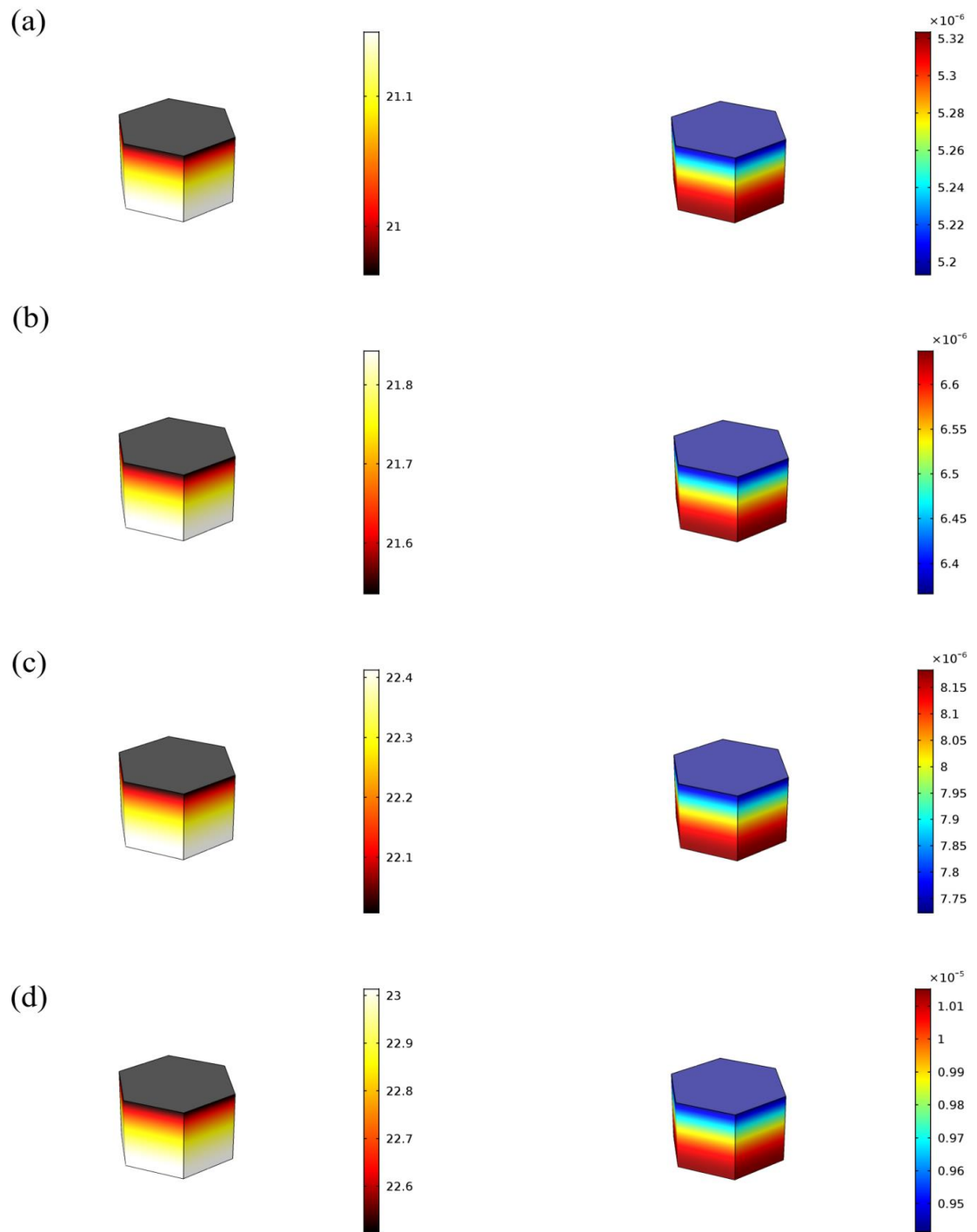


Figure 3-7 Temperature (°C) and oxygen consumption rate (kg/m³/s): (a) 1 day; (b) 2 days; (c) 3 days and (d) 4 days

3.3.2.4 Carbon dioxide production

Carbon dioxide production followed the same trend as the oxygen consumption. In the areas of higher temperature, more carbon dioxide was produced. These areas will show the greatest biodegradation rate of MSW. Figure 3-8 shows this trend as time progresses. Figure 3-4(a) shows the maximum carbon dioxide volume fraction as time progresses. There was a sharp decrease just after time 0 due to the carbon dioxide being pushed out of the bioreactor by the incoming air. Initially, little carbon dioxide was produced when compared to the flow of air coming in, diluting the carbon dioxide. However, as time progressed, the rate of production of carbon dioxide increased. As a result, the volume fraction increased, with the oxygen volume fraction decreasing.

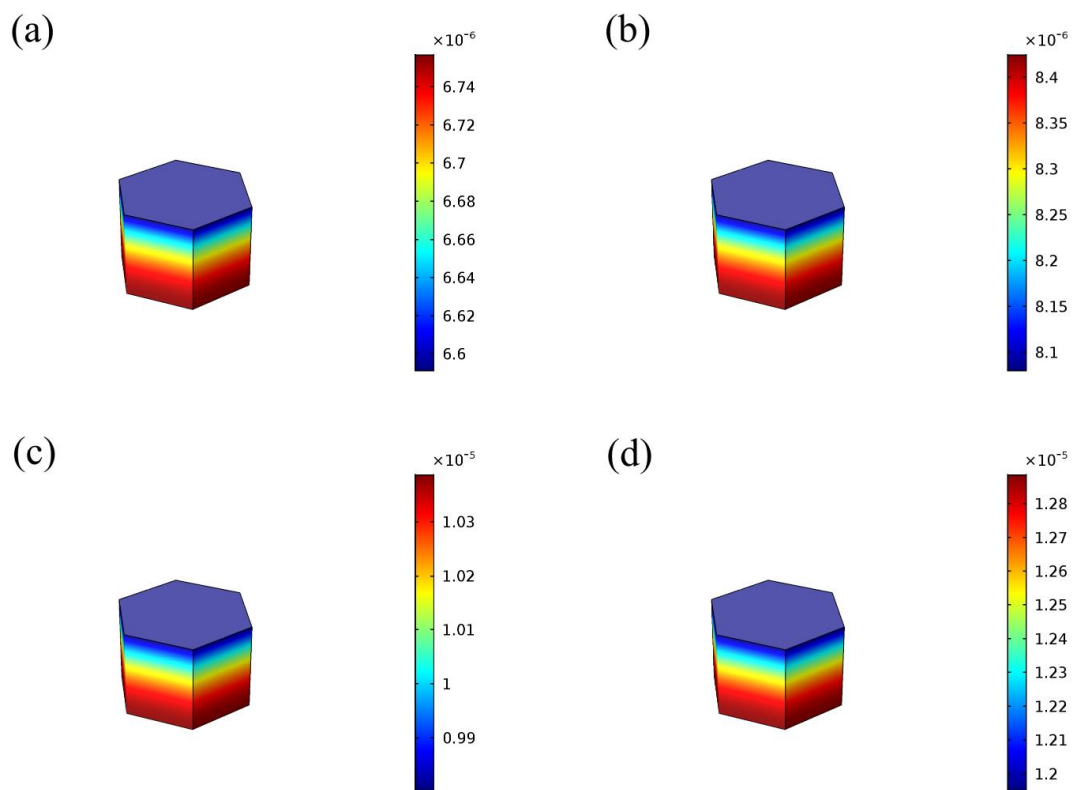


Figure 3-8 Carbon dioxide production rate ($\text{kg}/\text{m}^3/\text{s}$): (a) 1 day; (b) 2 days; (c) 3 days and (d) 4 days

3.3.2.5 Methane production

The initial gas composition was 54.2% CH₄ and 45.8% CO₂ (anaerobic conditions) based on the stoichiometry in Equation 3-33. Before air injection began there was no oxygen, meaning the system was under complete anaerobic conditions. At the onset of air injection, the methane production in the areas with oxygen, ceased, shown in Figure 3-9. This model was run assuming homogeneous isotropic porous media. This means air reached the entire bioreactor. This assumption holds true for lab scale bioreactors but full scale landfills are not ideal and this assumption may not hold true. There are locations where air cannot reach (e.g. if a large non-biodegradable obstruction is in the waste) and there will be pockets of anaerobic bacterial growth.

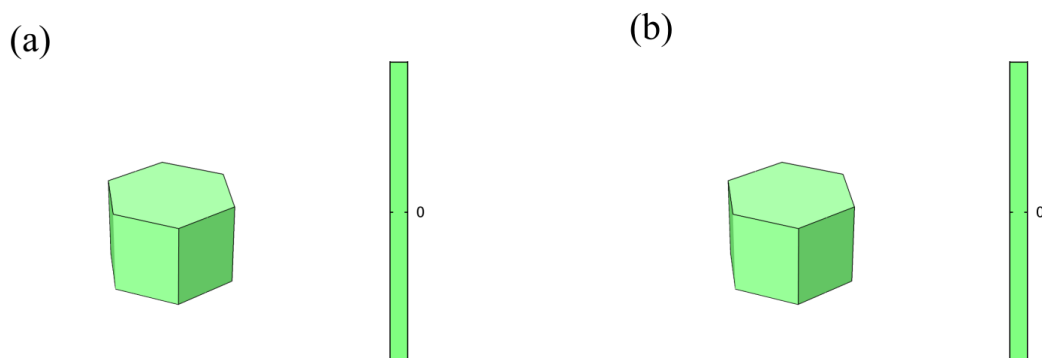


Figure 3-9 Methane production rate (kg/m³/s): (a) 4 hrs and (b) 24 hrs

3.3.3 Higher aerobic biomass concentration

In Section 3.3.2, the parameters used were set with the intention of replicating results found in Borglin et al. in order to find estimates for the heat of reaction and the initial biomass concentration. Here, the intention was to use the model to predict the behaviour in a larger scale system (e.g. a condition in which the oxygen composition in the reactor is less than that of atmospheric composition), and to investigate the landfill behaviour that may not be physically feasible (e.g. a very high initial aerobic biomass concentration of 10 kg/m³).

3.3.3.1 Full scale landfill aerobic biomass concentration

The initial aerobic biomass concentration was increased to decrease the oxygen concentration and investigate its effect on temperature and aerobic biomass growth rate. The initial aerobic biomass concentration was increased to 1 kg/m^3 used in Fytanidis and Voudrias (2014). At this initial aerobic concentration, oxygen still reached the entire reactor and as a result the methane production rate was 0. The behaviour of the biomass growth was similar to that of Section 3.3.2 in which the gradient of aerobic biomass growth rate decreased from areas of high temperature to low temperature. The main differences were the higher temperatures due to the greater heat production by the higher biomass concentration leading to higher rate of biodegrading of MSW and lower concentration of oxygen at the outlet (Figure 3-10).

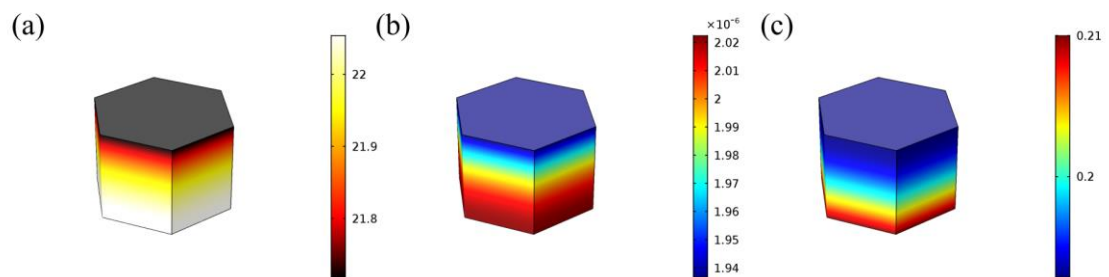


Figure 3-10 After 24 hours: (a) temperature ($^{\circ}\text{C}$); (b) aerobic growth rate ($\text{kg/m}^3/\text{s}$) and (c) oxygen volume fraction (-)

3.3.3.2 High aerobic biomass concentration

The initial aerobic biomass concentration was increased by an order of magnitude to 10 kg/m^3 to investigate its effect. Since MSW biodegradation is directly related to the growth of the aerobic bacteria, a higher concentration of aerobic biomass would lead to faster MSW biodegradation. However, other variables (e.g. temperature, consumption/production rates, etc.) are not simple to discern.

The large aerobic biomass concentration rapidly increased the temperature in the reactor (Figure 3-11(a)). Although the higher temperature will decrease the growth rate of the biomass (Equation 3-31), the large concentration of biomass will increase the growth rate enough to compensate for the high temperature. Figure 3-11(b) shows a plot of the first time derivative of the concentration of aerobic biomass (the growth rate). Even though temperature was at the maximum allowed temperature for growth, the biomass were still growing at a fast rate when compared to the aerobic growth rates in Figure 3-6. The problem with allowing the temperature to remain this high, is the safety concerns. There is potential for combustion to occur. Incomplete combustion inside landfill mass has been reported in literature^{46,47} when trace amounts of carbon monoxide have been found in the gas being extracted. Therefore, temperature needs to be controlled, via increased leachate injection (or air injection). Assuming the aerobic biomass starts near 1 kg/m^3 , it will take time for the concentration to increase to 10 kg/m^3 . In that time, enough MSW may have been biodegraded to slow down the rapid growth and help limit the heat generation.

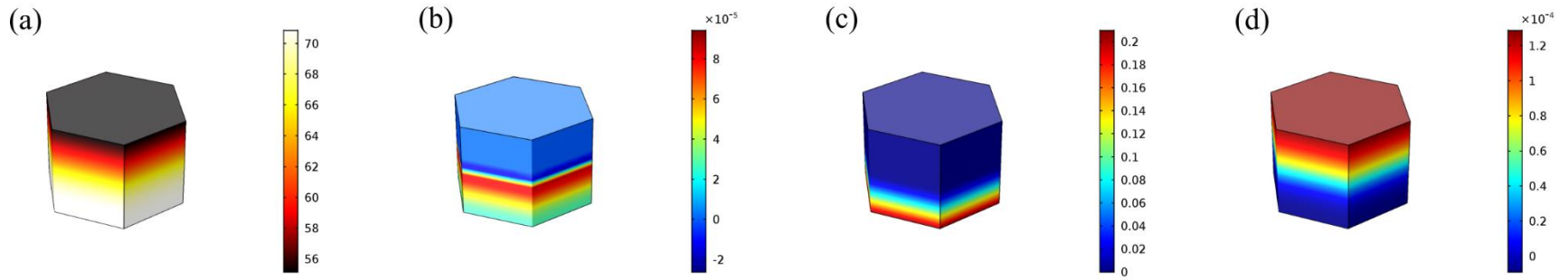


Figure 3-11 After 24 hours: (a) temperature ($^{\circ}\text{C}$); (b) aerobic biomass growth rate ($\text{kg}/\text{m}^3/\text{s}$); (c) oxygen volume fraction (-) and (d) rate of methane production ($\text{kg}/\text{m}^3/\text{s}$)

The gradient of aerobic biomass growth is in stark contrast to Section 3.3.2, where a higher temperature meant a higher biodegradation rate. In Section 3.3.2, the temperature had not exceeded the optimal temperature for aerobic growth. Further increase in the temperature increased the rate of growth of the aerobic bacteria. Here, the temperature was above the optimal temperature. Increasing temperature decreased the aerobic growth rate as the temperature deviated further from the optimal temperature; shown in Figure 3-11(a) and (b). Up until the point where there was no more oxygen (approximately half way along the z-axis in Figure 3-11(b)), the aerobic growth rate increased. This corresponded to a slight temperature gradient in Figure 3-11(a).

As can be seen in Figure 3-11(b) and (c), oxygen did not reach the top portion of the bioreactor. This means that aerobic bacteria cannot grow in the top portion of the bioreactor (shown by the negative aerobic growth rate in Figure 3-11(b), indicating aerobic bacterial death). Aerobic bacteria will only biodegrade the portions where growth is occurring. Eventually these areas will biodegrade and the aerobic bacteria will have no MSW to sustain growth and will perish. The air is then no longer used up in the bottom portion and will reach higher in the waste and allows aerobic growth and biodegradation. In this way, in this configuration, with high aerobic biomass concentration, the bioreactor acts similar to a plug flow reactor. Figure 3-11(d) shows the methane production rate. Methane is produced in the top portion of the bioreactor where no oxygen reached.

3.3.4 Temperature control

As shown in Section 3.3.2, temperature is an important variable for the aerobic biodegradation rate. Equations 3-25 and 3-26 show that the aerobic bacterial growth rate is dependent on temperature. If the temperature exceeds the optimal temperature shown in Table 3-2, the aerobic bacteria growth rate will decrease. Therefore, temperature control is required. This is typically done in two ways: (1) increasing air flowrate and/or (2) increasing the leachate flowrate⁴². Figure 3-12(a) shows the effect of increasing and decreasing air flowrate on the average temperature of the bioreactor and Figure 3-12(b)

shows the effect on maximum temperature in the bioreactor (middle point is the actual air flow condition). Figure 3-12(c) shows the effect of increasing and decreasing leachate flowrate on the average temperature of the bioreactor and Figure 3-12(d) shows the effect on the maximum temperature in the bioreactor (middle point is the actual leachate flow condition).

Increasing air flowrate did not appreciably decrease the temperature of the landfill. However, increasing leachate flowrate did. The rate at which the temperature decreased when increasing leachate flowrate began to level off as shown by Figure 3-12(b). The higher the leachate flowrate, the closer the temperature was to the injection temperature of the leachate (20°C). The specific heat capacity of leachate is approximately 4 times larger than that of air. However, varying air flowrate has more consequences than simply acting as a heat sink. Decreasing air flowrate can potentially cause some aerobic bacteria to perish due to lack of oxygen. Since the growth of the aerobic bacteria causes the heat production, less aerobic bacteria will decrease the temperature. However, this is not a suitable method if the landfill is to operate aerobically. It would require a significant increase in air flowrate to accomplish the same cooling as leachate. From an economic standpoint, this is not always feasible. Increasing the air flowrate will also strip more moisture from the landfill requiring more leachate injection to compensate. Therefore, varying leachate flowrate is a more effective temperature control method.

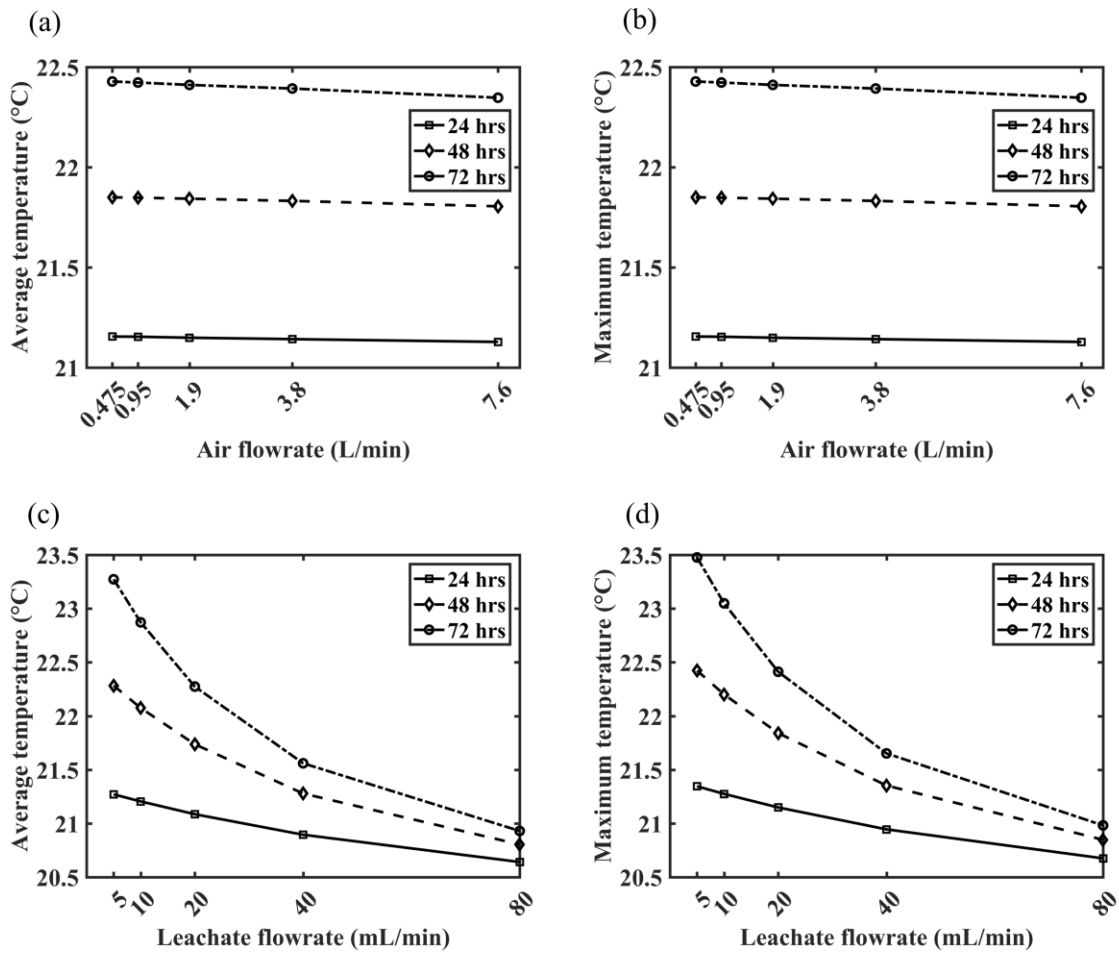


Figure 3-12 Varying air flowrate: (a) average temperature (°C); (b) maximum temperature (°C); varying leachate flowrate: (c) average temperature (°C); (d) maximum temperature (°C)

3.4 Conclusions and summary

A 3-dimensional dynamic mathematical model for a landfill operation was developed using coupled partial differential equations representing the governing mass, energy and momentum balances. The model was solved using the finite element method using COMSOL Multiphysics. The model was used to determine the transport phenomena that occurred upon the conversion of an anaerobic bioreactor landfill into an aerobic bioreactor landfill. The fitted model parameters were consistent with values found in the literature.

In the initial stages of conversion of an anaerobic landfill to an aerobic landfill, the initial aerobic biomass concentration was the main factor that limited the growth of aerobic bacteria (assuming the presence of sufficient oxygen). The more bacteria present, the faster they grew and the faster they dominated. Once the aerobic bacteria have begun to grow, heat will be produced, increasing the temperature of the waste. Higher temperatures promoted the rate of the growth of aerobic bacteria (until the temperature increased beyond the optimal growth temperature). The areas with higher aerobic activities will biodegrade at a faster rate. However, areas where aerobic bacteria activity was significant enough to increase the temperature beyond the optimal temperature, showed less aerobic growth. Controlling temperatures (and by extension, biodegradation) was found to be more effective by varying the leachate flowrate when compared to varying the air flowrate. An increase in aerobic biomass concentration (simulated using 10 kg/m^3) showed that the biodegradation occurs at a rapid rate. However, the temperature increases quickly and does not decrease. This can have safety issues and temperature needs to be controlled.

At large aerobic biomass concentrations, oxygen may not reach the entire solid waste mass and areas may not biodegrade. The waste will biodegrade in “plugs”. When areas of the waste become biodegraded enough, the aerobic bacteria cannot sustain growth with the remaining organic portion of the waste. The oxygen will then not be consumed in these areas and will flow to the areas where oxygen did not initially reach.

Future work can be performed to scale-up the model and test different geometries and air injection well placements to optimize the aerobic process. Work is being done to test how multiple aerobic-anaerobic conversions would behave¹⁰. A model that starts aerobically and is converted to anaerobic would also be useful. Other factors (e.g. pH, moisture content) can be included in the reaction rates, to examine their effects on conversion of the landfills and on the transport phenomena. This can also be extended to determine the effect on the MSW biodegradation. The results show this model can be useful in tracking the conversion process and provide useful insights in full scale landfills operations.

3.5 References

1. Baltoukas D. *1-D approximation for the simulation of preferential flow in heterogeneous landfill conditions*. Delft University of Technology, Delft, Netherlands, 2012.
2. Westlake K. Sustainable Landfill—Possibility or Pipe-Dream? *Waste Manag Res.* 1997;15(5):453–61. Doi: 10.1177/0734242X9701500502.
3. Kulkarni HS, Reddy KR. Moisture distribution in bioreactor landfills: A review. *Indian Geotech J.* 2012;42(3):125–49. Doi: 10.1007/s40098-012-0012-8.
4. Erses AS, Onay TT, Yenigun O. Comparison of aerobic and anaerobic degradation of municipal solid waste in bioreactor landfills. *Bioresour Technol.* 2008;99(13):5418–26. Doi: 10.1016/j.biortech.2007.11.008.
5. Zhang Y, Yue D, Liu J, Lu P, Wang Y, Liu J, et al. Release of non-methane organic compounds during simulated landfilling of aerobically pretreated municipal solid waste. *J Environ Manage.* 2012;101:54–8. Doi: 10.1016/j.jenvman.2011.10.018.
6. Omar H, Rohani S. Treatment of landfill waste, leachate and landfill gas: A review. *Front Chem Sci Eng.* 2015;9(1):15–32. Doi: 10.1007/s11705-015-1501-y.
7. El-Fadel M, Findikakis AN, Leckie JO. Numerical Modelling of Generation and Transport of Gas and Heat in Landfills I. Model Formulation. *Waste Manag Res.* 1996;14(5):483–504. Doi: 10.1177/0734242X9601400506.
8. Gholamifard S, Eymard R, Duquennoi C. Modeling anaerobic bioreactor landfills in methanogenic phase: Long term and short term behaviors. *Water Res.* 2008;42(20):5061–71. Doi: 10.1016/j.watres.2008.09.040.

9. Themelis NJ, Kim YH. Material and energy balances in a large-scale aerobic bioconversion cell. *Waste Manag Amp Res J Int Solid Wastes Public Clean Assoc ISWA*. 2002;20(3):234–42. Doi: 10.1177/0734242X0202000304.
10. Kim S-Y, Tojo Y, Matsuto T. Compartment model of aerobic and anaerobic biodegradation in a municipal solid waste landfill. *Waste Manag Res*. 2007;25(6):524–37. Doi: 10.1177/0734242X07079148.
11. Slezak R, Krzystek L, Ledakowicz S. Mathematical model of aerobic stabilization of old landfills. *Chem Pap*. 2012;66(6):543–9. Doi: 10.2478/s11696-012-0133-7.
12. Fytanidis DK, Voudrias EA. Numerical simulation of landfill aeration using computational fluid dynamics. *Waste Manag*. 2014;34(4):804–16. Doi: 10.1016/j.wasman.2014.01.008.
13. Omar H, Rohani S. Transport Phenomena in the Conversion of an Anaerobic Landfill Into an Aerobic Landfill. *Proceedings of the 2015 COMSOL Conference in Boston*. Boston; 2015.
14. Duquennoi C, Weisse S, Clement R, Oxarango L. Coupling Hydrodynamics and Geophysics with COMSOL Multiphysics: First Approach and Application to Leachate Injection in Municipal Waste Landfills. *Proceedings of the COMSOL Conference 2011 Boston*. Stuttgart, Germany; 2011.
15. McCreanor P, Reinhart D. Hydrodynamic modeling of leachate recirculating landfills. *Waste Manag Res*. 1999;17(6):465–9.
16. Ishimori H, Sakanakura H, Endo K, Yamada M, Osako M. Numerical Model for Leaching and Transporting Behavior of Radiocesium in MSW Landfill. *Proceedings of the COMSOL Conference 2013 Boston*. Boston; 2013.
17. Ishimori H, Endo K, Ishigaki T, Sakanakura H, Yamada M. Coupled fluid flow and thermal and reactive transport in porous media for simulating waste stabilization

phenomena in semi-aerobic landfill. *Proceedings of the 2011 COMSOL Conference in Boston*. Boston; 2011.

18. Ishimori H, Endo K, Yamada M. Reliability Evaluation for Static Chamber Method at Landfill Sites. *Proceedings of the COMSOL Conference 2009 Boston*. Boston; 2009.
19. Hettiarachchi H, Meegoda J, Hettiaratchi P. Effects of gas and moisture on modeling of bioreactor landfill settlement. *Waste Manag.* 2009;29(3):1018–25. Doi: 10.1016/j.wasman.2008.08.018.
20. Xi Y, Xiong H. Numerical simulation of landfill gas pressure distribution in landfills. *Waste Manag Res.* 2013;31(11):1140–7. Doi: 10.1177/0734242X13502380.
21. Faour AA, Reinhart DR, You H. First-order kinetic gas generation model parameters for wet landfills. *Waste Manag.* 2007;27(7):946–53. Doi: 10.1016/j.wasman.2006.05.007.
22. Abushammala MFM, Basri NEA, Basri H, Kadhum AAH, El-Shafie AH. Estimation of methane emission from landfills in Malaysia using the IPCC 2006 FOD model. *J Appl Sci.* 2010;10(15):1603–9. Doi: 10.3923/jas.2010.1603.1609.
23. Amini HR, Reinhart DR, Mackie KR. Determination of first-order landfill gas modeling parameters and uncertainties. *Waste Manag.* 2012;32(2):305–16. Doi: 10.1016/j.wasman.2011.09.021.
24. Van Genuchten MT. A closed-form equation for predicting the hydraulic conductivity of unsaturated soils. *Soil Sci Soc Am J.* 1980;44(5):892–8.
25. COMSOL. Two-phase flow in column. Available at <http://www.comsol.com/model/two-phase-flow-in-column-499>.

26. Stoltz G, Tinet A, Staub M, Oxarango L, Gourc J. Moisture Retention Properties of Municipal Solid Waste in Relation to Compression. *J Geotech Geoenvironmental Eng.* 2012;138(4):535–43. Doi: 10.1061/(ASCE)GT.1943-5606.0000616.
27. Jayakody KPK, Shimaoka T, Komiya T, Ehler P. Laboratory Determination of Water Retention Characteristics and Pore size Distribution in Simulated MSW Landfill Under Settlement. *Int J Environ Res.* 2014;8(1):79–84.
28. COMSOL. COMSOL Documentation. Available at www.comsol.com.
29. Borglin SE, Hazen TC, Oldenburg CM, Zawislanski PT. Comparison of aerobic and anaerobic biotreatment of municipal solid waste. *J Air Waste Manag Assoc.* 2004;54(7):815–22. Doi: 10.1080/10473289.2004.10470951.
30. Fairbanks DF, Wilke CR. Diffusion Coefficients in Multicomponent Gas Mixtures. *Ind Eng Chem.* 1950;42(3):471–5. Doi: 10.1021/ie50483a022.
31. Chapman S, Cowling TG. *The Mathematical Theory of Non-uniform Gases: An Account of the Kinetic Theory of Viscosity, Thermal Conduction and Diffusion in Gases.* Cambridge University Press; 1970.
32. Brodkey RS, Hershey HC. *Transport phenomena: a unified approach.* New York ; Montreal: McGraw-Hill; 1988.
33. Rosso L, Lobry JR, Flandrois JP. An Unexpected Correlation between Cardinal Temperatures of Microbial Growth Highlighted by a New Model. *J Theor Biol.* 1993;162(4):447–63. Doi: 10.1006/jtbi.1993.1099.
34. Baptista M, Antunes F, Gonçalves MS, Morvan B, Silveira A. Composting kinetics in full-scale mechanical–biological treatment plants. *Waste Manag.* 2010;30(10):1908–21. Doi: 10.1016/j.wasman.2010.04.027.

35. Themelis NJ, Ulloa PA. Methane generation in landfills. *Renew Energy*. 2007;32(7):1243–57. Doi: 10.1016/j.renene.2006.04.020.
36. Beaven RP, White JK, Braithwaite P. Application of the University of Southampton Landfill Degradation and Transport Model (LDAT) to an aerobic treatment field experiment. *Proceedings of Global Waste Management Symposium*. Colorado, USA; 2008.
37. Sole-Mauri F, Illa J, Magrí A, Prenafeta-Boldú FX, Flotats X. An integrated biochemical and physical model for the composting process. *Bioresour Technol*. 2007;98(17):3278–93. Doi: 10.1016/j.biortech.2006.07.012.
38. Tchobanoglous G, Theisen H, Vigil SA. *Integrated solid waste management: engineering principles and management issues*. New York ; Montreal: McGraw-Hill; 1993.
39. Yeşiller N, Hanson JL, Liu W-L. Heat Generation in Municipal Solid Waste Landfills. *J Geotech Geoenvironmental Eng*. 2005;131(11):1330–44.
40. Manna L, Zanetti MC, Genon G. Modeling biogas production at landfill site. *Resour Conserv Recycl*. 1999;26(1):1–14. Doi: 10.1016/S0921-3449(98)00049-4.
41. Bilgili MS, Demir A, Özkaya B. Influence of leachate recirculation on aerobic and anaerobic decomposition of solid wastes. *J Hazard Mater*. 2007;143(1–2):177–83. Doi: 10.1016/j.jhazmat.2006.09.012.
42. Green LC. Method and system for treating bio-degradable waste material through aerobic degradation. 5,888,022, 1999.
43. Zanetti MC. Aerobic Biostabilization of Old MSW Landfills. *Am J Eng Appl Sci*. 2008;1(4):393–8. Doi: 10.3844/ajeassp.2008.393.398.
44. Wadkar DV, Modak PR, Chavan VS. Aerobic thermophilic composting of municipal solid waste. *Int J Eng Sci Technol*. 2013;5(3):716–8.

45. Giannis A, Makripodis G, Simantiraki F, Somara M, Gidakos E. Monitoring operational and leachate characteristics of an aerobic simulated landfill bioreactor. *Waste Manag.* 2008;28(8):1346–54. Doi: 10.1016/j.wasman.2007.06.024.
46. Crutcher AJ, Rovers FA, McBean EA. Temperature as an indicator of landfill behavior. *Water Air Soil Pollut.* 1982;17(2):213–23. Doi: 10.1007/BF00283304.
47. Powell J, Jain P, Kim H, Townsend T, Reinhart D. Changes in Landfill Gas Quality as a Result of Controlled Air Injection. *Environ Sci Technol.* 2006;40(3):1029–34. Doi: 10.1021/es051114j.

Chapter 4

4 Removal of CO₂ from landfill gas and Pb²⁺ from leachate using a hybrid sorption process

Landfills produce methane and carbon dioxide as the waste is biodegraded. Typically, this gas is flared and the energy is lost. The objective of this study was the removal of carbon dioxide for the purification of methane from landfill gas and removal of heavy metals from leachate using a hybrid sorption column (both adsorption and absorption). The column had a 6 cm diameter and 70 cm height. The heavy metals were removed via adsorption/ion exchange using the natural zeolite clinoptilolite. The experimental results agreed with the theoretical results found using Aspen HYSYS®. Using leachate as the liquid phase resulted in slightly more removal of carbon dioxide than water (60.6% and 56.8%, respectively using zeolite; 63.4% and 61.5%, respectively using glass beads). Using zeolite as packing compared to glass beads showed slightly less removal (56.8% and 61.5%, respectively using water and 60.6% and 63.4%, respectively when using leachate). When zeolite was used as packing and leachate as the sorbent, the gas composition was in equilibrium after 2 recycles at a composition of 55% methane and 45% carbon dioxide. When glass beads were used as packing, the carbon dioxide removal was high enough (63.4%) that the carbon dioxide desorbed at the inlet of the pump and did not allow further recycles. The initial pH of the model leachate (prepared using distilled water and lead(II) nitrate) was tested in batch experiments to see how the efficacy of lead removal varied with pH. At pH 2.8, 4.9 and 5.6 the removal of lead was $99.64 \pm 0.07\%$, $99.77 \pm 0.06\%$ and $99.84 \pm 0.07\%$, respectively. Increasing pH higher than this point caused precipitation and decreased the lead concentration to 2.5 ppm. The subsequent removal at pH 10.3 was $91.64 \pm 2.25\%$. The experimental and simulation results indicated that the hybrid sorption column can be useful for the removal of CO₂ at higher pressures from landfill gas but requires a longer column length for the effective removal of heavy metals from leachate.

4.1 Introduction

Greenhouse gases (GHGs) have been steadily rising every year. This is due to the increasing human population. Carbon dioxide is nearly always blamed for the increase because of the large amounts produced via energy production by fossil fuels and cement manufacturing. However, methane is a more potent greenhouse gas, 25 times as potent as carbon dioxide. Methane traps more infrared radiation and has a longer atmospheric residence time¹. In the year 2004 – 2005, anthropogenic GHG emissions from the waste sector totaled 1.4 million metric tons of CO₂ equivalent. From the GHG emissions produced by the waste sector, 90% was made up of methane and 18% of the global anthropogenic methane emissions². Furthermore, the concentration of methane in the atmosphere is more than twice its concentration 150 years ago. This is indirectly caused by the increase in human population³. Anaerobic landfills primarily produce both methane and carbon dioxide. Table 4-1 shows a range of volume fractions of the various components of anaerobic landfill gas (LFG). Different authors provide different compositions for anaerobic landfill but this reference was used because ranges of the different gases were given. The gas composition used in this work was 50% CH₄ and 50% CO₂. This composition falls inside the range given in Table 4-1 and is reported in literature⁴.

Table 4-1 Typical anaerobic landfill gas composition

Component	Volume fraction (%)	Reference
CH ₄	40-55	
CO ₂	35-50	
N ₂	0-20	5
O ₂	0	
H ₂ S	Up to 200 ppm	

In landfills, attempts are made to reduce the amount of methane released to the atmosphere by capturing the LFG and flaring it. However, flaring has the unwanted consequence of potentially producing harmful gases (SO_x, NO_x, CO) depending on the composition of the LFG⁶. Furthermore, flaring has to be done at a temperature of 1200°C or higher to reduce the risk of toxic compounds (e.g. dioxins) being produced⁷. An alternative to wasting the

energy is to use the LFG for other applications such as power generation⁸⁻¹⁰ or fuel production^{10,11}. However, anaerobic LFG has approximately half the heating value of natural gas¹². Removing carbon dioxide can increase the heating value.

Research has been conducted on removing CO₂ using chemical scrubbing¹³⁻¹⁶. Water scrubbing is simple, effective and versatile. It has not been as extensively researched¹⁷⁻¹⁹ as chemical scrubbing because it is not as widely used. In landfills there is access to leachate that can be used as an absorbent in place of water.

Removing heavy metals from wastewaters (in this case leachate) can be accomplished in numerous methods. In this study the method to be used is adsorption/ion exchange by zeolites. The heavy metal that is focused on is lead. Lead has the highest adsorption/ion exchange selectivity of the common heavy metals found in landfill leachate for the natural zeolite clinoptilolite²⁰. The adsorption/ion exchange for lead using zeolite is shown in Equation 4-1.



where M designates the zeolite cation being exchanged (Na, K, Ca or Mg), n designates the ionic charge, which can vary for the transition metals, and the subscripts (s) and (z) designate in solution and bonded to the zeolite, respectively.

Various adsorbents can be used to remove heavy metals such as activated carbons²¹⁻²⁴, natural/synthetic zeolites^{20,25-27} and metal-organic frameworks²⁸. Clinoptilolite, a natural zeolite, is the most heavily studied zeolite for use in the removal of heavy metals²⁹⁻³¹ and is the choice for use in this study.

Both heavy metal removal using adsorption/ion exchange and gas separation using absorption are most often carried out in packed bed columns. The purpose of this study is to combine the two methods in one column and test its efficacy when compared to the best case scenario (i.e. two single columns). The goal of this study is to prove the efficacy of this hybrid sorption system and spawn further research and development to eventually scale

up this system. Combining two columns in one, simplifies the design requirements and reduces the capital cost.

4.2 Economic incentive for the landfill gas purification

This section provides the economics of using the methane from the LFG as an energy source. The prices are taken from distributors in the Province of Ontario³² and are shown in Table 4-2.

$$F_{LFG} = 84,000 \frac{m^3}{day} \quad 33$$

$$x_{CH_4} = 0.40 - 0.55^5$$

Table 4-2 Ontario natural gas prices

Distributor	Cost ($\text{\$/m}^3$)
Union Gas Ltd.	9.4846
Enbridge Gas Distribution Inc.	11.7485
Natural Resource Gas Ltd.	18.7001

Assuming 40% CH₄

$$F_{CH_4} = F_{LFG} x_{CH_4} = 33,600 \frac{m_{CH_4}^3}{day}$$

Assuming 55% CH₄

$$F_{CH_4} = F_{LFG} x_{CH_4} = 46,200 \frac{m_{CH_4}^3}{day}$$

Union Gas

$$\text{Total savings} = F_{CH_4} \$_{CH_4} = \left(33,600 \frac{m_{CH_4}^3}{day} \right) \left(9.4846 \frac{\text{\$}}{m^3} \right) \approx \$1,163,000 / \text{year}$$

$$\text{Total savings} = \left(46,200 \frac{m^3_{CH_4}}{\text{day}} \right) \left(9.4846 \frac{\text{¢}}{m^3} \right) \approx \$1,599,000 / \text{year}$$

Using Union Gas prices, between \$1,163,000 and \$1,599,000 per year can be saved on natural gas.

Enbridge Gas Distribution Inc.

$$\text{Total savings} = \left(33,600 \frac{m^3_{CH_4}}{\text{day}} \right) \left(11.7485 \frac{\text{¢}}{m^3} \right) \approx \$1,441,000 / \text{year}$$

$$\text{Total savings} = \left(46,200 \frac{m^3_{CH_4}}{\text{day}} \right) \left(11.7485 \frac{\text{¢}}{m^3} \right) \approx \$1,981,000 / \text{year}$$

Using Enbridge Gas prices, between \$1,441,000 and \$1,981,000 per year can be saved on natural gas.

Natural Resource Gas Ltd.

$$\text{Total savings} = \left(33,600 \frac{m^3_{CH_4}}{\text{day}} \right) \left(18.7001 \frac{\text{¢}}{m^3} \right) \approx \$2,293,000 / \text{year}$$

$$\text{Total savings} = \left(46,200 \frac{m^3_{CH_4}}{\text{day}} \right) \left(18.7001 \frac{\text{¢}}{m^3} \right) \approx \$3,153,000 / \text{year}$$

Using Natural Resource Gas prices, between \$2,293,000 and \$3,153,000 per year can be saved on natural gas.

4.3 Materials and methods

4.3.1 Zeolite preparation

The natural zeolite sample used in this project was a commercial product provided by Earth Innovations Inc. (Toronto, ON, Canada) with the particle size of 7.6 ± 1.6 mm. The natural zeolite clinoptilolite was used for heavy metal removal and as packing for absorption. The chemical formula of clinoptilolite is given by $(\text{Na,K,Ca})_4\text{Al}_6\text{Si}_{30}\text{O}_{72} \cdot 24\text{H}_2\text{O}$ ³⁴. The chemical composition is found in Table 4-3. The chemical composition was found using X-ray fluorescence (XRF) technique. This clinoptilolite contained mostly Al_2O_3 (11.5%) and SiO_2 (67.5%) and little amounts of other oxides. To regenerate the zeolite, the zeolite was soaked in a 10% (by weight) NaCl, 1% HCl (by volume) in distilled water solution for 24 hours³⁵. After 24 hours the zeolite was thoroughly washed with distilled water and dried at 110°C overnight. The cation exchange capacity (CEC) values of zeolites used in both the column and the batch tests are found in Section 4.4.1.5.

4.3.2 Leachate preparation

Leachate used in the absorption experiments was obtained from the W12A Landfill in London, Ontario, Canada. Before use, the leachate was filtered through VWR Grade 413 mesh filter to remove fine particles that may clog the nozzle used to spray the absorbent. When not in use, the leachate was stored at 4°C to minimize potential degradation of the leachate. When experiments are performed, the leachate is allowed to return to room temperature for use and subsequently refrigerated after the experiments are finished.

4.3.3 Model leachate solution preparation

The model leachate solution was prepared by dissolving $\text{Pb}(\text{NO}_3)_2$ in deionized water to get a concentration of 100 ppm. Lead was used due to its having the highest adsorption/ion exchange uptake selectivity by clinoptilolite. The pH of the solutions were varied using HNO_3 and NaOH.

4.3.4 Characterization techniques

The zeolite sample was washed with deionized water and dried at 100°C for 5 hours then characterized using XRF (for chemical composition), X-ray diffraction (XRD) (for crystallinity and phase composition), scanning electron microscope (SEM) for morphology, thermogravimetric analysis (TGA) (for thermal stability and water content) and BET method (for surface area). Furthermore, CEC of the zeolite was measured using ammonium acetate standard technique³⁵. Characterizations were done on zeolite samples with particle sizes between 250 and 425 µm except for the CEC which was done on samples with particle sizes of between 5.5 and 6 mm.

XRF results were obtained using PANalytical PW2400 Wavelength Dispersive instrument. The powder XRD patterns of the zeolite sample was obtained using a Rikagu Miniflex XRD (Japan) machine at CuK α radiation ($\lambda= 0.154$ nm), with a step size of 0.05° in the 2 θ range of 5–60°. Morphology was observed using Hitachi S 2600N SEM (Tokyo, Japan) operating at 5 kV of acceleration voltage. The TGA curves were obtained under nitrogen atmosphere from ambient temperature up to 1050°C with heating rate of 10 °C/min using a Mettler Toledo TGA/SDTA 851e model (Switzerland) with version 6.1 STARe software. The BET and Langmuir surface areas were obtained using a Micrometrics ASAP 2010 (Micrometrics, Norcross, USA). Known amounts of sample was loaded into the BET sample tube and degassed under vacuum (10^{-5} Torr) at 150 °C.

The CEC values of the zeolitic samples were measured using the ammonium acetate saturation (AMAS)³⁵ technique followed by using UV-VIS spectroscopy to determine the ammonium concentration. A known mass of the zeolite sample was contacted with 1 N solution of ammonium acetate (NH₄OAc). The samples were shaken in an end-over-end shaker for 5 days. After 5 days, the samples were allowed to air dry. The dried samples were then put in contact with 10% NaCl, 1% HCl in distilled water for 6 hours and the zeolite was filtered out. The supernatant was mixed with sodium salicylate, sodium hydroxide and sodium hypochlorite to determine the ammonium concentration. The sample was then analyzed using UV-VIS spectroscopy (Cary 100 UV-Visible

Spectrophotometer, Agilent, Santa Clara, USA) and correlated to the ammonium concentration (correlation shown in Figure A-1).

Lead concentration was determined by inductively coupled plasma optical emission spectrometry (ICP-OES) using a Varian Vista Pro ICP-OES with SPS-3 Auto-sampler (Australia). The wavelengths used in the ICP analysis were 182.143 nm, 217.00 nm, 220.353 nm, 261.417 nm and 283.305 nm. The lead concentration results from the 5 wavelengths were averaged to give the lead concentration reported in this work. Prior to ICP-OES analysis, the samples were filtered through 0.45 μm polyethersulfone membrane filters.

4.3.5 Experimental setup and procedure

4.3.5.1 Experimental setup

Figure 4-1 shows the experimental set-up used. The experiments were carried out at room temperature (21-25°C). The gas flow rate was controlled with a 50-500 mL/min rotameter. A diaphragm pump was used to introduce water/leachate to the column at a flow rate of 50-150 mL/min. Liquid was sprayed at the column top using a 90° full cone 303SS spray nozzle. All of the experiments were carried out in a column with 6 cm diameter and 70 cm height. The column pressure was adjusted with a ¼" back pressure regulator. The column was filled with Winsted precision glass balls. To avoid high pressure drop ¼" glass balls were used for absorption tests.

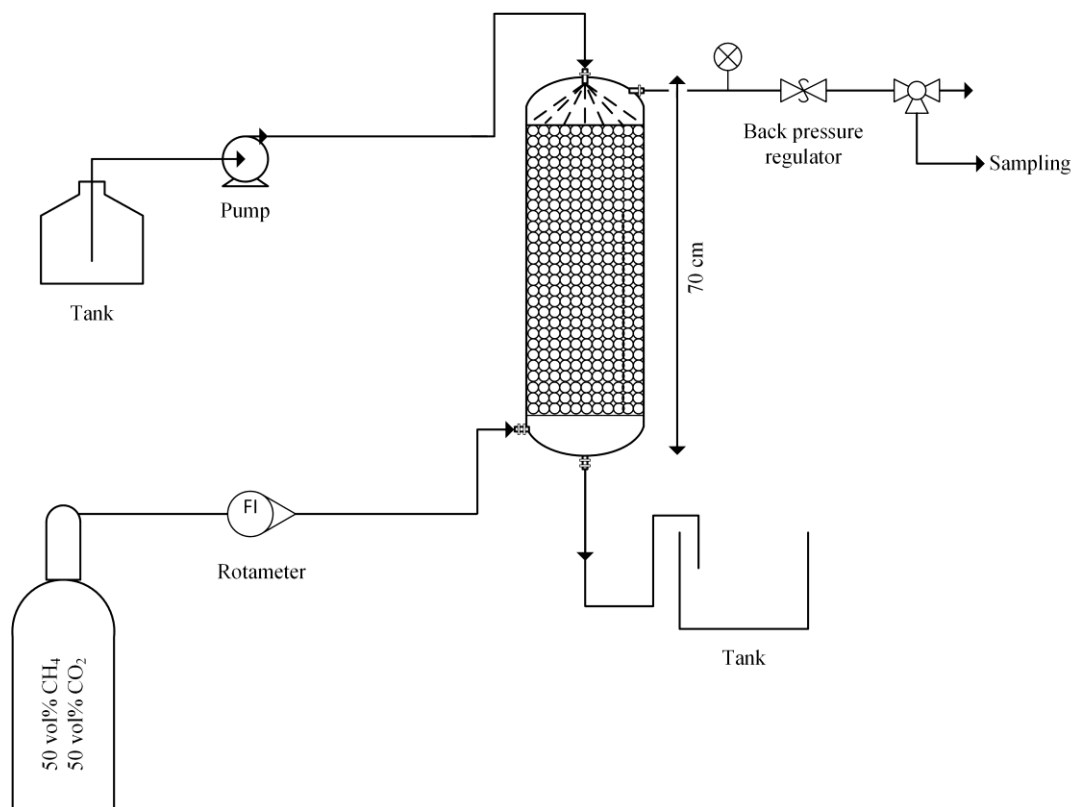


Figure 4-1 Hybrid sorption system schematic

4.3.5.2 Absorption column experimental procedure

The objective of this study was to remove CO_2 from a CO_2 - CH_4 mixture representing anaerobic LFG to increase the concentration of CH_4 . The mixture of gases was 50% CO_2 and 50% CH_4 , measured gravimetrically to 1% error. A premixed gas cylinder with this combination was supplied from Praxair (London, ON). The simulated LFG mixture pressure was kept constant using a pressure regulator.

Water was first pumped into the column. Once the water had reached the bottom, the gas was introduced in the bottom of the column to begin. A constant level of liquid (liquid holdup) was allowed at the bottom of the column to force the gas up through the bed. The constant level was controlled using a valve on the outlet tube. Without liquid, the gas preferentially chooses to go through the liquid outlet due to less pressure drop when

compared to the packed bed. The gas and water/leachate were allowed to run for 10 minutes before a gas sample was taken, to allow the column to reach equilibrium (equilibrium time found experimentally in the preliminary experiments; shown in Figure A-2) and to ensure results were independent of one another. Tests were all done in triplicates. Absorption tests were carried out with water and the results were compared with Aspen HYSYS® V8.6 to ensure the adequacy of the experimental system. The sour gas Peng-Robinson fluid package was used. Carbon dioxide is an acidic gas, therefore this had to be accounted for in the selection of fluid package. A GEM5000 (LANDTEC NORTH AMERICA, Colton, California) landfill gas analyzer was used to measure the gas composition (CO_2 and CH_4 vol%) in output stream. The compositions were normalized by subtracting the trace O_2 and N_2 from the gas analyzer results. All the leachate was collected at the bottom of the column and was reused for multipass leachate experiments.

4.3.5.3 Batch adsorption/ion exchange experimental procedure

For batch adsorption/ion exchange studies, 3 g ($\pm 1\%$) of zeolite was put in contact with 30 mL of the model leachate solution for 1 hour and 5 minutes in an end-over-end shaker in a PPCO tube at 20-30 rpm (average of 25 rpm) (equilibrium time is less than 6 hours; Figure A-3). Based on the concentration of lead, equilibrium concentration would be too low for accurate detection, so 1 hour and 5 minutes was chosen to ensure lead concentration was detectable. The batch tests were run in triplicate and 30 mL of model leachate solution was also mixed for 1 hour and 5 minutes in a PPCO tube as the baseline to account for any adsorption to the tube walls. The pH of the solutions was varied using HNO_3 and NaOH to determine the effect of pH on removal of lead. After both column and batch tests, the treated model leachate solutions were filtered through a 0.45 μm polyethersulfone membrane filter before being analyzed for lead concentration.

4.3.5.4 Adsorption/ion exchange column experimental procedure

The column was washed in 2% (by volume) nitric acid and the tanks and tubes were soaked in 2% nitric acid for 24 hours before the adsorption/ion exchange test to ensure any residual adsorbed heavy metals in the tanks were removed. Time was started when the first drops

of model leachate solution dropped into the column sump. Samples were taken from the outlet of the column and filtered through 0.45 μm polyethersulfone filters. In the previous sections, liquid holdup was used to force the gas upwards. However, to allow independent sample collections of treated model leachate, gas was not introduced into the column. The liquid holdup at the bottom would influence the future samples collected because the model leachate going through the column would mix with the liquid holdup.

4.4 Results and discussion

4.4.1 Adsorbent characterization

4.4.1.1 Chemical composition

XRF data for the clinoptilolite is summarized in Table 4-3. Si/Al ratio is an important characteristic of zeolites. The ratio affects physico-chemical properties of the zeolite. The ratio was calculated from the XRF data. The Si/Al ratio was 10.37 (mass basis) and 9.96 (mole basis), supporting data gathered from XRD patterns that the sample is a clinoptilolite-rich tuff zeolite belonging to the heulandite (HEU) family³⁶.

Loss on ignition (LOI) was determined by heating the sample at 1050°C for 3 hours in an electrical furnace and was 10.50%. Given the TGA (Figure 4-4) and LOI data, it can be concluded that the main weight loss of the natural samples resulted from water evaporation rather than decomposition of any component due to the large mass decrease at approximately 100°C.

Table 4-3 Chemical composition of the zeolite sample by XRF technique

	MRL^a (wt %)	Zeolite sample
SiO₂	0.2	67.50
TiO₂	0.04	0.30
Al₂O₃	0.1	11.50
Fe₂O₃	0.04	1.65
MnO	0.06	0.01
MgO	0.11	0.50
CaO	0.03	2.20
K₂O	0.06	4.11
Na₂O	0.08	0.91

P₂O₅	0.01	0.10
Cr₂O₃	0.01	<0.01
BaO	0.02	0.04
SrO	0.02	0.01
LOI^b	0.01	10.50
Total	--	99.54
Si/Al (wt)	--	10.37
Si/Al (mol)	--	9.96

^aMRL: Method Reporting Limit

^bLOI: Loss on Ignition

4.4.1.2 Phase purity (crystallinity) and morphology

The XRD result is shown in Figure 4-2. According to the XRD patterns presented in Figure 4-2, the main zeolitic phase pointed to the HEU structure, which can be either heulandite or clinoptilolite. Since the Si/Al ratio is higher than 4, clinoptilolite can be considered the major phase of the sample³⁶.

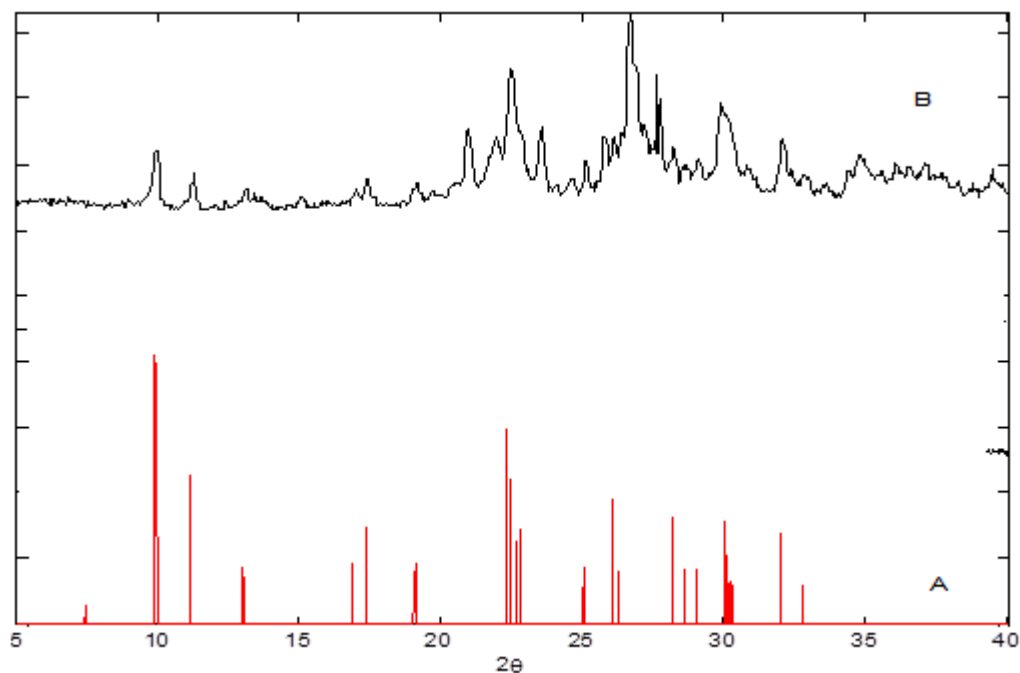


Figure 4-2 XRD Patterns of (A) pure clinoptilolite (simulated XRD pattern) compared with (B) zeolite sample

The zeolite sample was viewed under magnification using a SEM. Figure 4-3 shows the crystalline structure of clinoptilolite. Clinoptilolite is characterized by broad flat rectangular faces with angled corners³⁷.

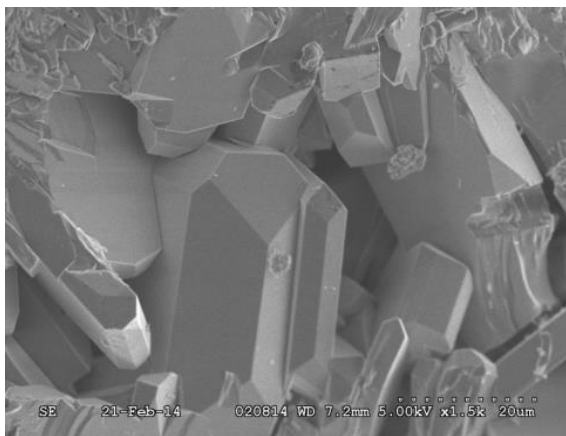


Figure 4-3 SEM micrograph of the zeolite sample

4.4.1.3 Thermal analysis

Figure 4-4 shows the TGA curve of the fresh (unused) zeolite sample. Approximately 9.5% weight loss occurred at 100°C. Another peak of about 1% weight loss at approximately 750°C leads to a total weight loss of 10.5%. This is in good agreement with the LOI value in Table 4-3.

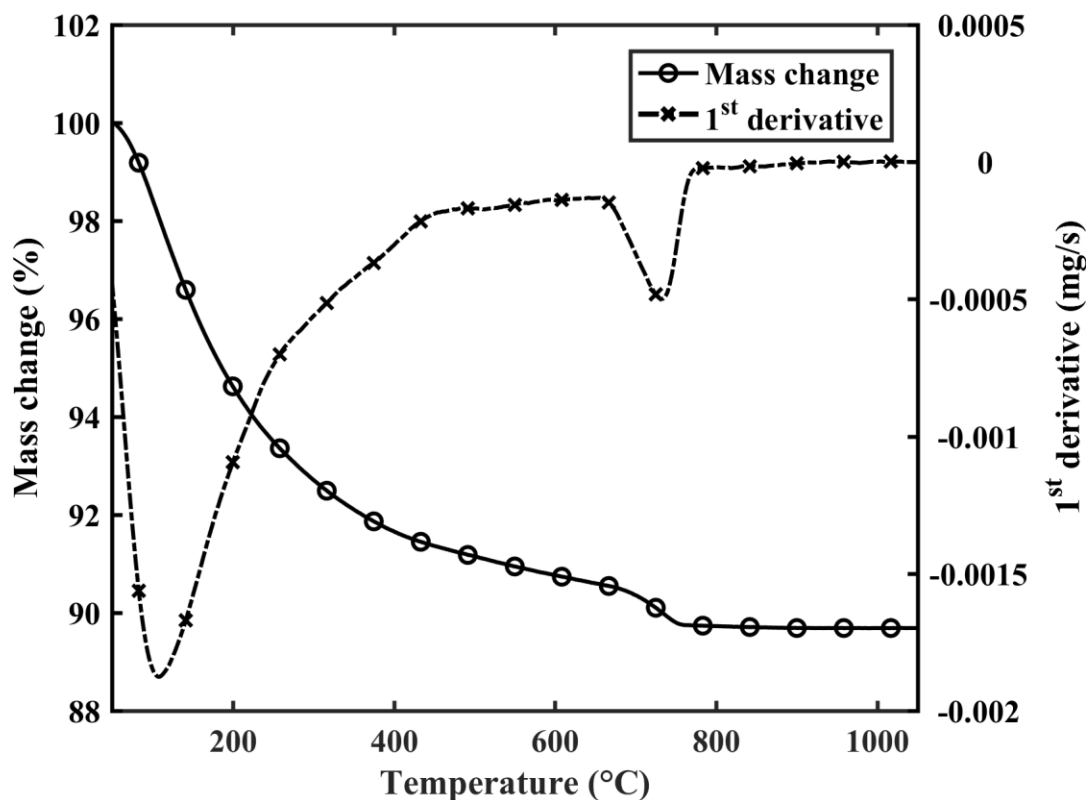


Figure 4-4 TGA curve of the zeolite sample (heating rate 10°C/min, under N₂ atmosphere)

The small peak (at approximately 750°C) can be attributed to minerals containing the carbonate ion (i.e. CO₃²⁻) such as calcium carbonate³⁸. Calcium carbonate decomposes around 700-900°C³⁹. The weight loss of the sample at approximately 750°C is close to 1%.

4.4.1.4 Surface area

The BET surface area was found to be 28.2 m²/g. The Langmuir surface area was found to be 38.9 m²/g. The micropore area was found to be 7.2 m²/g and the external surface area was found to be 21.0 m²/g. The majority of the surface area was the external surface as it was 74.5% of the total surface area.

4.4.1.5 Cation exchange capacity

Cation exchange capacity is a specific characteristic of a zeolite, which depends on its structural chemistry. CEC is a measure of how many cation exchange sites are available.

After saturation for 5 days at room temperature, the supernatant was filtered and the saturated zeolite dried thoroughly at room temperature. After saturation, all of the exchange sites are occupied by NH_4^+ ions. The amount of NH_4^+ (concentration) ions is a measure of CEC. To measure CEC, the NH_4^+ ions have to be removed from the zeolite and measured. To accomplish this the NH_4^+ -saturated samples were soaked in a 10% NaCl, 1% HCl solution to exchange the NH_4^+ ions with Na^+ ions according to the following reaction:



The ammonium saturated zeolite was soaked in 25 mL of 10% NaCl, 1% HCl solution for 6 hours. The ammonium concentration was measured using an assay made by mixing the supernatant with sodium salicylate, sodium hydroxide and sodium hypochlorite. The colour of the solutions was calibrated with known ammonium concentrations using UV-VIS spectroscopy (Figure A-1).

According to the results, the CEC of the zeolite used for the column was 0.85 ± 0.16 meq/g and the CEC of the zeolite used for the batch pH tests was 0.98 ± 0.09 meq/g. The CEC values are comparable to clinoptilolite CEC values reports in literature³⁸.

4.4.2 Absorption

4.4.2.1 Agreement between the experimental and simulated results of absorption

The first step for this study was to determine if the designed column performed correctly. To accomplish this, experimental results using water as the absorbent and glass beads as packing were used. The experimental results were compared to simulation results obtained from Aspen HYSYS V.8.6. The results are shown in Figure 4-5.

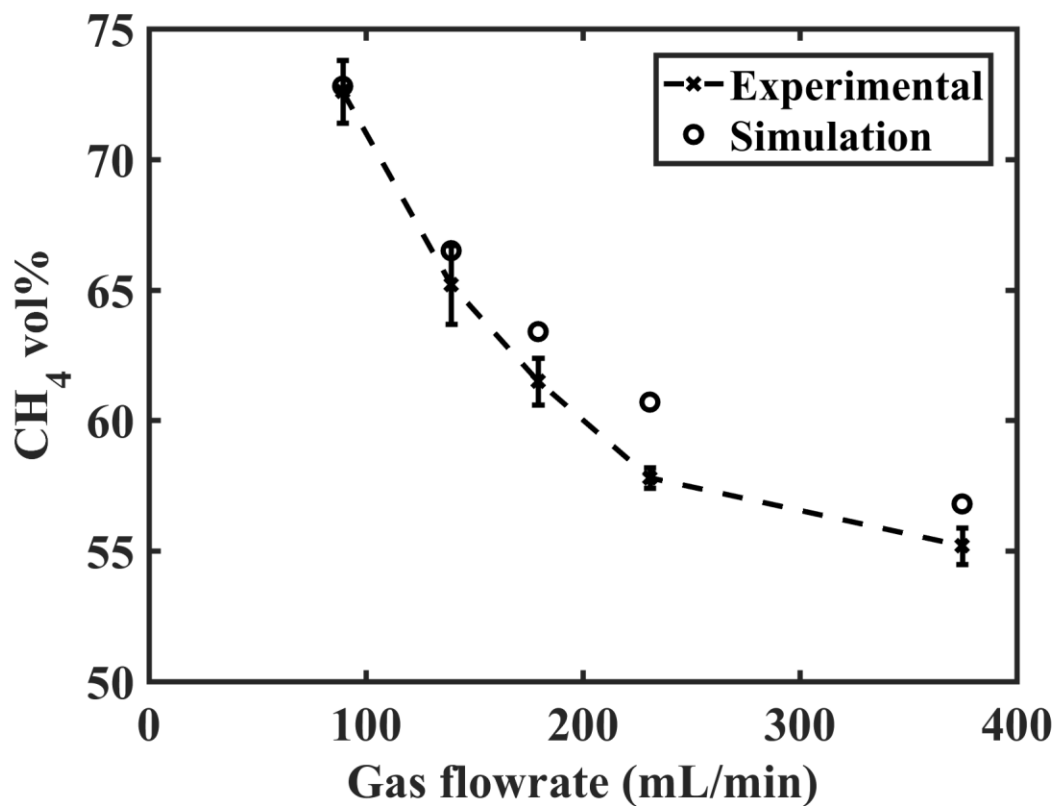


Figure 4-5 Experimental results vs. Aspen HYSYS simulation results

Figure 4-5 shows the agreement between the experimental and simulated results. This verified the column's operational functionality.

4.4.2.2 Comparison of the performance of different packings and absorbents

Using leachate as an absorbent was compared to water to test its performance in removing carbon dioxide. The performance of the zeolite particles was also compared to glass beads to test its efficacy as packing material.

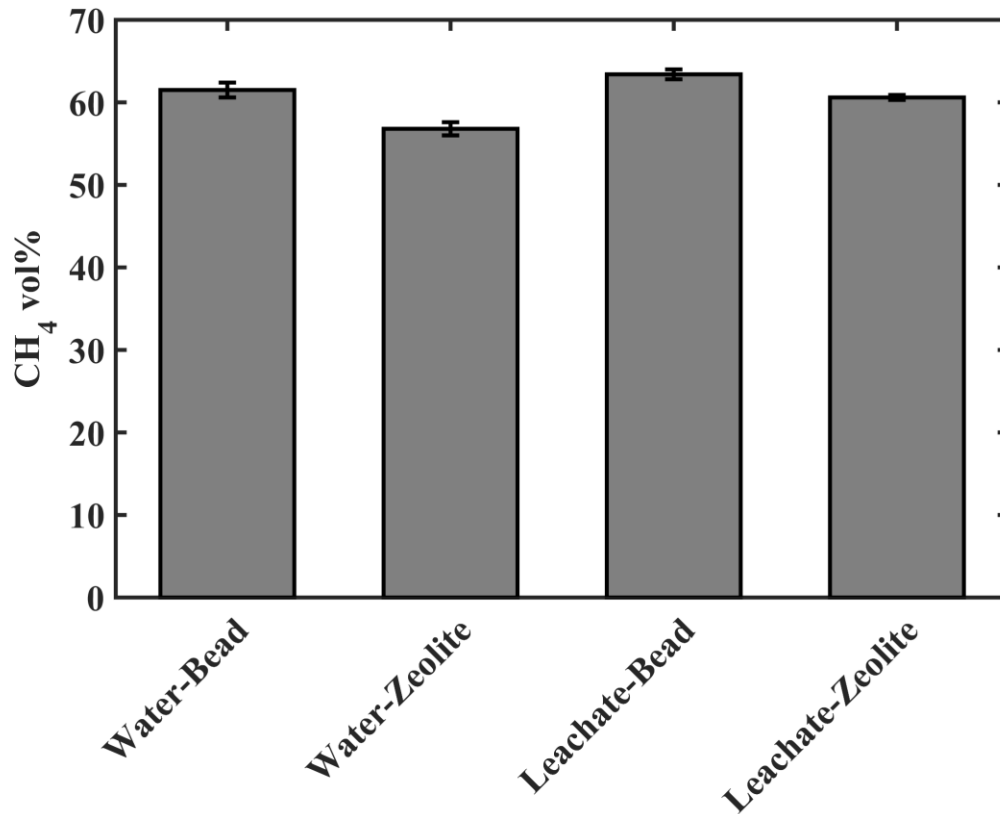


Figure 4-6 Methane vol% with different packing and absorbents

Figure 4-6 shows that using glass beads as packing compared to zeolite provided a higher vol% of methane in the outlet gas stream (more carbon dioxide removal). Using beads, water and leachate achieved a CH₄ vol% of 61.5% and 63.4%, respectively. Using zeolite, water and leachate achieved a CH₄ vol% of 56.8% and 60.6%, respectively. The function of the packing is to provide a greater surface area and a longer residence time to allow for mass transfer of carbon dioxide from the gas phase to the liquid phase (either water or leachate). There was a slight increase in the methane volume fraction using glass beads when compared to zeolite. This was due to the uniformity of the spheres when compared to the zeolite. Due to the non-uniformity of the zeolite particles, some channeling in the liquid phase occurred. Some portions of the column did not become wet. The channeling decreased residence time and did not allow the water to become saturated with carbon

dioxide. While performing the experiments with zeolite, it was seen that the water/leachate was more evenly distributed in the top half of the column and channeling was more apt to occur in the bottom half.

Also, leachate provided a greater removal of carbon dioxide from the gas (Figure 4-6). Using leachate, beads and zeolite achieved a CH₄ vol% of 63.4% and 60.6%, respectively. Using water, beads and zeolite achieved a CH₄ vol% of 61.5% and 56.8%, respectively. The pH of the leachate was 7.56 (slightly basic) and the pH of the water was 6.53 (slightly acidic). The basicity of the leachate favours the dissolution of carbon dioxide more than the water. The dissolution of carbon dioxide in water proceeds via the following equilibrium reaction:



The basicity (hydroxide ions) neutralized some of the carbonic acid produced, favouring the forward reaction when the leachate was used.

4.4.2.3 Simulation results at higher pressures

Absorption columns are typically run at pressures much higher than atmospheric pressure^{17,18}. Figure 4-7 shows the methane vol% simulation results at higher pressures using water. The sorption system was limited in increasing pressure due to safety requirements. However, as shown by Figure 4-5, experimentation and simulation results at atmospheric pressure were in close agreement. Therefore, simulation can be used to provide results at higher pressures. At 20 atm, the vol% of CH₄ was greater than 95%. The simulation was run using the same water flowrate and the same gas molar flowrate. In Section 4.4.2.2, leachate showed a slightly higher methane vol% than water (beads – 63.4% and 61.5%, respectively and zeolite – 60.6% and 56.8%, respectively) when compared to water (Figure 4-6).

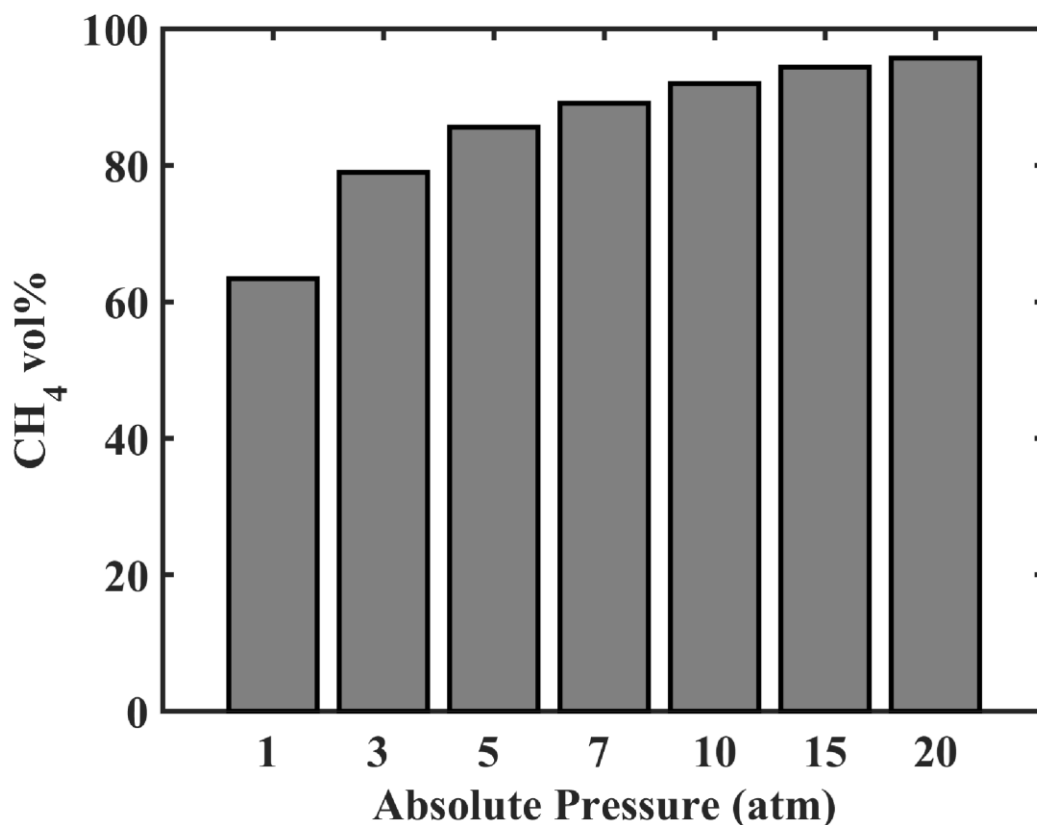


Figure 4-7 Methane vol% simulation results at higher pressures using water

At higher pressures, leachate can be used to separate carbon dioxide and methane. At 20 atm, water increased the methane vol% to approximately 95%. Using leachate can provide similar (or slightly increased) methane purity.

4.4.2.4 Multipass leachate absorption

After the leachate was used as an absorbent, the leachate was subsequently reused to test its efficacy as an absorbent. Figure 4-8 shows the methane vol% as the leachate is used multiple times. Gas composition reached equilibrium after the second recycle for the zeolite packing at approximately 55% methane. The pH reached an equilibrium of approximately 6.5 after the first recycle (Figure 4-9). The equilibrium pH achieved using

the glass beads was lower than the zeolite after the first recycle. This could be due to more carbon dioxide dissolved, producing more acid.

On the first leachate use, the glass bead packing removed more carbon dioxide than the zeolite packing; 26.8% and 21.2% CO₂ removal, respectively. This caused the leachate to become saturated in carbon dioxide. After the first recycle, carbon dioxide desorbed from the carbon dioxide in the suction line, near the inlet of the pump. This caused tiny bubbles to form and severely affected the pump operation, and did not allow any further recycles. The zeolite packing did not achieve the same dissolution of carbon dioxide and did not have this problem.

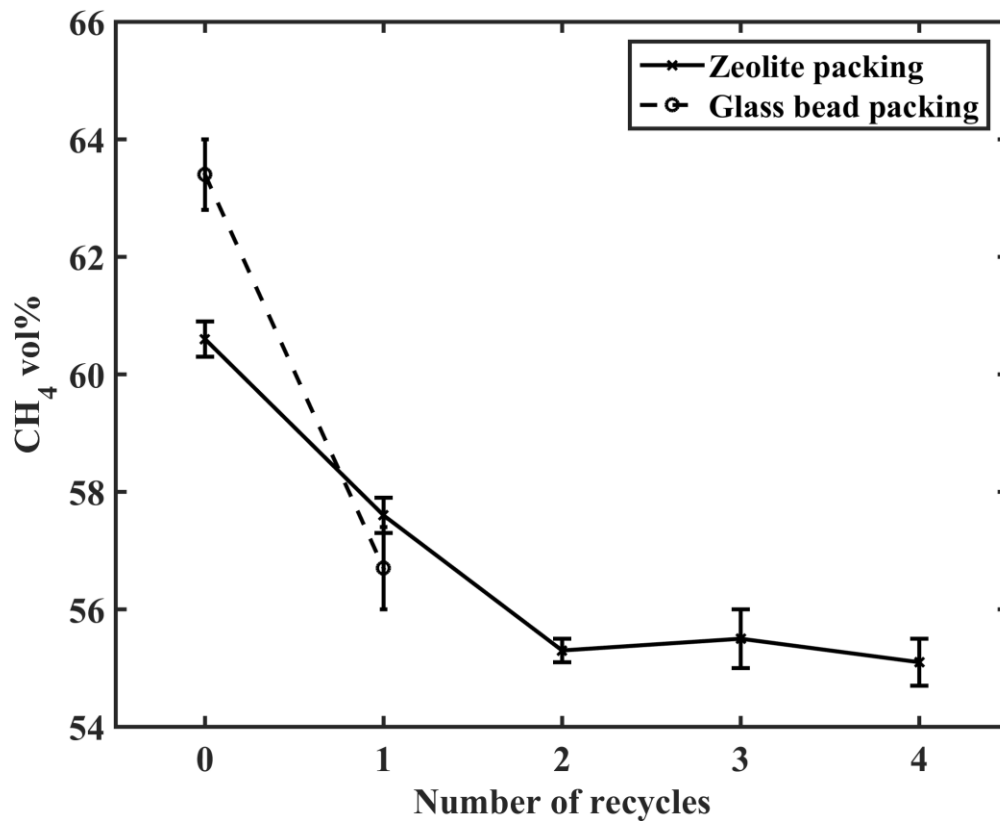
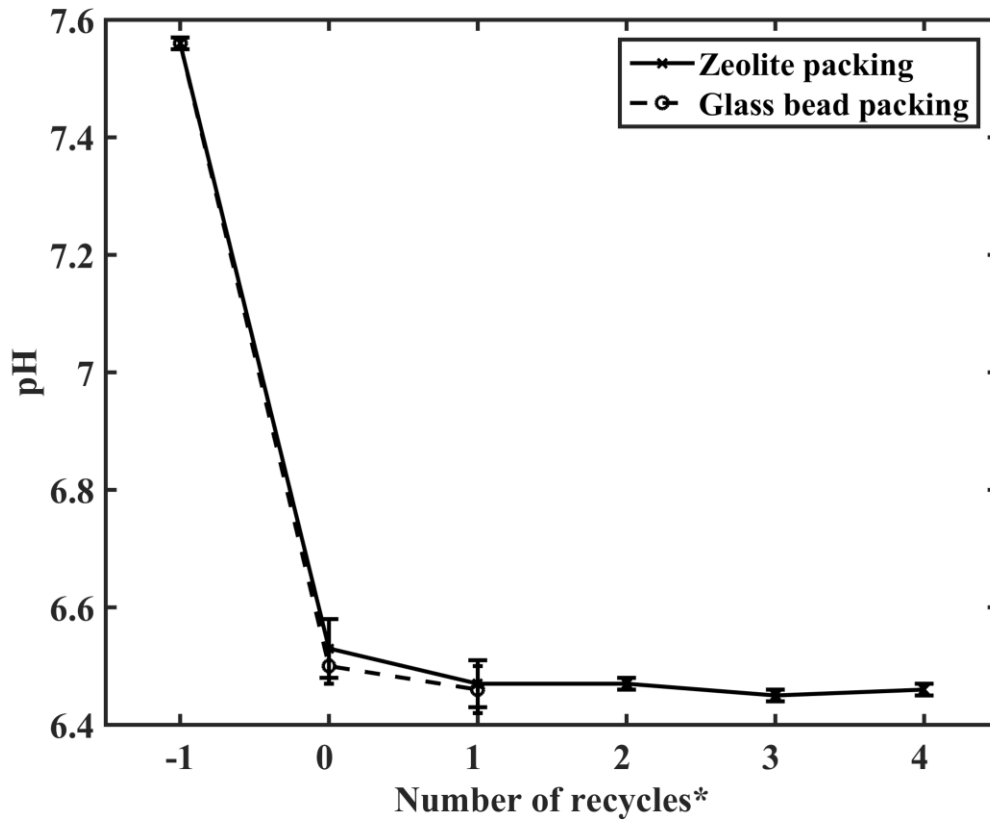


Figure 4-8 CH₄ vol% after multiple leachate reuse



*-1 indicates initial pH (before use)

Figure 4-9 pH after multiple leachate reuse

Due to the absorption being performed at atmospheric pressure, little carbon dioxide was desorbed after completion. If the absorption were performed at elevated pressures, a return to atmospheric pressure would have removed the majority of the carbon dioxide, and allowed more carbon dioxide to be absorbed in subsequent uses and prevented cavitation occurring.

4.4.3 Adsorption/ion exchange

4.4.3.1 Batch adsorption/ion exchange test; pH in the batch tests

A batch adsorption/ion exchange test was performed using the zeolite particles to determine how much lead could be removed from the model leachate solution under ideal batch conditions. Depending on the age of the landfill (and the subsequent age of the leachate), the pH can vary between acidic and basic conditions. Anaerobic landfills are characterized by acidic leachate early in their lives as acidic compounds are produced. The landfills become less acidic over time as the acidic species are consumed⁴⁰. Figure 4-10 shows the initial pH and final pH after 1 hour of contact time between the model leachate solution and the zeolite. Figure 4-11 shows the removal of lead with varying pH. Starting at 100 ppm lead concentration, at pH 2.8, 4.9 and 5.6 the removal of lead was $99.64 \pm 0.07\%$, $99.77 \pm 0.06\%$ and $99.84 \pm 0.07\%$, respectively. The most acidic samples showed the least removal of lead. This is due to the hydronium ions being in competition with the lead ions for the cation sites on the zeolite. This results in an increase in pH (Figure 4-10). As the pH increased (B and C in Figure 4-10), less hydronium ions were in competition for the cation sites, the removal of lead increased and the pH increase was not as large (Figure 4-10). Since less hydronium ions are present, the driving force is less than A (Figure 4-10) and less hydronium ions are exchanged. Once the pH became basic (D), the lead precipitated out. The precipitate was filtered out and adsorption/ion exchange experiments were carried out. The pH decreased (became more acidic) due to the slight acidic nature of zeolites. Removal at D (Figure 4-11) conditions were $91.64 \pm 2.25\%$. The initial precipitation decreased the concentration from 100 ppm to approximately 2.5 ppm. Removal at basic conditions decreased due to the competition between the Pb^{2+} and the Na^+ ions for the cation exchange sites. The Na^+ ions are added when the pH is increased using NaOH.

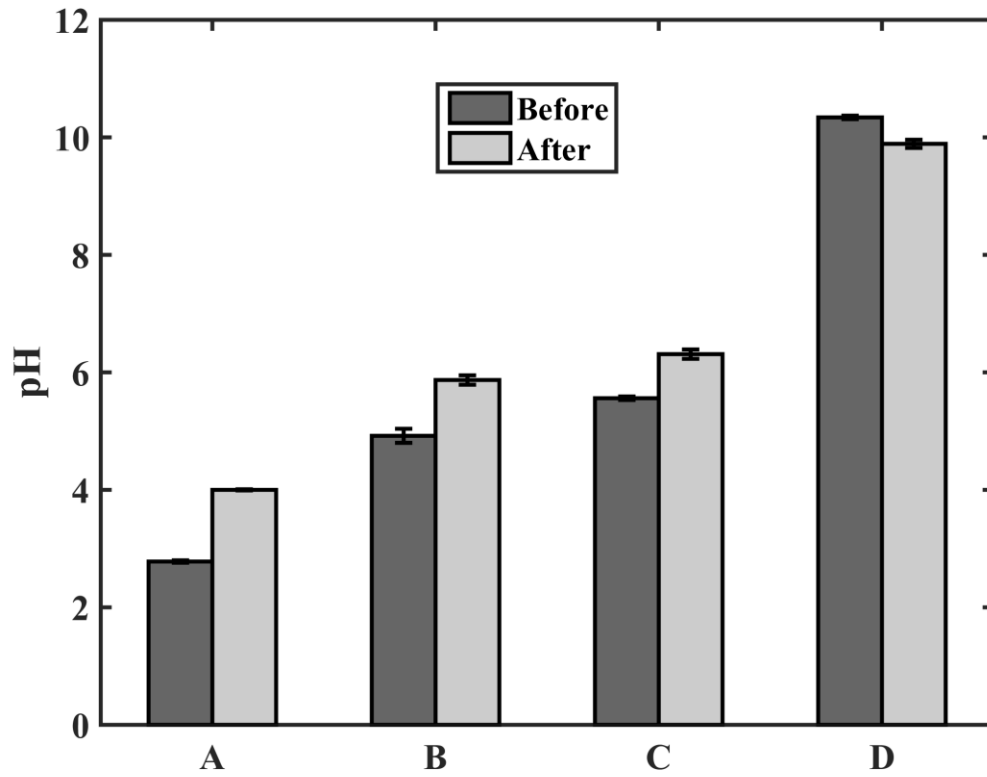


Figure 4-10 pH before and after zeolite contact

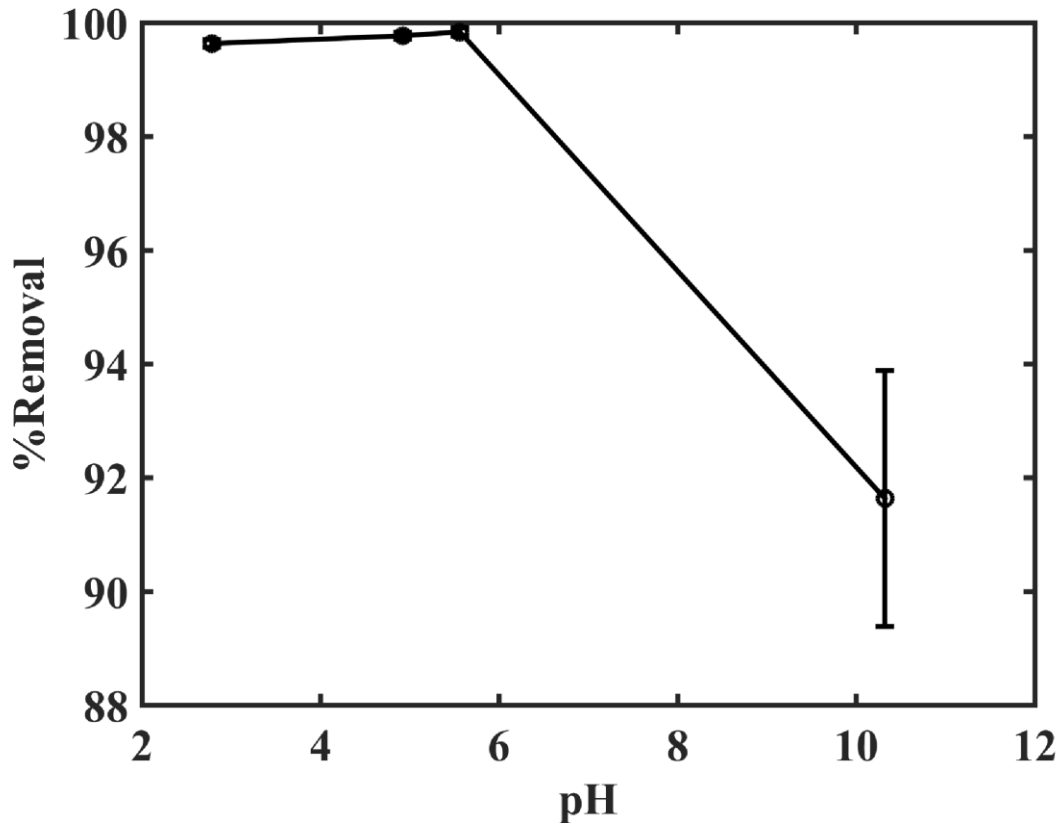


Figure 4-11 %Removal at different initial pH values

The lead precipitation (via hydroxide precipitation) is given by the following equilibrium reaction:



From this reaction, the pH at which precipitation occurs can be determined. This is done using the following equation (K_{sp} value was found from the CRC Handbook⁴¹ with a value of $1.43e-20$):

$$K_{sp} = [Pb^{2+}][OH^-]^2 \Rightarrow [OH^-] = \sqrt{\frac{K_{sp}}{[Pb^{2+}]}}$$

$$pOH = -\log[OH^-] \Rightarrow pH = 14 - pOH = 5.74$$

Therefore, based on this calculation, at 100 ppm, lead precipitates at a pH of 5.74.

The Ontario guidelines for daily lead discharge in process effluent is 0.4 ppm⁴². After 1 hour, the lead concentration did not decrease below the guidelines for discharge. However, 1 hour was not enough contact time to reach equilibrium (Figure A-3). After 12 hours of contact time (equilibrium time surpassed) the concentration of lead was below 0.4 ppm. This was below the discharge limit.

4.4.3.2 Continuous adsorption/ion exchange column test

Figure 4-12 shows the concentration divided by the initial concentration of lead as time progresses while flowing through the adsorption/ion exchange column. The lead concentration decreased to between 8 and 10 ppm at the column exit. The removal was not enough for safe discharge and meeting the environmental guidelines. Therefore, the leachate would need further treatment to decrease the lead concentration. Clinoptilolite with a particle size of 7.6 ± 1.6 mm was used as packing. Due to the shape of the zeolite particles, the lead did not have access to the sites inside of the zeolite for ion exchange/adsorption due to the short residence time. The lead ions only had access to the surface sites, significantly decreasing the area available for removal of lead. By increasing the height of the column, the lead concentration can decrease below 8 ppm. The highest removal of lead occurs at the start of the adsorption/ion exchange process. Furthermore, due to the particle shape of the zeolites, channeling was observed. A small portion of the zeolite particles were in contact with the zeolite.

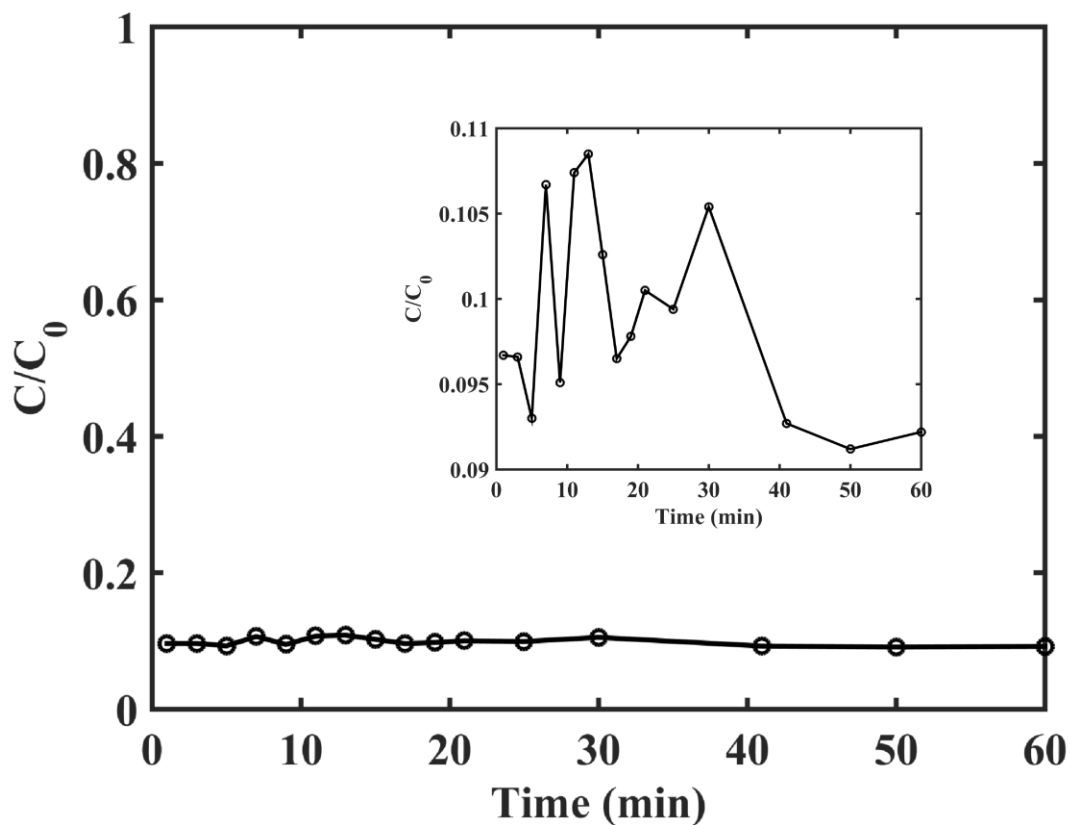


Figure 4-12 Lead concentration divided by initial lead concentration over time (inset is a zoomed in view of the line)

4.5 Conclusions

Clinoptilolite was characterized and used for lead removal from model leachate solution. It was also partially used as packing in a hybrid sorption column for absorption to purify methane by removing carbon dioxide from a 50-50 mixture of CO_2 and CH_4 representing the LFG.

The column efficacy was tested by comparing experimental results at different gas flowrates with Aspen HYSYS V8.6 simulation results. The experimental results agreed with the results found using Aspen HYSYS at atmospheric pressure. When used as packing for absorption, clinoptilolite showed slightly less carbon dioxide removal efficiency

compared to traditional inert spherical glass bead (56.8% to 61.5% for water and 60.6% to 63.4% for leachate). The non-uniformity of the clinoptilolite particles was proposed to have caused channeling of the liquid and did not allow sufficient residence time for equilibrium between the liquid and gas phases. Landfill leachate was tested for use as an absorbent in the place of water. At the same gas and liquid flowrates, there was a 1.9% increase in removal of carbon dioxide using leachate instead of water using glass bead packing and 3.8% increase using zeolite packing. Simulation results showed at 10 atm, the methane vol% was greater than 90%, showing an approximately 80% removal of carbon dioxide. Reusing leachate as an absorbent showed potential when using zeolite packing. Gas composition equilibrium was reached after 2 recycles at 55% of methane. However, when using glass beads, carbon dioxide saturated the leachate and caused desorption (cavitation) at the inlet of the pump, negatively affecting performance.

During batch adsorption/ion exchange tests, removal of lead increased as pH increased until neutral pH. The higher the pH, the less hydronium ions were in competition for the ion exchange sites. At basic pH (pH 10.3), the sodium ions (from sodium hydroxide) were in competition with the lead ions, showing less lead removal. Precipitation decreased the lead concentration to 2.5 ppm. Starting from 2.5 ppm, at pH 10.3, $91.64 \pm 2.25\%$ removal of lead was observed. Starting at 100 ppm lead concentration, at pH 2.8, 4.9 and 5.6 the removal of lead was $99.64 \pm 0.07\%$, $99.77 \pm 0.06\%$ and $99.84 \pm 0.07\%$, respectively. Increasing pH greater than 5.74 causes lead precipitation. After contact with the zeolite, the lower the pH, the higher the pH increased. This was due to a higher concentration of hydronium ions causing a larger driving force for uptake of the hydronium ions.

Further work can be done on scaling up and increasing the pressure of the column to examine the removal of carbon dioxide. More work can also be done on the kinetics of the removal of the heavy metals. The complexity of the processes that are occurring (absorption, adsorption/ion exchange, fluid flow) should also be modelled to better understand what is occurring.

4.6 References

1. Huber-Humer M, Kjeldsen P, Spokas KA. Special issue on landfill gas emission and mitigation. *Waste Manag.* 2011;31(5):821–2.
2. Bogner J, Pipatti R, Hashimoto S, Diaz C, Mareckova K, Diaz L, et al. Mitigation of global greenhouse gas emissions from waste: conclusions and strategies from the Intergovernmental Panel on Climate Change (IPCC) Fourth Assessment Report. Working Group III (Mitigation). *Waste Manag Res.* 2008;26(1):11–32. Doi: 10.1177/0734242X07088433.
3. Rasmussen RA, Khalil MAK. Atmospheric methane in the recent and ancient atmospheres: Concentrations, trends, and interhemispheric gradient. *J Geophys Res Atmospheres.* 1984;89(D7):11599–605. Doi: 10.1029/JD089iD07p11599.
4. Aguilar-Virgen Q, Taboada-González P, Ojeda-Benítez S. Analysis of the feasibility of the recovery of landfill gas: a case study of Mexico. *J Clean Prod.* 2014;79:53–60. Doi: 10.1016/j.jclepro.2014.05.025.
5. Bove R, Lunghi P. Electric power generation from landfill gas using traditional and innovative technologies. *Energy Convers Manag.* 2006;47(11–12):1391–401. Doi: 10.1016/j.enconman.2005.08.017.
6. Solov'yanov AA. Associated petroleum gas flaring: Environmental issues. *Russ J Gen Chem.* 2011;81(12):2531–41. Doi: 10.1134/S1070363211120218.
7. Ménard C, Ramirez AA, Nikiema J, Heitz M. Biofiltration of methane and trace gases from landfills: A review. *Environ Rev.* 2012;20(1):40–53. Doi: 10.1139/a11-022.
8. Goossens MA. Landfill gas power plants. *Renew Energy.* 1996;9(1–4):1015–8. Doi: 10.1016/0960-1481(96)88452-7.

9. Morgan SM, Yang Q. Use of Landfill Gas for Electricity Generation. *Pract Period Hazard Toxic Radioact Waste Manag.* 2001;5(1):14–24. Doi: 10.1061/(ASCE)1090-025X(2001)5:1(14).
10. Themelis NJ, Ulloa PA. Methane generation in landfills. *Renew Energy.* 2007;32(7):1243–57. Doi: 10.1016/j.renene.2006.04.020.
11. Mostbauer P, Lombardi L, Olivieri T, Lenz S. Pilot scale evaluation of the BABIU process – Upgrading of landfill gas or biogas with the use of MSWI bottom ash. *Waste Manag.* 2014;34(1):125–33. Doi: 10.1016/j.wasman.2013.09.016.
12. Jewaskiewitz B. Landfill gas recovery, green energy, and the clean development mechanism. *Civ Eng Mag South Afr Inst Civ Eng.* 2010;18(7):19–23.
13. Dang H, Rochelle GT. CO₂ Absorption Rate and Solubility in Monoethanolamine/Piperazine/Water. *Sep Sci Technol.* 2003;38(2):337–57. Doi: 10.1081/SS-120016678.
14. Diao Y-F, Zheng X-Y, He B-S, Chen C-H, Xu X-C. Experimental study on capturing CO₂ greenhouse gas by ammonia scrubbing. *Energy Convers Manag.* 2004;45(13-14):2283–96. Doi: 10.1016/j.enconman.2003.10.011.
15. Gaur A, Park J-W, Maken S, Song H-J, Park J-J. Landfill gas (LFG) processing via adsorption and alkanolamine absorption. *Fuel Process Technol.* 2010;91(6):635–40. Doi: 10.1016/j.fuproc.2010.01.010.
16. Kim GH, Park SY, You JK, Hong WH, Kim J-N, Kim J-D. CO₂ absorption kinetics in a CO₂-free and partially loaded aqueous ammonia solution 2014;250:83–90.
17. Rasi S, Lantelä J, Veijanen A, Rintala J. Landfill gas upgrading with countercurrent water wash. *Waste Manag.* 2008;28(9):1528–34. Doi: 10.1016/j.wasman.2007.03.032.

18. Rasi S, Läntelä J, Rintala J. Upgrading landfill gas using a high pressure water absorption process. *Fuel*. 2014;115:539–43. Doi: 10.1016/j.fuel.2013.07.082.
19. Cozma P, Wukovits W, Mămăligă I, Friedl A, Gavrilesco M. Modeling and simulation of high pressure water scrubbing technology applied for biogas upgrading. *Clean Technol Environ Policy*. 2015;17(2):373–91. Doi: 10.1007/s10098-014-0787-7.
20. Zamzow MJ, Eichbaum BR, Sandgren KR, Shanks DE. Removal of Heavy Metals and Other Cations from Wastewater Using Zeolites. *Sep Sci Technol*. 1990;25(13-15):1555–69. Doi: 10.1080/01496399008050409.
21. Kobya M, Demirbas E, Senturk E, Ince M. Adsorption of heavy metal ions from aqueous solutions by activated carbon prepared from apricot stone. *Bioresour Technol*. 2005;96(13):1518–21. Doi: 10.1016/j.biortech.2004.12.005.
22. Zaini MAA, Amano Y, Machida M. Adsorption of heavy metals onto activated carbons derived from polyacrylonitrile fiber. *J Hazard Mater*. 2010;180(1–3):552–60. Doi: 10.1016/j.jhazmat.2010.04.069.
23. Kanawade SM, Gaikwad RW. Adsorption of heavy metals by activated carbon synthesized from solid wastes. *Int J Chem Eng Appl*. 2011;2(3):207–11.
24. Rahman MM, Adil M, Yusof AM, Kamaruzzaman YB, Ansary RH. Removal of Heavy Metal Ions with Acid Activated Carbons Derived from Oil Palm and Coconut Shells. *Materials*. 2014;7(5):3634–50. Doi: 10.3390/ma7053634.
25. Malliou E, Loizidou M, Spyrellis N. Uptake of lead and cadmium by clinoptilolite. *Sci Total Environ*. 1994;149(3):139–44. Doi: 10.1016/0048-9697(94)90174-0.
26. Ouki SK, Kavannagh M. Performance of natural zeolites for the treatment of mixed metal-contaminated effluents. *Waste Manag Res*. 1997;15(4):383–94. Doi: 10.1177/0734242X9701500406.

27. Erdem E, Karapinar N, Donat R. The removal of heavy metal cations by natural zeolites. *J Colloid Interface Sci.* 2004;280(2):309–14. Doi: 10.1016/j.jcis.2004.08.028.
28. Fang Q-R, Yuan D-Q, Sculley J, Li J-R, Han Z-B, Zhou H-C. Functional Mesoporous Metal–Organic Frameworks for the Capture of Heavy Metal Ions and Size-Selective Catalysis. *Inorg Chem.* 2010;49(24):11637–42. Doi: 10.1021/ic101935f.
29. Tuncan A, Tuncan M, Koyuncu H, Guney Y. Use of natural zeolites as a landfill liner. *Waste Manag Res.* 2003;21(1):54–61. Doi: 10.1177/0734242X0302100107.
30. Turan NG, Ergun ON. Removal of Cu(II) from leachate using natural zeolite as a landfill liner material. *J Hazard Mater.* 2009;167(1-3):696–700.
31. Ozel U, Akdemir A, Ergun ON. Utilization of natural zeolite and perlite as landfill liners for in situ leachate treatment in landfills. *Int J Environ Res Public Health.* 2012;9(5):1581–92. Doi: 10.3390/ijerph9051581.
32. Ontario Energy Board. Natural gas rate updates. Natural Gas Rate Updates. Available at <http://www.ontarioenergyboard.ca/OEB/Consumers/Natural+Gas/Natural+Gas+Rates>.
33. Martín S, Marañón E, Sastre H. Landfill gas extraction technology: study, simulation and manually controlled extraction. *Bioresour Technol.* 1997;62(1-2):47–54.
34. Kowalczyk P, Sprynskyy M, Terzyk AP, Lebedynets M, Namieśnik J, Buszewski B. Porous structure of natural and modified clinoptilolites. *J Colloid Interface Sci.* 2006;297(1):77–85. Doi: 10.1016/j.jcis.2005.10.045.
35. Bain DC, Smith BFL. A Handbook of Determinative Methods in Clay Mineralogy. *A Handbook of Determinative Methods in Clay Mineralogy*. Glasgow: Blackie & Son Ltd.; 1987. p. 248–74.

36. Cotton A. Dissolution kinetics of clinoptilolite and heulandite in alkaline conditions. *Biosci Horiz.* 2008;1(1):38–43. Doi: 10.1093/biohorizons/hzn003.
37. Snellings R, Haren TV, Machiels L, Mertens G, Vandenberghe N, Elsen J. Mineralogy, Geochemistry, and Diagenesis of Clinoptilolite Tuffs (miocene) in the Central Simav Graben, Western Turkey. *Clays Clay Miner.* 2008;56(6):622–32. Doi: 10.1346/CCMN.2008.0560603.
38. Du Q, Liu S, Cao Z, Wang Y. Ammonia removal from aqueous solution using natural Chinese clinoptilolite. *Sep Purif Technol.* 2005;44(3):229–34. Doi: 10.1016/j.seppur.2004.04.011.
39. Galan I, Glasser FP, Andrade C. Calcium carbonate decomposition. *J Therm Anal Calorim.* 2012;111(2):1197–202. Doi: 10.1007/s10973-012-2290-x.
40. Erses AS, Onay TT, Yenigun O. Comparison of aerobic and anaerobic degradation of municipal solid waste in bioreactor landfills. *Bioresour Technol.* 2008;99(13):5418–26. Doi: 10.1016/j.biortech.2007.11.008.
41. William Haynes. *CRC Handbook of Chemistry and Physics*. Boca Raton: CRC Press; 2014.
42. Government of Ontario. O. Reg. 560/94: Effluent monitoring and effluent limits - metal mining sector. Ontario.ca. Available at <https://www.ontario.ca/laws/regulation/940560#BK27>. Accessed February 12, 2016.

Chapter 5

5 Conclusions and recommendations

5.1 Conclusions

A mathematical model was developed that captured the phenomena occurring during the conversion of an anaerobic landfill into an aerobic landfill. In the beginning of the conversion process, the main limiting factor in the conversion from an anaerobic to aerobic landfill, was the initial aerobic biomass. Aerobic biodegradation is an exothermic process. Therefore, temperature can be used to observe the efficacy of the conversion. At initial aerobic concentrations of 0.01, 0.1, 0.6, 1 and 5 kg/m³ showed average waste temperatures of approximately 20.0, 20.2, 21.0, 21.9 and 49.6°C. The higher the initial biomass concentration, the faster the temperature increased (indicating aerobic biomass growth). However, at 5 kg/m³ the model showed that the oxygen was being consumed before it reached the entire reactor (waste). In reality, this will cause the waste to be biodegraded in plugs (like in a plug flow reactor). The model demonstrated that increasing the temperature up to the optimum growth temperature of aerobic bacteria (58.6°C), increased the aerobic biomass growth rate, oxygen consumption rate and carbon dioxide production rate. However, if the temperature exceeded the optimal temperature (58.6°C) for aerobic biomass growth, the opposite behavior (lower aerobic biomass growth rate, oxygen consumption rate and carbon dioxide production rate) was observed. The model also showed that varying leachate flowrate was a more effective temperature control method when compared to varying air flowrate. This was due to leachate having a higher specific heat capacity compared to air.

A combined sorption (absorption and adsorption/ion exchange) column was proposed for the removal of carbon dioxide from LFG (absorption) and heavy metals from leachate (adsorption/ion exchange). The column had a diameter of 6 cm and a height of 70 cm. The heights of the beds (glass beads/zeolite) were between 52 and 55 cm. The sorption column's efficacy was tested by verifying the experimental data against simulation data

found using Aspen HYSYS. The experimental data agreed with the simulation results proving the operability of the column. The column was tested with both glass bead packing and granular zeolite packing to determine the difference in their ability to remove carbon dioxide from a gas mixture of 50% CO₂ and 50% CH₄ representing a typical landfill gas (LFG). The glass beads showed higher (water – 61.5% and 56.8%, respectively and leachate – 63.4% and 60.6%, respectively) removal of carbon dioxide than zeolite due to channeling that occurred with the zeolite packing. The short residence time did not allow equilibrium to be established between the liquid and gas phases.

Batch tests showed that the higher the pH (up to neutral pH), the more lead was removed. Contact was made with 30 mL of model leachate solution (100 ppm Pb, made using lead(II) nitrate) and 3 g of zeolite (clinoptilolite) for 1 hour and 5 minutes before being filtered to remove the zeolite. The zeolite particle size was 7.6 ± 1.6 mm. Zeolite and model leachate were in contact in a PPCO tube, mixing in a rotating oven at 25 rpm. The contact time was chosen so that the lead concentration was high enough (>0.01 ppm) for accurate measurement. Batch adsorption tests showed that removal of lead increased as pH became more neutral. The higher the pH (in the acidic pH range), the less H⁺ ions were competing for the ion exchange sites. At basic pH, the addition of sodium hydroxide added sodium ions. The sodium ions were in competition with the lead ions and less lead was removed. Starting at 100 ppm lead concentration, at pH 2.8, 4.9 and 5.6 the removal of lead was $99.64 \pm 0.07\%$, $99.77 \pm 0.06\%$ and $99.84 \pm 0.07\%$, respectively. At basic conditions, lead precipitation decreased the concentration to approximately 2.5 ppm. Starting at 2.5 ppm, the removal of lead was $91.64 \pm 2.25\%$. The pH has to be higher than 5.74 for precipitation to occur. After contact with the zeolite, the lower the pH, the higher the pH increased. This was due to a higher concentration of hydronium ions causing a larger driving force for uptake of the hydronium ions. Starting at an initial of pH 2.8, 4.9, 5.6 and 10.3 led to final pH values of 4.0, 5.9, 6.3 and 9.9, respectively. The decrease in pH for the basic sample (pH 10.3) was due to the acidic nature of clinoptilolite.

5.2 Recommendations

The modelling work presented in this thesis was validated using published experimental data. The validation was conducted to check that the results of the model were in agreement with the experimental data found in the open literature. A more thorough validation should be conducted using additional experimentation data. The model requires many parameters taken from literature. This model should also be validated against full scale landfill data. In small/pilot scale studies, not all potential complexities can be seen in experimental data (e.g. full scale physical parameters of the waste may not be isotropic). Temperature and oxygen concentration effects were included in the biokinetics of the anaerobic and aerobic bacteria. Other factors (e.g. pH, moisture content) should also be considered into the biokinetics. The waste dependence was taken out of the biokinetic equations due to the assumption that the model time length was short enough to keep substrate term in the biokinetic equation $\left(\frac{S}{k_s + S} \right)$ near unity. The model could also be modified to represent other types of landfills (i.e. anaerobic and semi-aerobic landfills) and can help understand the processes occurring.

With the sorption column, tests can be done at higher pressures. At atmospheric pressure, there was modest removal of carbon dioxide (approximately 20-30% CO₂ removal). At higher pressures, there will be much higher removal efficiency of carbon dioxide. Also, reuse of absorbent at higher pressures should be tested after desorbing at atmospheric pressures. Different lengths of the column should also be tested to determine if the concentration of lead can be decreased below the Ontario discharge standards. A mathematical model should also be developed that explains the processes that are occurring in the column (fluid flow, absorption, adsorption).

Appendices

Appendix A Preliminary adsorption/ion exchange column results

A.1 Ammonium assay calibration curve

The ammonium concentration in the NaCl solution can be determined using an assay made when sodium salicylate, sodium hydroxide and sodium hypochlorite are added. To find the calibration curve, known concentrations of ammonium (made from a known stock solution) were mixed with sodium salicylate, sodium hydroxide and sodium hypochlorite before using UV-VIS spectroscopy to determine the intensity of the absorbance peak. The peak absorbance intensity is correlated to the ammonium concentration. The graph showing the correlation is found in Figure A-1.

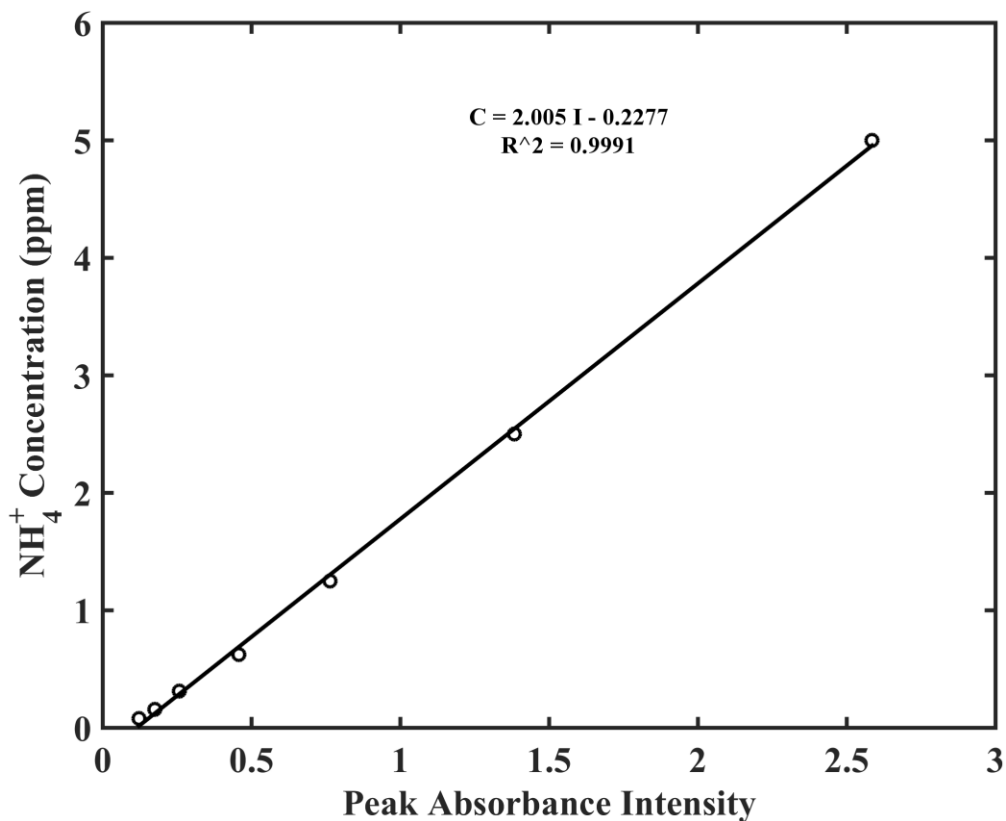


Figure A-1 Ammonium concentration calibration curve

A.2 Absorption equilibrium time determination

Water was sent into the top of the column (glass bead packing used). Gas was sent into the column from the bottom. At specific times, samples of water from the bottom of the column were taken. The pH of the samples was measured. As carbon dioxide is dissolved, water becomes more acidic (Equation 4-3). The plot of pH with respect to time is shown in Figure A-2. The pH reaches steady-state after approximately 5 minutes.

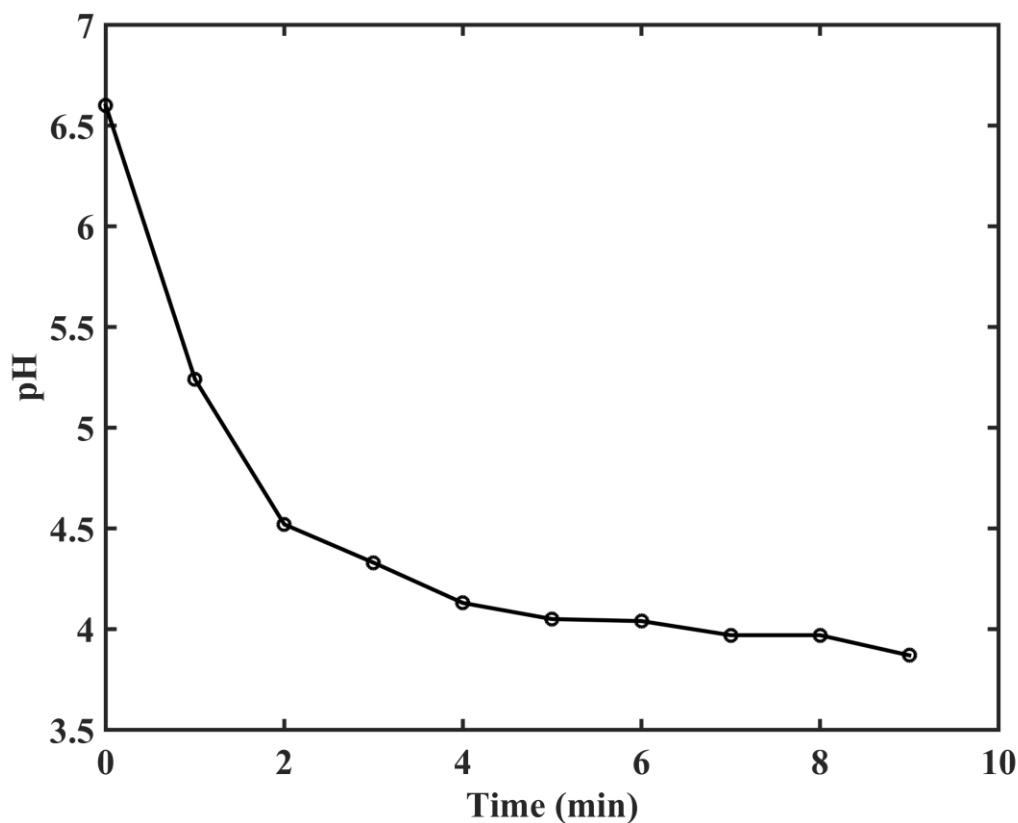


Figure A-2 Absorption equilibrium time

A.3 Adsorption equilibrium time determination

Leachate was pretreated as explained in Section 4.3.2 then 30 mL of leachate was put in contact with 3 g of zeolite. Individual samples were run for each time interval (1 h, 6 h, 12 h, 24 h, 48 h and 72 h). At each time interval, the leachate was filtered through a 0.45 μm polyethersulfone syringe filter and analyzed using inductively coupled plasma mass spectrometry (ICP-MS) to determine the concentration of chromium, copper, zinc, cadmium, lead and nickel. The equilibrium time graph is shown in Figure A-3.

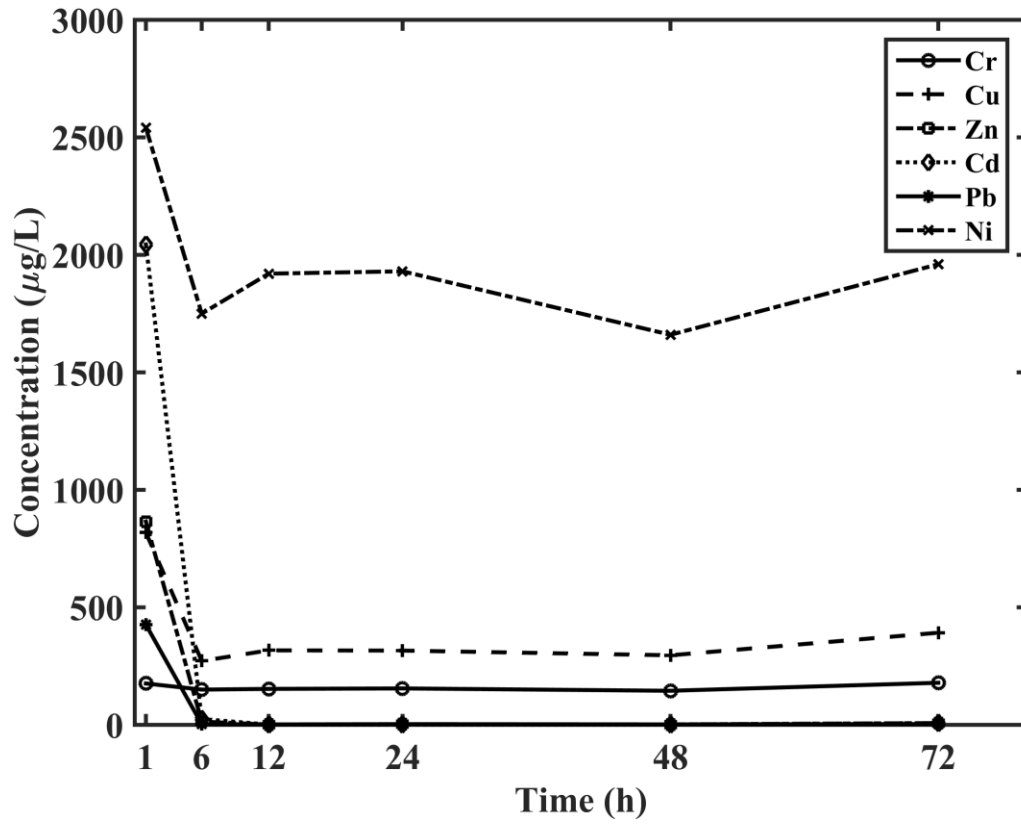


Figure A-3 Adsorption/ion exchange equilibrium time using landfill leachate

Appendix B Transport Phenomena in the Conversion of an Anaerobic Landfill into an Aerobic Landfill

Abstract: A two-dimensional dynamic model was developed using the concentrated reacting flow through porous media, heat transfer in porous media and mathematics interfaces. Initial aerobic biomass concentration was shown to be a very important parameter in the conversion of anaerobic landfills into aerobic landfills. Too low an initial aerobic concentration showed inefficient biodegradation whereas too high a concentration caused the biodegradation to proceed very quickly producing excess heat and killing the bacteria. Air flowrate was found to be less effective than leachate flowrate in controlling the landfill temperature. Increasing air flowrate by 4 times did little to change the temperature. The addition of leachate significantly cooled the waste.

B.1 Introduction

The growing human population has led to the accumulation of municipal solid waste (MSW). This has necessitated the creation of more landfills. However, these landfills come at a cost, land. In the future, there will be no land available to devote to landfills and a viable solution needs to be implemented. A potential solution that is gaining ground is the bioreactor landfill.

Traditional “dry-tomb” landfills entomb the MSW in an attempt to prevent moisture from infiltrating the landfill lessening the environment for microbial growth and activity. Moisture infiltration can lead to many environmental problems such as the production of landfill gas (a very potent mixture of greenhouse gases) caused by microbial activity, production of toxic leachate, and production of noxious odours¹.

Bioreactor landfills are the opposite of dry-tomb landfills because moisture (and air for aerobic landfills) is injected into the landfill to promote microbial activity. These landfills are highly monitored and controlled to safeguard the environment and ensure efficient

operation. The increased activity of the microbes in the MSW, increases the biodegradation rate, significantly decreasing the time required for waste stabilization.

Bioreactor landfills are split into two categories based on the dominant bacterial species present: anaerobic and aerobic. The type of bioreactor landfill has implications on the rate of biodegradation, composition of landfill gas and composition/toxicity of leachate. Experimental determination of the same information that a good model can provide, can take months or years, substantiating the need for a useful model to shorten the time considerably.

B.2 Governing equations

B.2.1 Gas flow equation

Air is injected into the waste mass to supply oxygen to the aerobic bacteria. The bacteria produce gases, which are extracted along with any unconsumed oxygen (the gases are collectively called landfill gas). The flow of air and landfill gas is defined by the Brinkman equation:

$$\frac{\rho}{\phi_p} \left(\frac{\partial \mathbf{u}}{\partial t} + (\mathbf{u} \cdot \nabla) \frac{\mathbf{u}}{\phi_p} \right) = \nabla \cdot \left[-P \mathbf{I} + \frac{\mu}{\phi_p} (\nabla \mathbf{u} + (\nabla \mathbf{u})^T) - \frac{2\mu}{3\phi_p} (\nabla \cdot \mathbf{u}) \mathbf{I} \right] - \left(\frac{\mu}{\kappa} + \beta_F |\mathbf{u}| + \frac{Q_{br}}{\phi_p^2} \right) \mathbf{u} \quad (\text{B-1})$$

Where ρ is the density of the gas (kg/m^3), \mathbf{u} is the velocity vector (m/s), ϕ_p is the porosity of the waste (-), P is the pressure (Pa), μ is the viscosity of the gas (Pa·s), κ is the permeability of the waste (m^2), β_F is the Forcheimer coefficient (kg/m^4) and Q_{br} is the volumetric mass source ($\text{kg/m}^3/\text{s}$).

$$\frac{\partial(\phi_p \rho)}{\partial t} + \nabla \cdot (\rho \mathbf{u}) = Q_{br} \quad (\text{B-245})$$

B.2.2 Gas transport equations

The flow of the gas species is dependent on bulk flow (convection) and molecular flow (diffusion) processes. Since no one species makes up greater than 90% of the composition of the gas, transport of concentrated species is used:

$$\phi_p \rho \frac{\partial \omega_i}{\partial t} + \nabla \cdot \mathbf{j}_i + \rho(\mathbf{u} \cdot \nabla) \omega_i = R_i \quad (\text{B-3})$$

Where ω_i is the mass fraction of component i (-), \mathbf{j}_i is the mass flux vector relative to the mass averaged velocity ($\text{kg/m}^2/\text{s}$), R_i is the rate of consumption/production for component i ($\text{kg/m}^3/\text{s}$).

$$\mathbf{j}_i = - \left(\rho D_i^F \nabla \omega_i + \rho \omega_i D_i^F \frac{\nabla M_n}{M_n} \right) \quad (\text{B-4})$$

Where D_i^F is the Fickian diffusion coefficient of component i (m^2/s) and M_n is the average molecular weight (kg/mol).

The multicomponent diffusion coefficients are found by the relationship proposed by Fairbanks and Wilke² using binary Fickian diffusion coefficients (found using the Chapman-Enskog equation).

$$D_i^F = \frac{1 - x_i}{\sum_{j, j \neq i} \frac{x_j}{D_{ij}}} \quad (\text{B-5})$$

Where D_{ij} is the binary Fickian diffusion coefficient of components i and j (m^2/s), x_i is the mole fraction of component i and x_j is the mole fraction of component j .

$$M_n = \left(\sum_i \frac{\omega_i}{M_i} \right)^{-1} \quad (\text{B-6})$$

Where M_i is the molecular weight of component i (kg/mol).

$$\mathbf{N}_i = \mathbf{j}_i + \rho \mathbf{u} \omega_i \quad (\text{B-7})$$

Where \mathbf{N}_i is the combined mass flux vector of component i (kg/m²/s).

B.2.3 Biokinetic equations

Anaerobic biomass growth

Initially, when no oxygen is present, the dominant bacterial species are anaerobic. The equation describing the anaerobic biomass growth rate is as follows:

$$R_N = \frac{\partial X_N}{\partial t} = K_{M,N} \frac{S}{k_{s,N} + S} X_N - R_{D,N} \quad (\text{B-8})$$

When the concentration of substrate (waste) is sufficiently high, ($S \gg k_{s,N}$), simplifies Eq. B-8 to:

$$R_N = \frac{\partial X_N}{\partial t} = K_{M,N} X_N - R_{D,N} \quad (\text{B-9})$$

Where R_N is the anaerobic biomass growth rate (kg/m³/day), X_N is the concentration of the anaerobic biomass (kg/m³), $K_{M,N}$ is the anaerobic Monod maximum growth rate constant (day⁻¹), S is the available substrate (kg/m³), $k_{s,N}$ is the substrate half-saturation constant for anaerobic growth (kg/m³) and $R_{D,N}$ is the anaerobic biomass decay rate (kg/m³/day).

Kim et al. assumed the decay rate of anaerobic biomass was given by the following³:

$$R_{D,N} = 0.05 K_{M,N} (X_N - X_{N,0}) \quad (\text{B-10})$$

Where $X_{N,0}$ is the initial concentration of anaerobic biomass (kg/m³).

Aerobic biomass growth

On the onset of aeration, the anaerobic bacteria begin to perish and aerobic bacteria begin to dominate. The equation describing the aerobic biomass growth rate is as follows:

$$R_A = \frac{\partial X_A}{\partial t} = K_{M,A} k_{temp} \frac{S}{k_{s,A} + S} \frac{c_{O_2}}{k_{O_2} + c_{O_2}} X_A - R_{D,A} \quad (\text{B-11})$$

If the substrate concentration is sufficiently high, ($S \gg k_{s,A}$), Eq. B-11 reduces to:

$$R_A = K_{M,A} k_{temp} \frac{c_{O_2}}{k_{O_2} + c_{O_2}} X_A - R_{D,A} \quad (\text{B-12})$$

Where R_A is the aerobic biomass production rate (kg/m³/day), X_A is the concentration of the aerobic biomass (kg/m³), $K_{M,A}$ is the aerobic Monod maximum growth rate constant (day⁻¹), k_{temp} is the temperature correction factor (-), c_{O_2} is the concentration of oxygen (kg/m³), k_{O_2} is the oxygen half saturation constant (kg/m³), $k_{s,A}$ is the substrate half-saturation constant for aerobic growth (kg/m³) and $R_{D,A}$ is the aerobic biomass decay rate (kg/m³/day).

Kim et al. assumed the decay rate of aerobic biomass was given by the following³:

$$R_{D,A} = 0.05 K_{M,A} (X_A - X_{A,0}) \quad (\text{B-13})$$

Where $X_{A,0}$ is the initial concentration of anaerobic biomass (kg/m³).

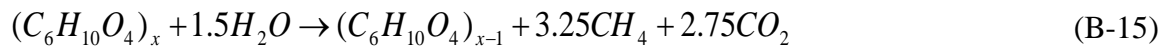
The temperature correction factor, shown in Eq. B-14, describes the temperature dependence of the growth of aerobic bacteria:

$$k_{temp} = \frac{(T - T_{max})(T - T_{min})^2}{(T_{opt} - T_{min})[(T_{opt} - T_{min})(T - T_{opt}) - (T_{opt} - T_{max})(T_{opt} + T_{min} - 2T)]} \quad (\text{B-14})$$

Where T is the temperature of the MSW (K), T_{\max} is the maximum temperature for aerobic bacterial growth (K), T_{\min} is the minimum temperature for aerobic bacterial growth (K) and T_{opt} is the optimal temperature for aerobic bacterial growth (K).

B.2.4 Species consumption/production equations

Themelis and Kim proposed the following generalized reaction for the anaerobic biodegradation of waste⁴:



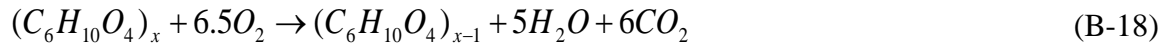
Based on this, the production of methane and carbon dioxide in the anaerobic state can be formulated:

$$\frac{R_{CO_2}}{2.75 \frac{M_{CO_2}}{M_{MSW}}} = \frac{R_N}{Y_{S/B,N}} = \frac{K_{M,N} X_N}{Y_{S/B,N}} \quad (B-16)$$

$$\frac{R_{CH_4}}{3.25 \frac{M_{CH_4}}{M_{MSW}}} = \frac{R_N}{Y_{S/B,N}} = \frac{K_{M,N} X_N}{Y_{S/B,N}} \quad (B-17)$$

Where R_{CO_2} is the production rate of carbon dioxide (kg/m³/s), M_{CO_2} is the molecular weight of carbon dioxide (kg/mol), M_{MSW} is the molecular weight of MSW (kg/mol), M_{CH_4} is the molecular weight of methane (kg/mol), $Y_{S/B,N}$ is the substrate/anaerobic biomass yield coefficient (kg_B/kg_S) and R_{CH_4} is the production rate of methane (kg/m³/s).

Themelis and Kim proposed the following generalized reaction for aerobic biodegradation of waste⁴:



Based on this, the consumption of oxygen and production of carbon dioxide in the aerobic state can be formulated:

$$\frac{R_{O_2}}{-6.5 \frac{M_{O_2}}{M_{MSW}}} = \frac{R_A}{Y_{S/B,A}} = \frac{K_{M,A} \frac{c_{O_2}}{k_{O_2} + c_{O_2}} X_A}{Y_{S/B,A}} \quad (B-19)$$

$$\frac{R_{CO_2}}{6 \frac{M_{CO_2}}{M_{MSW}}} = \frac{R_A}{Y_{S/B,A}} = \frac{K_{M,A} \frac{c_{O_2}}{k_{O_2} + c_{O_2}} X_A}{Y_{S/B,A}} \quad (B-20)$$

Where R_{O_2} is the consumption rate of oxygen (kg/m³/s), M_{O_2} is the molecular weight of oxygen (kg/mol), $Y_{S/B,A}$ and is the substrate/aerobic biomass yield coefficient (kg_B/kg_S).

Table B-1 Physical properties of waste

Parameter	Unit	Value	Reference
Waste porosity (ϕ_p)	-	0.3	⁵
Waste permeability (κ)	m ²	10 ⁻¹²	⁵
Waste density (ρ_{MSW})	kg/m ³	600	Assumed

Table B-2 Biokinetic parameters

Parameter	Unit	Value	Reference
Maximum anaerobic Monod growth rate constant ($K_{M,N}$)	day ⁻¹	0.2	³
Maximum aerobic Monod growth rate constant ($K_{M,A}$)	day ⁻¹	1.0	³
Oxygen half saturation constant (k_{O_2})	kg/m ³	7x10 ⁻⁶	^{6,7}

Substrate/anaerobic biomass yield coefficient ($Y_{S/B,N}$)	kg _B /kg _S	0.05	3
Substrate/aerobic biomass yield coefficient ($Y_{S/B,A}$)	kg _B /kg _S	0.1	8
Minimum aerobic growth temperature (T_{min})	°C	5	6,7,9
Optimal aerobic growth temperature (T_{opt})	°C	58.6	6,7,9
Maximum aerobic growth temperature (T_{max})	°C	71.6	6,7,9

Table B-3 Heat parameters

Parameter	Unit	Value	Reference
Specific heat capacity of MSW ($C_{P,MSW}$)	MJ/m ³ /K	2.0	10
Heat conductivity of MSW (k_{MSW})	W/m/K	0.0445	11
Aerobic biodegradation heat of reaction (ΔH_{reac})	kJ/mol	-460	3
Leachate injection flowrate ($F_{L,in}$)	L/day	2,100	12

B.2.5 Energy balance equations

The source of heat is the aerobic biodegradation of the waste (exothermic reaction). Anaerobic biodegradation is slightly exothermic and can be endothermic depending on the composition of the waste. The energy balance is given by:

$$V(\rho C_p)_{eq} \frac{\partial T}{\partial t} + V\rho C_p \mathbf{u} \cdot \nabla T = \nabla \cdot (k_{eq} \nabla T) + Q \quad (\text{B-21})$$

Where V is the volume of the MSW (m³), k_{eq} is the equivalent thermal conductivity (W/m/K), C_p is the specific heat of the gas (J/kg/K) and Q is the source/sink term of energy (W).

$$(\rho C_p)_{eq} = \theta_{MSW} \rho_{MSW} C_{p,MSW} + (1 - \theta_{MSW}) \rho C_p \quad (B-22)$$

Where θ_{MSW} is the mass fraction of the MSW (-), ρ_{MSW} is the density of MSW (kg/m^3) and $C_{p,MSW}$ is the specific heat of MSW (J/kg/K).

$$k_{eq} = \theta_{MSW} k_{MSW} + (1 - \theta_{MSW}) k \quad (B-23)$$

Where k_{MSW} is the heat conductivity of the MSW (W/m/K) and k is the heat conductivity of the gas (W/m/K).

$$Q = R\Delta H_{reac} - \rho_w F_{L,in} C_{p,w} (T - T_{L,0}) - \rho_g F_{g,in} C_p (T - T_{g,0}) \quad (B-24)$$

Where ΔH_{reac} is the reaction heat (kJ/mol), $F_{L,in}$ is the flowrate of leachate (mL/min), $C_{p,w}$ is the specific heat of water (J/kg/K), $T_{L,0}$ is the initial leachate temperature (K), $F_{g,in}$ is the flowrate of gas (L/min), and $T_{g,0}$ is the initial temperature of the gas (K).

B.3 Use of COMSOL Multiphysics

The model contains momentum, mass and energy transport phenomena. The momentum and mass balances are solved using the concentrated reacting flow in porous media interface. The energy balance was solved using the heat transfer in porous media interface. Due to the complex nature of the biokinetics involved in the process, COMSOL does not contain these equations by default. The equations had to be added using multiple distributed ODEs. COMSOL contained the option to couple the reacting flow in porous media and heat transfer in porous media interfaces. The biokinetics had to be coupled manually to both the reacting flow (gas consumption/production is dependent on biokinetics) and the heat transfer interfaces (reaction heat generation is dependent on biokinetics).

B.4 Analysis conditions

Model parameters used in the various equations are found from published literature. The parameters describing the physical properties of the waste are found in Table B-1. Kinetic parameters used for the model are found in Table B-2. Heat transfer parameters are found in Table B-3.

The geometry being used is a 20 m by 20 m cell (). Air injection wells are located at the corners and the extraction well is located in the center.

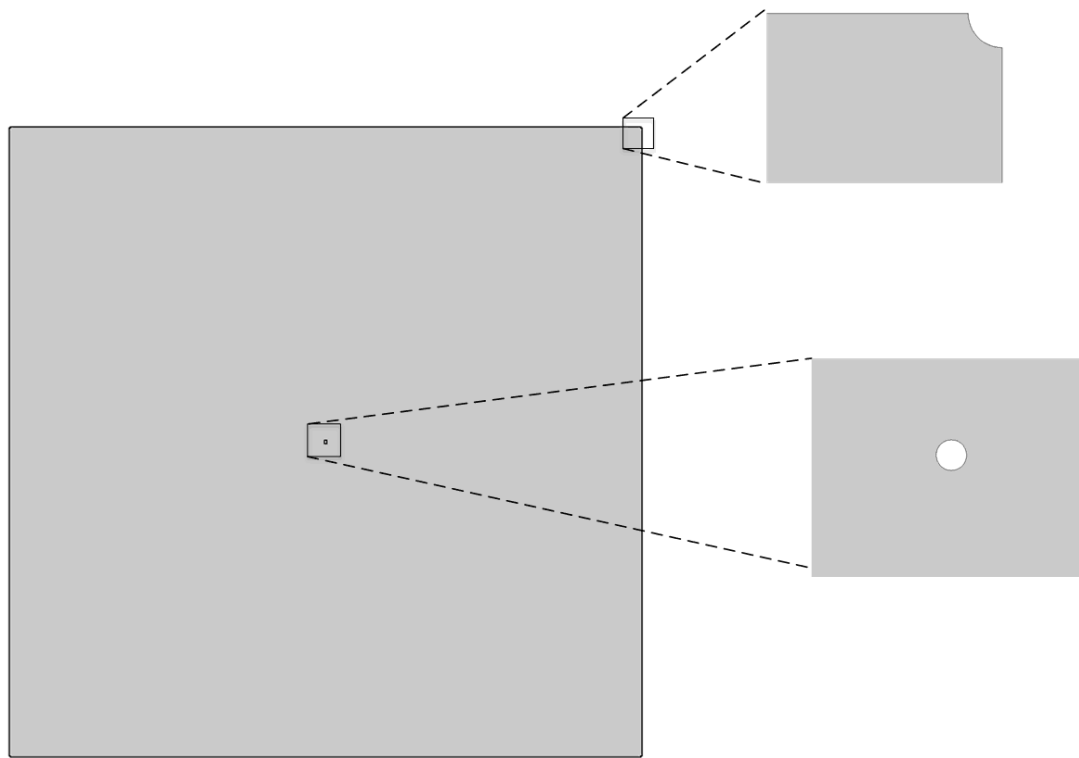


Figure B-1 Geometry of the landfill cell

B.5 Results

Figure B-2 shows the effect of initial aerobic biomass concentration on the conversion of anaerobic landfill into an aerobic landfill. Temperature is used as an indicator to give information about the biodegradation. Aerobic biodegradation is exothermic and the

temperature can give insight into the efficacy of the biodegradation. For example, landfill temperatures remaining near ambient temperature indicate minimal aerobic biodegradation. Figure B-2(a) shows a very small increase in temperature from the initial temperature. This indicates inefficient biodegradation. At the other end of the spectrum is Figure B-2(c). In this figure, the temperature has increased rapidly, indicating the requirement for control of the biodegradation. Figure B-2(c) shows the waste temperature nearing the maximum growth temperature shown in Table B-2. Exceeding this temperature will cause the aerobic bacteria to die, and will significantly decrease the biodegradation rate.

As can be seen from Figure B-2, if the landfill is left uncontrolled then the temperature will gradually climb. The temperature is generally controlled in two fashions: (1) by increasing the air flowrate or (2) by adding/increasing leachate injection.

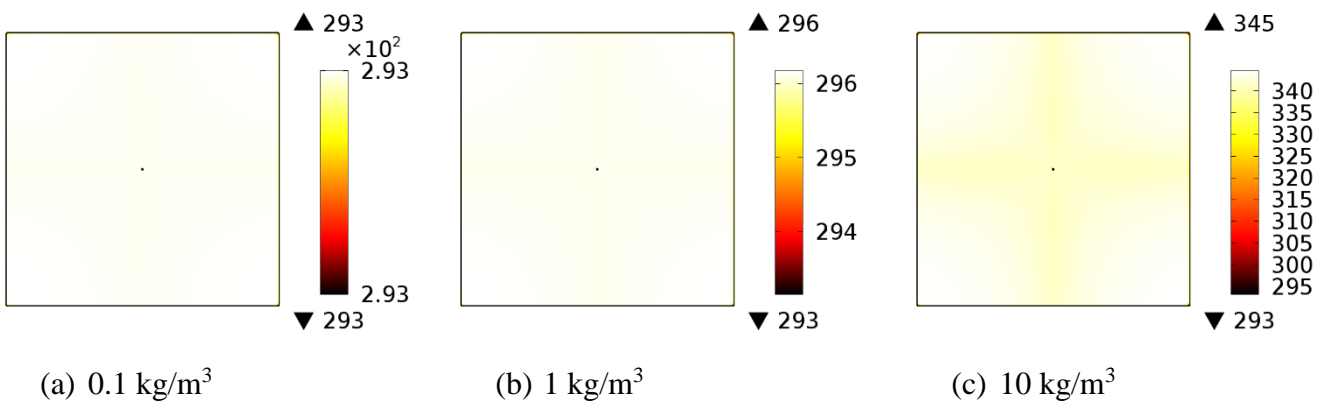


Figure B-2 Temperature after 1 day with varying initial aerobic biomass concentrations – initial temperature = 293K

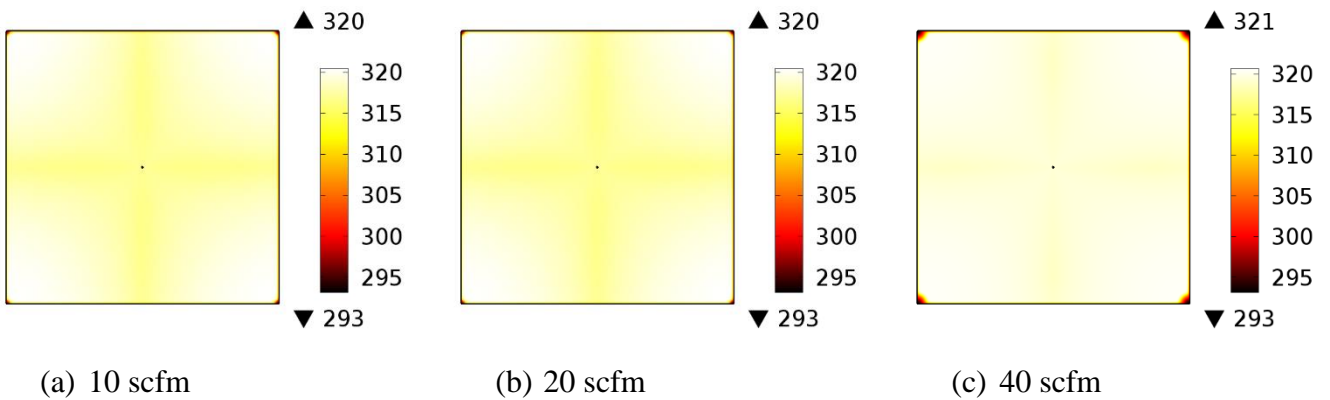


Figure B-3 Temperature after 1 day with varying air flowrates – initial temperature = 293K

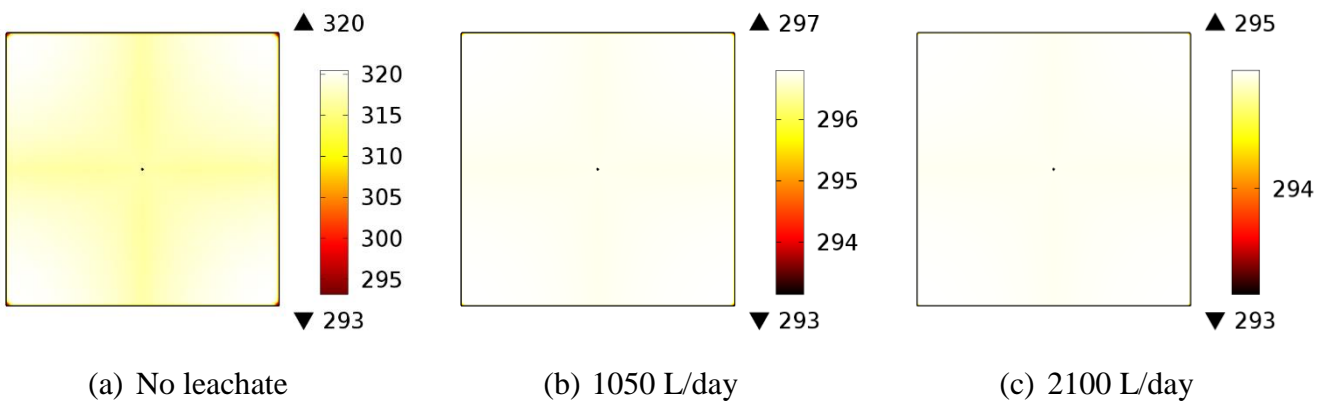


Figure B-4 Temperature after 1 day with varying leachate injection rates – initial temperature = 293K

Figure B-3 shows the effect of increasing air flowrate. Increasing the air flowrate by 4 times, did little to decrease the temperature. Increasing the air flowrate, increases the distance the air gets into the waste before the air heats to the waste temperature. Another effect of the increase in air flowrate, is the homogenization of temperature via convection. The cell temperature becomes more uniform as the air injection flowrate increases.

However, as shown by Figure B-4, the addition of leachate decreases the temperature significantly. The specific heat of leachate is approximately three orders of magnitude

greater than the air. This shows that air is not effective in decreasing temperature and leachate is effective. This would require a significant increase in air flowrate to cool as effectively as leachate and would increase operating costs.

B.6 Conclusions

Initial aerobic biomass concentration was shown to be an important parameter in the conversion of an anaerobic landfill into an aerobic landfill. Too low of an initial aerobic biomass concentration and the growth of the aerobic biomass was slow. Too high of an initial aerobic biomass concentration and the growth of the aerobic biomass was rapid and produced excessive heat. Aerobic sludge can be injected to adjust the initial aerobic biomass concentration to quicken the conversion of the landfill.

The model has yet to be validated by experimental/industrial data. It is consistent with expectations and literature. The aerobic biomass grow with time and show a pattern of higher growth in areas of greater oxygen. This translates to higher oxygen consumption and carbon dioxide production in these areas.

Kinetic parameters have come from published literature and may not exactly fit the experimental conditions, therefore parameter fitting will likely be required.

This model can provide a very useful tool for the operation of aerobic landfills. Testing many different scenarios/conditions (e.g. different air flowrates, different air injection temperature, different ambient temperature) can be done in a relatively short time when compared to testing these scenarios experimentally. Scenarios that are not physically realizable may also be tested to see their effects on the landfill to provide additional insight.

B.7 References

1. Omar H, Rohani S. Treatment of landfill waste, leachate and landfill gas: A review. *Front Chem Sci Eng*. 2015;9(1):15–32. Doi: 10.1007/s11705-015-1501-y.
2. Fairbanks DF, Wilke CR. Diffusion Coefficients in Multicomponent Gas Mixtures. *Ind Eng Chem*. 1950;42(3):471–5. Doi: 10.1021/ie50483a022.
3. Kim S-Y, Tojo Y, Matsuto T. Compartment model of aerobic and anaerobic biodegradation in a municipal solid waste landfill. *Waste Manag Res*. 2007;25(6):524–37. Doi: 10.1177/0734242X07079148.
4. Themelis NJ, Kim YH. Material and energy balances in a large-scale aerobic bioconversion cell. *Waste Manag Amp Res J Int Solid Wastes Public Clean Assoc ISWA*. 2002;20(3):234–42. Doi: 10.1177/0734242X0202000304.
5. Ishimori H, Endo K, Ishigaki T, Sakanakura H, Yamada M. Coupled fluid flow and thermal and reactive transport in porous media for simulating waste stabilization phenomena in semi-aerobic landfill. *Proceedings of the 2011 COMSOL Conference in Boston*. Boston; 2011.
6. Sole-Mauri F, Illa J, Magrí A, Prenafeta-Boldú FX, Flotats X. An integrated biochemical and physical model for the composting process. *Bioresour Technol*. 2007;98(17):3278–93. Doi: 10.1016/j.biortech.2006.07.012.
7. Fytanidis DK, Voudrias EA. Numerical simulation of landfill aeration using computational fluid dynamics. *Waste Manag*. 2014;34(4):804–16. Doi: 10.1016/j.wasman.2014.01.008.
8. Beaven RP, White JK, Braithwaite P. Application of the University of Southampton Landfill Degradation and Transport Model (LDAT) to an aerobic treatment field experiment. *Proceedings of Global Waste Management Symposium*. Colorado, USA; 2008.

9. Baptista M, Antunes F, Gonçalves MS, Morvan B, Silveira A. Composting kinetics in full-scale mechanical–biological treatment plants. *Waste Manag.* 2010;30(10):1908–21. Doi: 10.1016/j.wasman.2010.04.027.
10. Yeşiller N, Hanson JL, Liu W-L. Heat Generation in Municipal Solid Waste Landfills. *J Geotech Geoenvironmental Eng.* 2005;131(11):1330–44.
11. Manna L, Zanetti MC, Genon G. Modeling biogas production at landfill site. *Resour Conserv Recycl.* 1999;26(1):1–14. Doi: 10.1016/S0921-3449(98)00049-4.
12. Bilgili MS, Demir A, Özkaya B. Influence of leachate recirculation on aerobic and anaerobic decomposition of solid wastes. *J Hazard Mater.* 2007;143(1–2):177–83. Doi: 10.1016/j.jhazmat.2006.09.012.

Appendix C Microwave assisted zeolitization of coal fly ash using landfill leachate as the solvent

Coal fly ash (CFA) was converted to zeolite using microwave energy. Landfill leachate was used as the solvent, after increasing its pH with sodium hydroxide to precipitate the heavy metals contents, in three modes: filtered using a 0.45 μm filter (fine-filtered), filtered using a 1 μm filter (coarse filtered) and unfiltered. The experiments were performed using a self-adjusting microwave source (single-mode, 2.45 GHz, CEM cooperation, Discover, USA) in a cylindrical batch PTFE vessel (28 mm ID \times 108 mm). The XRD analysis of the product showed that using leachate inhibited the production of zeolite A (LTA) and favoured the production of hydroxysodalite (SOD). More heavy metals removal from leachate by precipitation and filtration favoured LTA production. Samples synthesized at 300 W of microwave irradiation for 30 minutes had a SOD/LTA ratio of 1.00, 1.06, and 2.28 for fine-filtered, coarse filtered and unfiltered leachate samples. SEM, TGA and CEC analyses further confirmed that more heavy metal precipitation and filtration favoured LTA over SOD production. CECs for zeolites synthesized using fine-filtered, coarse filtered and unfiltered leachate were 0.80, 0.72 and 0.67 meq/g, respectively. SOD production increased with increased microwave irradiation energy. There was an optimal microwave irradiation energy level per g of CFA (65.9 kJ/g) in which the most LTA was produced.

C.1 Introduction

Coal-fired energy production has gradually decreased in recent years. Despite this fact, due to the growth in population and world development, coal-fired energy still remains a very large segment of the energy production market. Coal-fired power plants burn pulverized coal to produce electricity. One of the waste products produced upon the combustion of coal is a particulate material called coal fly ash (CFA). Coal fly ash is potentially carcinogenic and has to be disposed of or used safely to mitigate the potential risks¹. CFA contains silicon and aluminum which can be utilized to synthesize zeolites. Zeolites are used as catalysts (mainly in the petroleum/petrochemical industry), to purify air and water,

as well as other uses in industrial settings. Many studies have been conducted²⁻¹² and reviews written^{13,14} on the production of zeolites from CFA.

Zeolitization of CFA involves the use of high quantities of water. Production of one metric ton of zeolite from CFA requires 20 metric tons of fresh water¹⁵. Most of the studies utilized pure water during the synthesis process. However, there has been growing interest in utilizing liquid waste streams in the production of zeolite. Eliminating the use of fresh water can significantly reduce the cost and environmental impact associated with the zeolitization process. Furthermore, if a source of wastewater is used instead of fresh water, two waste streams (CFA and wastewater) are used for the production of a value added material. Belviso et al.¹⁶ synthesized zeolite X from CFA and seawater as the solvent by fusion with NaOH followed by hydrothermal crystallization. A comparison was done between the results obtained from the use of seawater and distilled water. The synthesis yield was higher using seawater than using distilled water at different crystallization temperatures. Hussar et al.¹⁷ synthesized zeolite A by a hydrothermal process using sodium silicate, sodium aluminate and the by-product of an aluminum etching process. The chemical composition of the aluminum etching by-product consisted of the following main oxides expressed as percentage by weight; Al₂O₃, 92%; Na₂O, 6%; SiO₂, 0.5%. Their results indicated that a higher synthesis reaction temperature and longer reaction time favored synthesis of zeolite A. The effect of using industrial waste brine solution instead of ultra-pure water was investigated during the synthesis of zeolite by Musyoka¹⁸. They used coal fly ash as the Si feedstock and high halide brine obtained from the retentate effluent of a reverse osmosis water treatment plant of a mine, as the solvent. The brine contained high sodium and potassium and low concentrations of toxic elements. Also there was trace amounts of aluminum equal to 48.38 µg/L and no silicon. The use of brine as a solvent resulted in the formation of hydroxysodalite zeolite although unconverted mullite and hematite from the fly ash feedstock were also present in the product. Musyoka et al.⁵ used two types of mine waters (acidic and circumneutral). The important cationic species of circumneutral water were: Na: 952 mg/L, Mg: 38 mg/L, Ca: 19 mg/L and Si: 1.2 mg/L (no detectable Al); and in the acidic drainage water were: Fe: 4694 mg/L, Na: 68 mg/L,

Mg: 386 mg/L, Ca: 458 mg/L, Al: 613 mg/L and Si: 31 mg/L. Zeolites Na-X and Na-P1 were synthesized by fusion and hydrothermal method, respectively. The use of circumneutral mine water resulted in similar zeolite forms, i.e. Na-P1 and X, whereas the use of acidic mine drainage led to the formation of a single phase hydroxysodalite zeolite. Studies were also conducted by Behin et al.¹⁹ utilizing a liquid waste stream from plasma electrolytic oxidation (PEO), which is a relatively novel technique to produce functional oxide coatings on the surface of metals such as aluminum, magnesium, and titanium alloys²⁰. The wastewater from the PEO process had a pH of 12 and contained Na (63 mg/L), K (497 mg/L), Si (295 mg/L) and Al (10 mg/L) metal cations. The zeolite produced with PEO wastewater was comparable with the zeolite produced with fresh water in terms of BET surface area, water carrying capacity and cation exchange capacity (CEC). The wastewater streams used in the above experiments did not contain any heavy metals. Landfill leachates, however may contain heavy metal ions and would be an interesting study to conduct on the zeolitization process of CFA.

Landfill leachate is produced when water infiltrates a landfill and leaches out from the landfill. Depending on the composition of the waste, leachate can contain soluble organic, inorganic, bacteriological constituents, heavy metals and suspended solids²¹. It presents many potential environmental hazards and due to its complex nature is difficult and expensive to treat. A significant portion of the landfilling cost is due to leachate treatment. Many studies have been conducted²²⁻²⁵ and reviews written²⁶⁻²⁸ on leachate treatment. Here the goal is to use leachate instead of water for the production of zeolite A. There have been studies conducted using wastewater to synthesize zeolites, however, in these studies the major constituents have been alkali and alkali-earth metals. The use of leachate in this experiment helps to shed light on the effects of heavy metal ions in the reaction mixture on the zeolitization process.

C.2 Materials and methods

C.2.1 Materials

Coal fly ash was obtained from a coal fired power plant (Ontario Power Generation, Nanticoke, Canada) and was stored in a sealed container before use. Sodium hydroxide (Alphachem, Mississauga, Canada) and sodium aluminate anhydrous (Sigma-Aldrich, USA) were of analytical grade and used as received. The leachate was obtained from the W12A Landfill (London, Canada). Upon collection of the leachate, the leachate was filtered through VWR Grade 415 Filter Paper (Mississauga, Canada) to remove any particulate matter present in the leachate. When not in use, the leachate was stored at 4°C to limit degradation of the leachate. When used during experiments, the leachate was allowed to reach room temperature before each experiment. The unused leachate was subsequently refrigerated after use. Other chemicals used for characterization tests were of analytical grade. Other chemicals used for characterization tests were of analytical grade.

C.2.2 Experimental procedure

Coal fly ash was converted into zeolite by a single step hydrothermal alkaline treatment². Zeolitization of coal fly ash was carried out as follows: 2.18 g of sodium hydroxide granules with 1.82 g of fly ash (NaOH/CFA ratio of 1.2) were dissolved in 17 mL of leachate. Upon increase of pH (required for digestion of CFA) using NaOH, heavy metal hydroxides precipitated. One set of experiments was conducted with leachate that was filtered through 0.45 µm polyethersulfone syringe filters (VWR, Canada) (fine-filtered). Another set of experiments was conducted with the leachate filtered through 1 µm filter paper (coarse filtered). A third set using the unfiltered leachate. The digestion of CFA was conducted at 60°C for 12 h using an end-over-end shaker in a cylindrical PPCO vessel (25.5 mm ID × 104.5 mm). After digestion, 3 mL of the aqueous sodium aluminate solution (0.155 g/mL) were added and the reaction solution aged for 2 hours. Subsequently, the mixture was subjected to microwave radiation for crystallization. The experiments were performed using a self-adjusting microwave source (single-mode, 2.45 GHz, CEM cooperation, Discover, USA) at atmospheric pressure. A cylindrical batch PTFE vessel (28

mm ID × 108 mm) equipped with a reflux condenser was placed in the microwave chamber for varied periods of time (10, 20 and 30 min) and microwave power (100, 200, 300 W). In a single mode microwave, electromagnetic irradiation is directed through a precisely-designed wave guide that produces a standing wave, whereas in multimode microwave there is a mixture of many waves with different phase shifts. The microwave field density in a single mode microwave is much higher compared to a multimode microwave. Therefore, similar results can be achieved in a single-mode microwave using lower power input²⁹. After a given period of MW irradiation, the solid products were filtered, washed with deionized water and dried overnight.

C.2.3 Characterization

Inductively coupled plasma atomic emission spectroscopy (ICP-AES) was used to measure the concentration of different ions in the leachate. Concentrations were found using a Perkin-Elmer Optima-3300 DV ICP-Atomic Emission Spectrometer (USA). Chemical composition of the CFA sample was determined by means of X-ray fluorescence spectroscopy (XRF) utilizing PANalytical PW2400 Wavelength Dispersive. Rigaku–Miniflex powder diffractometer (Japan) was used to collect XRD data of the synthesized zeolites using CuK_α (λ for $\text{K}_\alpha = 1.54059 \text{ \AA}$) over the range of $5^\circ < 2\theta < 25^\circ$ with a step width of 0.02° . The obtained crystalline phase was identified based on standard peaks in literature³⁰. The thermogravimetric analysis (TGA) of the samples was performed using a Mettler Toledo TGA/SDTA 851e model (Switzerland) with version 6.1 STARe software. The samples were heated from 25°C to 600°C at a heating rate of $10^\circ\text{C}/\text{min}$ under nitrogen purge. The crystal size distribution and morphology of the zeolites were studied by scanning electron microscope (SEM); Hitachi S 2600N SEM (Tokyo, Japan) operating at 5 kV of acceleration voltage. CEC was measured using ammonium acetate saturation method (5 days) based on Bain and Smith³¹. The zeolite samples were soaked in a 1 N solution of ammonium acetate for 5 days in the same end-over-end shaker. After 5 days, the zeolite samples were filtered and allowed to air dry. The dried samples were then washed using 100 mL (5 × 20 mL) of an aqueous solution of 10 wt% NaCl and 1 vol% HCl to remove the fixated ammonium. The ammonium concentration in the supernatant was

then measured. The ammonium concentration was correlated to peak absorbance intensity between 550 and 800 nm measured using UV-VIS spectroscopy (Figure C-5). To prepare the samples for the UV-VIS spectroscopy, sodium salicylate, sodium hydroxide and sodium hypochlorite were added and 5 minutes allowed to elapse for the reaction to proceed to completion.

C.3 Results and discussion

C.3.1 Inductively coupled plasma atomic emission spectroscopy (ICP-AES)

The ions concentrations and pH of the leachate are found in Table C-1

Table C-1 Cation concentrations (mg/L) and pH of leachate

Cation	Concentration (mg/L)
Ag	< 0.01
Al	0.14
As	< 0.01
B	3.95
Be	< 0.01
Ca	206.08
Cd	4.15
Co	0.03
Cr	0.27
Cu	1.71
Fe	0.62
Hg	< 0.01
K	252.27
Li	0.05
Mg	141.46
Mn	1.01
Mo	< 0.01
Na	810.80
Ni	5.92
P	0.53
Pb	0.62
S	99.13
Sb	< 0.01
Se	< 0.01
Si	21.94

Sn	< 0.01
Tl	< 0.01
V	< 0.01
Zn	7.61
pH*	7.56

* Unitless

The leachate contained high levels of Ca (206.08 mg/L), K (252.27 mg/L), Mg (141.46 mg/L), Na (810.80 mg/L) and S (99.13 mg/L). Ca, K, Mg and Na are most likely a result of the leaching of salts from the soil covers of the landfill³². Sulfur is most likely from the leaching of the landfill waste³³. Silicon and Al are required for the synthesis of zeolites. The landfill leachate had only trace amounts of both elements; concentrations of Si and Al were 21.94 and 0.14 mg/L, respectively.

C.3.2 X-ray analysis (XRF and XRD)

The chemical compositions of the CFA that was used as the main source of Si and Al for hydrothermal zeolitization process are summarized in Table C-2. The SiO₂/Al₂O₃ ratio was found to be 2.13, which was appropriate for the synthesis of low silica zeolite crystallites such as LTA type zeolite. According to the XRD data, the main components of the CFA were amorphous aluminosilicate as well as quartz and mullite that existed as crystalline structures as indicated in Table C-2.

Table C-2 XRF analysis of chemical composition of CFA

Parameter	Weight percent (%)
<i>Major oxide</i>	
SiO ₂	41.78
Al ₂ O ₃	19.61
CaO	13.64
Fe ₂ O ₃	5.79
MgO	3.23
TiO ₂	1.39
K ₂ O	1.1
Na ₂ O	0.94
P ₂ O ₅	0.71
BaO	0.36
SrO	0.25

Cr ₂ O ₃	0.01
MnO	0.02
<i>Loss On Ignition</i>	10.89
Total	99.72

Phases analysis

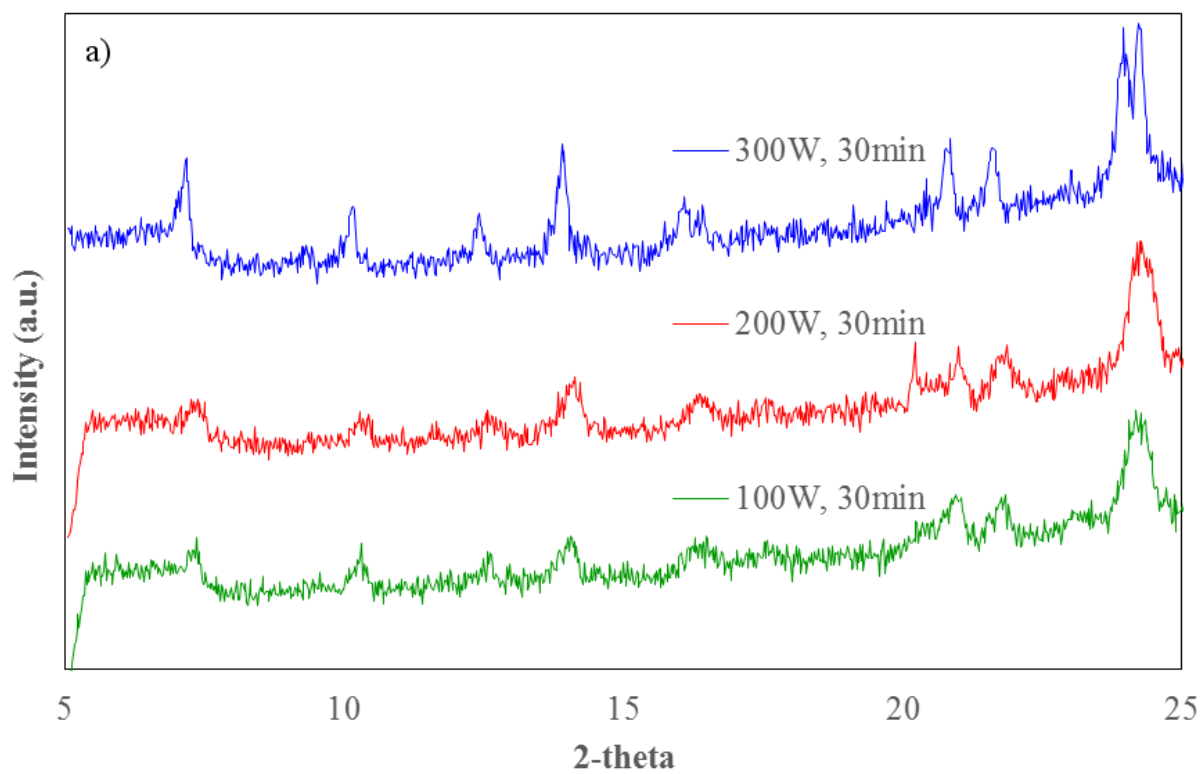
Amorphous aluminosilicate

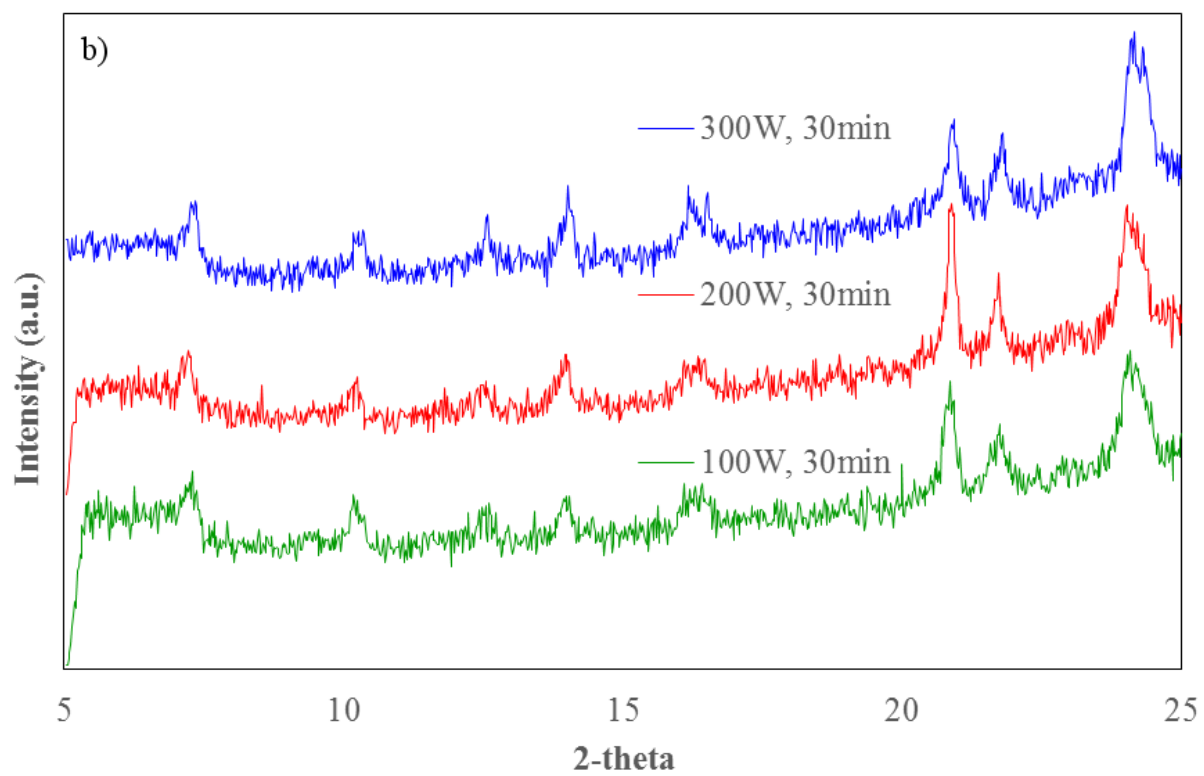
Quartz (SiO₂)

Mullite (3Al₂O₃.2SiO₂)

*SiO₂/Al₂O₃: 2.13

The XRD analysis was conducted for all the samples after microwave irradiation in order to identify the zeolite phases present. Two major zeolitic phases were observed, namely zeolite A (LTA) and hydroxysodalite (SOD). The XRD patterns for the different leachates are shown in Figure C-1.





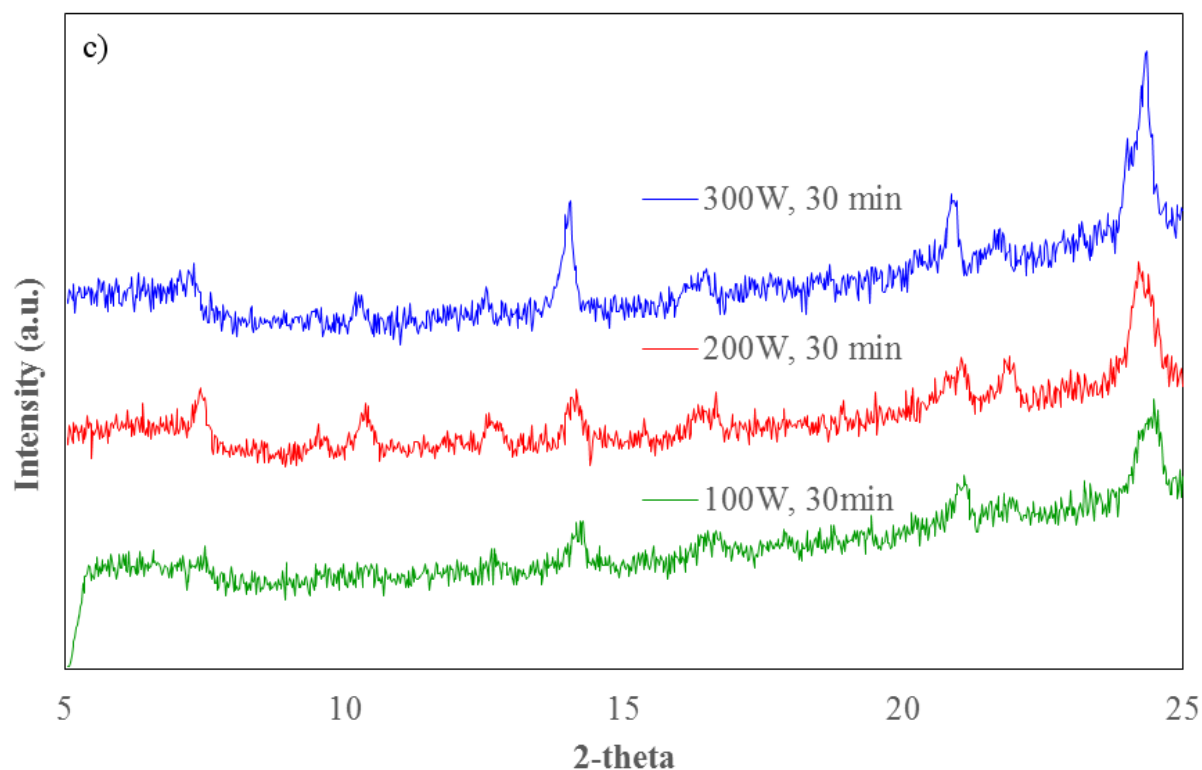


Figure C-1 The XRD patterns of zeolitized coal fly ash utilizing: a) fine-filtered leachate b) coarse filtered leachate and c) unfiltered leachate as the reaction solvent

The relative peak intensities were defined as the ratio of the characteristic peak of each product species to the highest characteristic peak observed.

$$RI_{LTA} = \frac{I_{LTA,Sample}}{I_{LTA,Sample}} \quad (C-1)$$

$$RI_{SOD} = \frac{I_{SOD,Sample}}{I_{SOD,Sample}} \quad (C-2)$$

Table C-3 shows the relative peak intensities of the samples irradiated with different microwave power and using different leachates as the reaction solvent. It was observed that higher microwave power for 30 min irradiation time favoured the production of SOD over

LTA. Furthermore, the fine-filtered leachate solvent produced more zeolite A and higher crystallinity. This indicates that microwave irradiation favours the production of SOD which has also been reported by previous works³⁴. It can also be concluded that the presence of cations other than Na⁺ can disrupt the production of zeolite A thus lowering the crystallinity of the product and strongly favouring the production of SOD over LTA.

Table C-3 Relative characteristic XRD Peak Intensity for fine-filtered, coarse filtered and unfiltered synthesis after 30 minutes of microwave irradiation

Leachate	Power (W), time (min)	LTA	SOD
Fine-filtered	300, 30	1.00	1.00
	200, 30	0.346	0.471
	100, 30	0.495	0.345
Coarse filtered	300, 30	0.495	0.525
	200, 30	0.407	0.404
	100, 30	0.445	0.318
Unfiltered	300, 30	0.390	0.888
	200, 30	0.495	0.444
	100, 30	0.297	0.395

In order to study the effect of total microwave energy irradiation on the zeolite phase produced, relative intensities of characteristic peaks of both LTA and SOD were plotted against microwave irradiation energy. Figure C-2 illustrates the results for both coarse filtered and unfiltered leachate used as the zeolitization reaction solvent. In both cases it is observed that there is an optimal microwave irradiation energy level for the production of LTA, however as the amount of irradiation energy is increased, more SOD was produced. While the production of LTA plateaus, the production of SOD increases linearly.

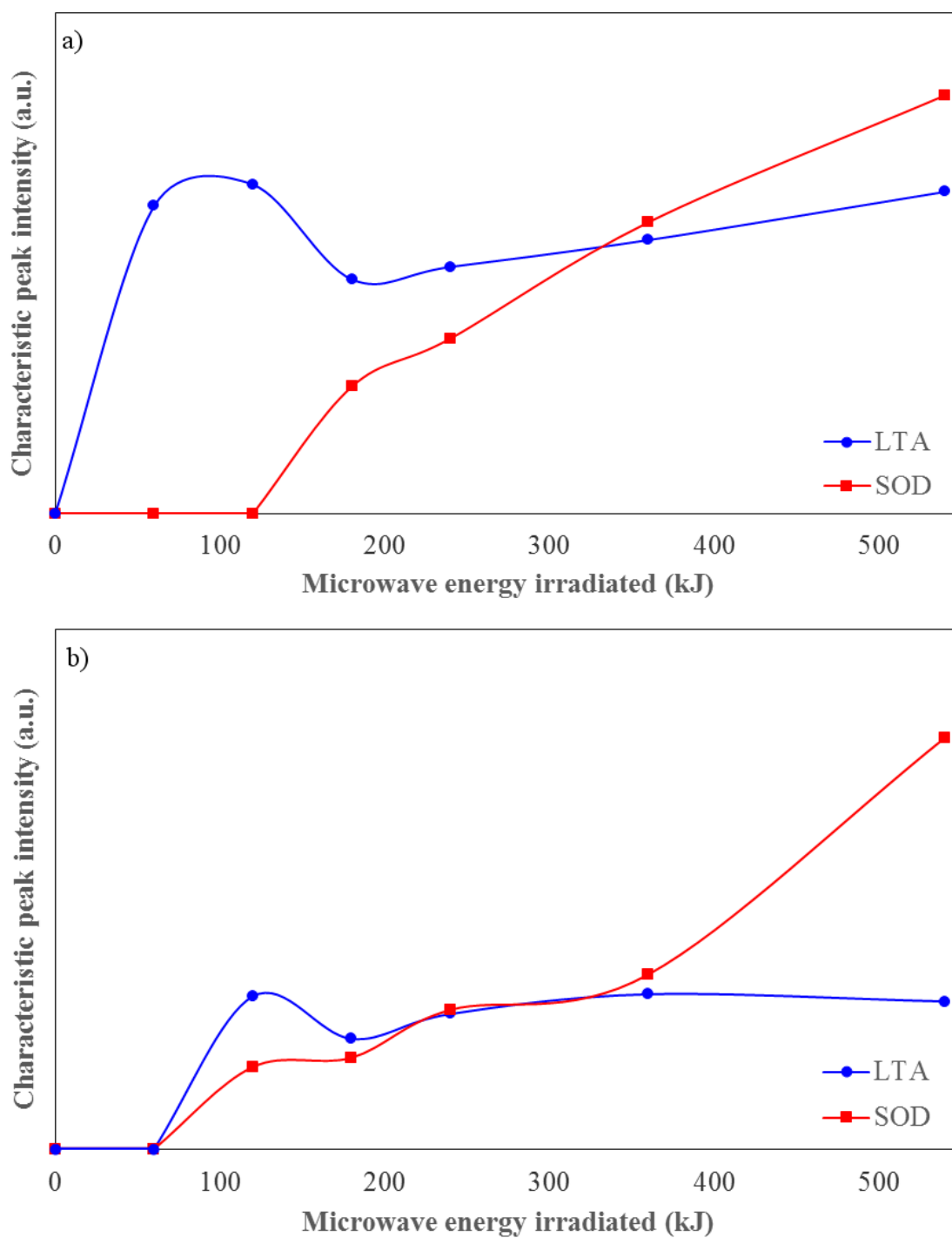


Figure C-2 The characteristic XRD peak intensities with respect to microwave irradiation utilizing: a) coarse filtered leachate and b) unfiltered leachate as reaction solvent

This trend is more pronounced for the zeolite synthesized in the unfiltered leachate. Much more SOD is produced compared to LTA for unfiltered leachate experiments than the coarse filtered leachate. This again indicates that the heavy metals in the reaction solution retard the production of LTA and significantly favour the production of SOD.

From Figure C-2, it is observed that zeolitic characteristic peaks occur sooner for coarse filtered leachate solvent experiments compared to the unfiltered leachate solvent experiments. This indicates that heavy metal constituents prevent nucleation of LTA zeolite crystals. Our research group has earlier conducted similar experiments with pure water³⁵ and wastewater produced from plasma electrolytic oxidation process¹⁹ (both lacking heavy metal ions) and produced pure LTA unlike for leachate experiments that produced a mixture of LTA and SOD. This indicates the significant role that heavy metal ions play in suppressing the nucleation of LTA.

The presence of various alkali metal cations in otherwise identical gels, results in the synthesis of different zeolites. For example, Na⁺, K⁺, Cs⁺ result in crystallization of zeolite A, chabazite, and edingtonite, respectively³⁶. The interactions between negatively charged silicate, aluminate and aluminosilicate species and the cation species are extremely important in determining the zeolite crystallized. LTA is a less stable phase compared to SOD¹¹ and requires germination of multiple composite building units (CBU's) as opposed to SOD which has only one CBU (beta cage). The presence of heavy metal oxides may favour the production of a stable phase by preventing the germination of "d4r" and "lta" cages which are the CBU's required for LTA synthesis³⁷. Abundance of beta cages ("sod" CBU) in the solution in lieu of "d4r" and "lta" favours the production of stable SOD phase.

C.3.3 Scanning electron microscope (SEM)

The scanning electron microscope (SEM) images of the synthesized zeolites utilizing unfiltered, coarse filtered and fine-filtered leachate as zeolitization solvent are illustrated in Figure C-3(a-f). In all of the SEM images, two distinct main structures can be observed, cubic and rough surfaced spheres. The cubic structures are associated with LTA

framework, while the rough sphere are SOD framework^{10,38,39}. The zeolitic frameworks are crystallized on the surface of the undissolved coal fly ash particles in accordance with an earlier suggested mechanism^{13,35}.

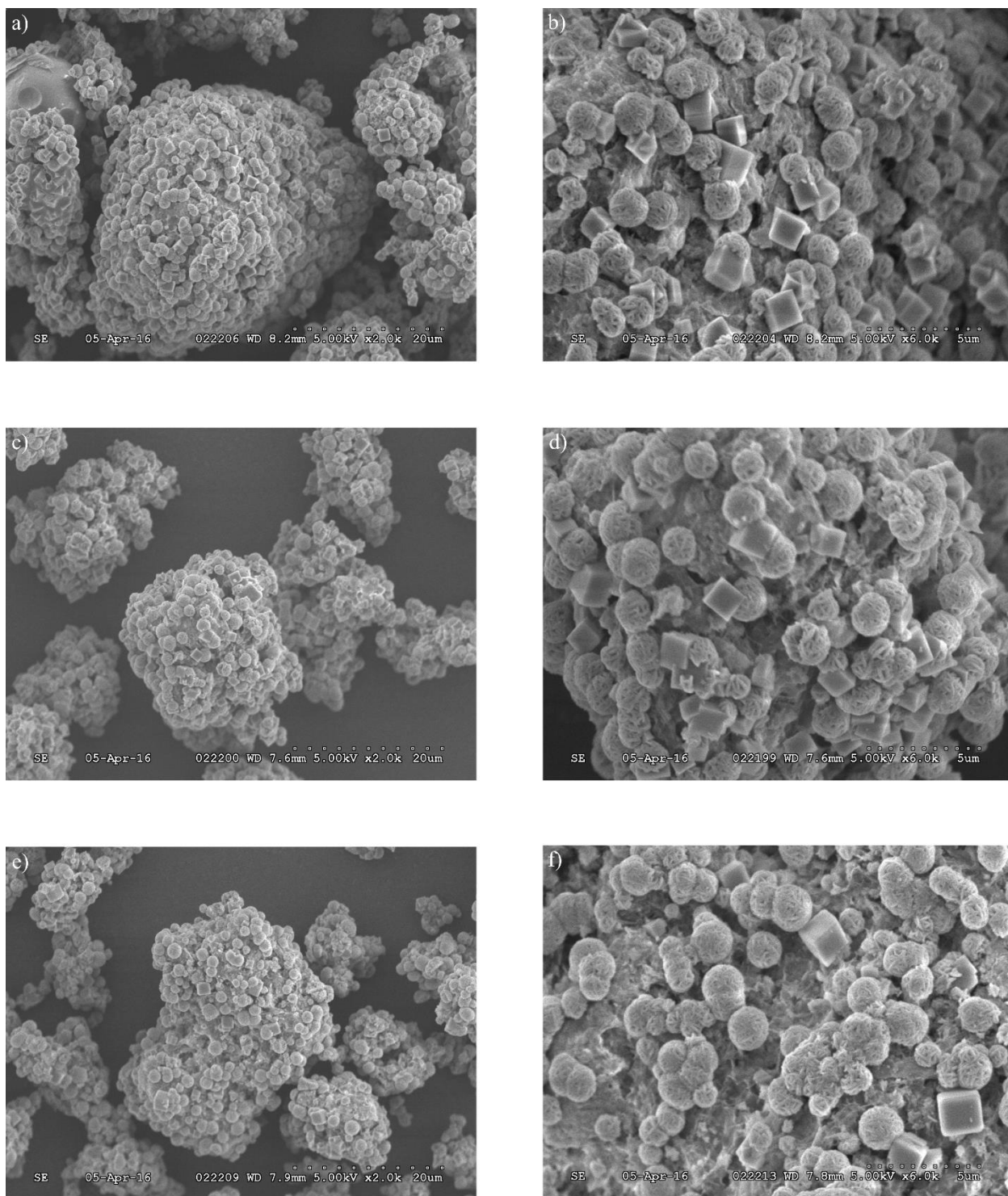


Figure C-3 The SEM images of zeolitized coal fly ash utilizing: a, b) fine-filtered c, d) coarse filtered and e, f) unfiltered leachate as solvent

The SEM images indicate that the cubic structures associated with the LTA are more abundant than spherical structures in both fine-filtered and coarse filtered leachate experiments. In the case of unfiltered experiments, the spherical SOD crystals clearly outnumber the cubic LTA. These results corroborate the results and conclusions drawn from XRD analysis.

C.3.4 Thermogravimetric analysis (TGA)

The TGA curves of the synthesized zeolites using unfiltered, coarse filtered and fine-filtered leachate as reaction solvent are shown in Figure C-4.

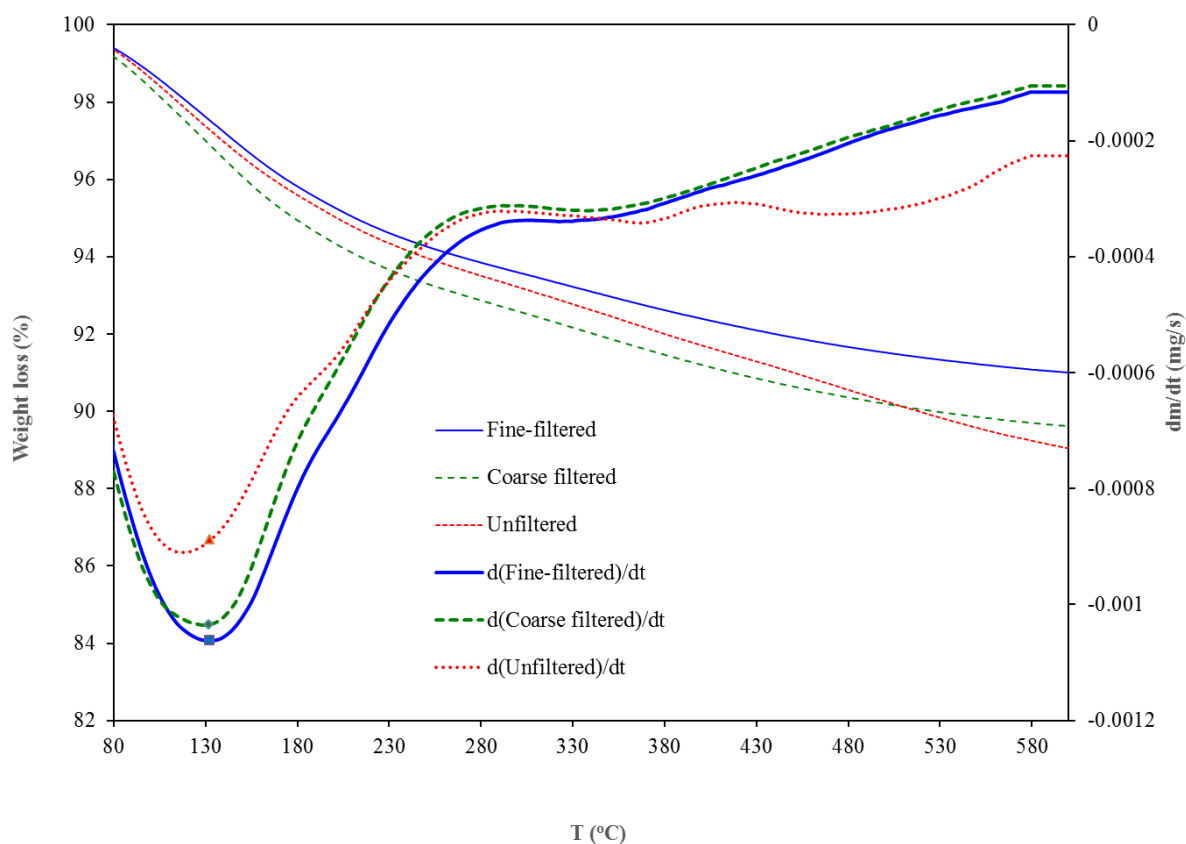


Figure C-4 The TGA of synthesized zeolites using fine-filtered, coarse filtered and unfiltered leachate as solvent

All three samples showed major weight loss at approximately 120-130°C (shown by the derivative lines). The synthesized zeolite using fine-filtered leachate, coarse filtered leachate, and unfiltered leachate lost approximately 9.0%, 10.4% and 11.0%, respectively (shown by the weight loss lines of the three samples; Figure C-4). The derivative of the weight loss of the synthesized zeolites samples using coarse filtered and fine-filtered leachates decreased in magnitude at approximately 340-350°C (seen as an upward trend in the derivative curves), whereas that of the synthesized zeolite using unfiltered leachate was relatively flat after 340-350°C. This indicates that more weight was lost by the zeolite produced using unfiltered leachate. A possible explanation for the higher weight loss of the zeolite synthesized using unfiltered leachate is due to the thermal decomposition of heavy metal hydroxides present in the unfiltered leachate. The difference between the three synthesized zeolite samples was the amount of heavy metal precipitate in the leachate. Upon filtration of the precipitates, the concentration of heavy metal hydroxide decreased. The unfiltered leachate had the highest heavy metal hydroxides concentration.

Another result of the heavy metal hydroxides concentration difference between the samples was the water carrying capacity. This is shown in Figure C-4 by the depth of the large peak of the first derivatives at approximately 100-140°C. The lower the peak, the more water is held in the zeolite structure. This can be ascribed to an increase in surface area compared to the initial CFA¹⁰. The lowest peak in the first derivatives (most negative), was that of the zeolite synthesized using fine-filtered leachate, showing the most water carrying capacity. The highest peak (least negative) was that of the zeolite synthesized using unfiltered leachate, showing the least water carrying capacity.

C.3.5 Cation exchange capacity (CEC)

Figure C-5 shows the correlation between ammonium concentration and peak absorbance intensity. The R^2 value was found to be 0.9991 indicating a very strong linear correlation between ammonium concentration and peak absorbance intensity. After removal of the ammonium ions from the zeolite, the ammonium concentration was measured using UV-VIS method as explained in Section C.2.3.

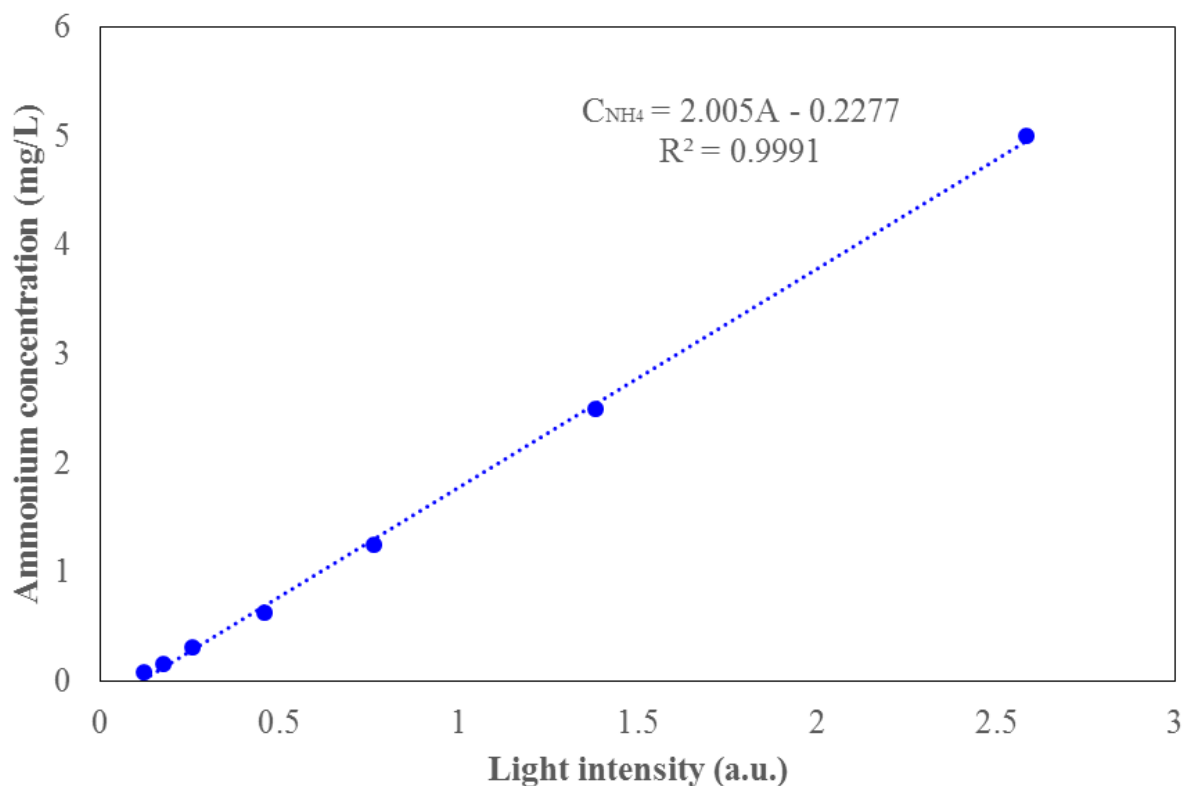


Figure C-5 The correlation between the NH_4^+ concentration and peak absorbance intensity

The CEC values of the zeolites synthesized using fine-filtered, coarse filtered and unfiltered leachate are shown in Figure C-6. The CEC values of the zeolites synthesized using fine-filtered, coarse filtered and unfiltered leachate were 0.80, 0.72 and 0.67 meq/g, respectively.

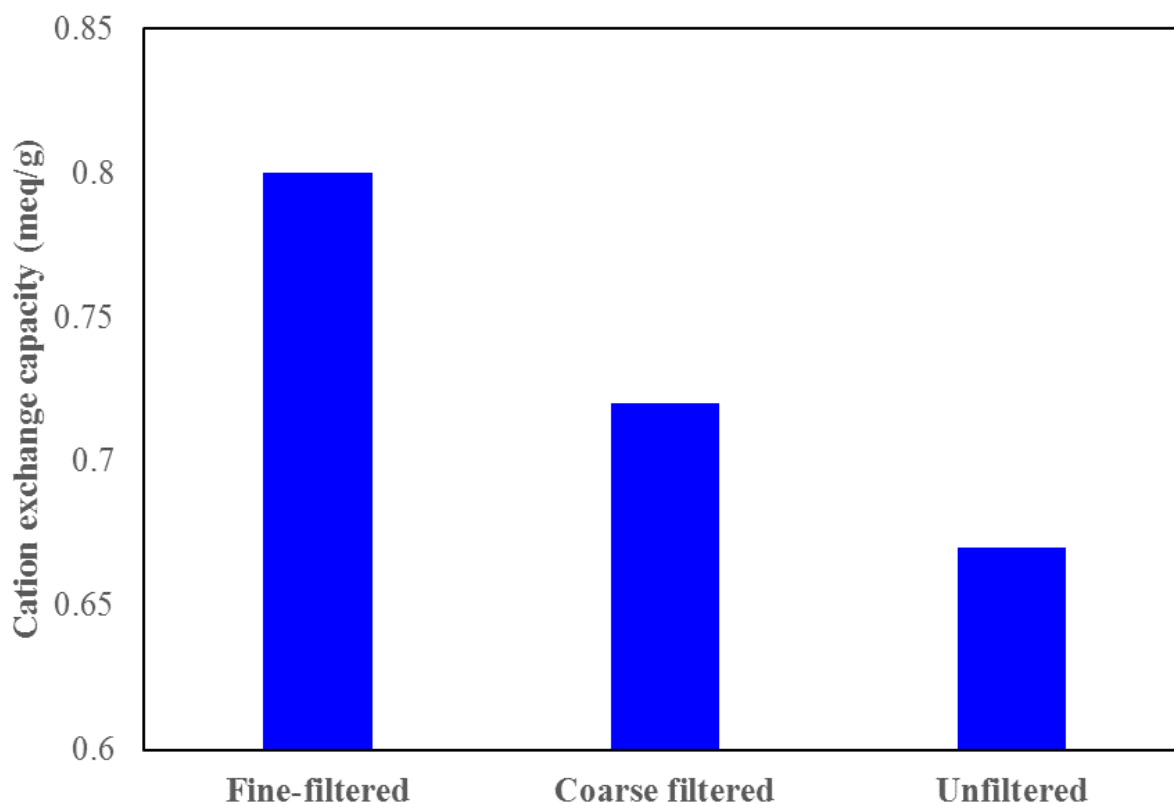


Figure C-6 The CEC values of fine-filtered, coarse filtered and unfiltered leachate prepared zeolites

The CEC value depends on the amount of zeolite A produced. Raw CFA has a CEC value of 0.3 meq/g¹⁰. Whereas CEC values of zeolite A are reported in the range of 2-5 meq/g^{10,40,41}. Sodalite has a CEC value ranging from 0.099-1.22 meq/g (various ions were used to determine the CEC of sodalite in literature)⁴². Since, raw CFA and sodalite have lower CEC values than zeolite A, the presence of either of these will decrease the CEC of the produced sample. Table C-3 shows that the zeolite synthesized using fine-filtered leachate had the highest amount of zeolite A. The zeolite synthesized using coarse filtered leachate had more zeolite A than the zeolite synthesized using unfiltered leachate and this corresponds to a higher CEC value (0.72 and 0.67 meq/g, respectively; Figure C-6). The SEM micrographs (Figure C-3) also confirm the larger quantity of zeolite A using fine-

filtered and coarse filtered leachate compared to the zeolite synthesized using unfiltered leachate.

C.4 Conclusions

Landfill leachate was used for coal fly ash zeolitization. Sodium hydroxide added to the leachate solution resulted in a large amount of heavy metal precipitation. In order to investigate the effects of the presence of heavy metal cations and precipitation on the zeolitization process, three sets of experiments were performed. In one set, the precipitate was removed using 0.45 μm filters. In another set, filtration was performed with 1 μm filters. In a third set of experiments, no filtration was performed. After the zeolitization process utilizing single mode microwave, multiple analyses, including XRD, SEM, CEC and TGA were conducted.

The XRD analysis indicated that utilizing leachate for the synthesis of zeolites suppressed the production of LTA and favoured the production of SOD. Unfiltered leachate produced the highest ratio of SOD to LTA. Whereas, fine-filtered leachate, with the least amount of heavy metal precipitate, produced the highest amount of LTA even though there was still SOD present. This indicated that the presence of heavy metal ions leads to the production of SOD; the higher the amount of heavy metal in the solution, the higher the ratio of SOD to LTA.

Microwave power was associated with both higher crystallinity and production of SOD. There was an optimal level of microwave energy irradiated for the production of LTA. Further increasing the irradiated energy, reduced the production of LTA which eventually plateaued while SOD production increased linearly. This trend was more pronounced for experiments conducted with unfiltered leachate.

The SEM, CEC and TGA results corroborated the XRD results. The SEM micrographs showed approximately equal amounts of LTA and SOD structures deposited on CFA particles for both zeolites produced using coarse filtered and fine-filtered leachate solutions while zeolite produced using unfiltered leachate samples showed more SOD structures.

The CEC values were the highest for the zeolite synthesized using fine-filtered leachate followed by the zeolite synthesized using coarse filtered leachate and lowest for the unfiltered leachate. The TGA results showed the same trend for the water carrying capacity.

C.5 References

1. Fisher GL, Chrisp CE, Raabe OG. Physical Factors Affecting the Mutagenicity of Fly Ash from a Coal-Fired Power Plant. *Science*. 1979;204(4395):879–81.
2. Holler H, Wirsching U. Zeolite formation from fly ash. *Fortschr Mineral*. 1985;63(1):21–43.
3. Kazemian H, Naghdali Z, Ghaffari Kashani T, Farhadi F. Conversion of high silicon fly ash to Na-P1 zeolite: Alkaline fusion followed by hydrothermal crystallization. *Adv Powder Technol*. 2010;21(3):279–83.
4. Murayama N, Takahashi T, Shuku K, Lee H, Shibata J. Effect of reaction temperature on hydrothermal syntheses of potassium type zeolites from coal fly ash. *Int J Miner Process*. 2008;87(3–4):129–33.
5. Musyoka NM, Petrik LF, Fatoba OO, Hums E. Synthesis of zeolites from coal fly ash using mine waters. *Miner Eng*. 2013;53:9–15.
6. Park M, Choi CL, Lim WT, Kim MC, Choi J, Heo NH. Molten-salt method for the synthesis of zeolitic materials: I. Zeolite formation in alkaline molten-salt system. *Microporous Mesoporous Mater*. 2000;37(1):81–9.
7. Shigemoto N, Hayashi H, Miyaura K. Selective formation of Na-X zeolite from coal fly ash by fusion with sodium hydroxide prior to hydrothermal reaction. *J Mater Sci*. 1993;28(17):4781–6.
8. Shoumkova A, Stoyanova V. Zeolites formation by hydrothermal alkali activation of coal fly ash from thermal power station “Maritsa 3”, Bulgaria. *Fuel*. 2013;103:533–41.
9. Tanaka H, Fujii A. Effect of stirring on the dissolution of coal fly ash and synthesis of pure-form Na-A and -X zeolites by two-step process. *Adv Powder Technol*. 2009;20(5):473–9.

10. Bukhari SS, Behin J, Kazemian H, Rohani S. A comparative study using direct hydrothermal and indirect fusion methods to produce zeolites from coal fly ash utilizing single-mode microwave energy. *J Mater Sci*. 2014;49(24):8261–71. Doi: 10.1007/s10853-014-8535-2.
11. Bukhari SS, Rohani S, Kazemian H. Effect of ultrasound energy on the zeolitization of chemical extracts from fused coal fly ash. *Ultrason Sonochem*. 2016;28:47–53. Doi: 10.1016/j.ultsonch.2015.06.031.
12. Chen Y, Xu T, Xie C, Han H, Zhao F, Zhang J, et al. Pure zeolite Na-P and Na-X prepared from coal fly ash under the effect of steric hindrance. *J Chem Technol Biotechnol*. 2015:n/a – n/a. Doi: 10.1002/jctb.4794.
13. Bukhari SS, Behin J, Kazemian H, Rohani S. Conversion of coal fly ash to zeolite utilizing microwave and ultrasound energies: A review. *Fuel*. 2015;140:250–66.
14. Querol X, Moreno N, Umaña JC, Alastuey A, Hernández E, López-Soler A, et al. Synthesis of zeolites from coal fly ash: an overview. *Int J Coal Geol*. 2002;50(1–4):413–23. Doi: 10.1016/S0166-5162(02)00124-6.
15. Behin J, Bukhari SS, Kazemian H, Rohani S. Developing a zero liquid discharge process for zeolitization of coal fly ash to synthetic NaP zeolite. *Fuel*. 2016;171:195–202.
16. Belviso C, Cavalcante F, Lettino A, Fiore S. Zeolite synthesised from fused coal fly ash at low temperature using seawater for crystallization. *Coal Combust Gasifica-Tion Prod*. 2009;1:8–13.
17. Hussar K, Teekasap S, Somsuk N. Synthesis of Zeolite A from By-Product of Aluminum Etching Process: Effects of Reaction Temperature and Reaction Time on Pore Volume. *Am J Environ Sci*. 2011;7(1):35.

18. Musyoka NM, Petrik LF, Balfour G, Gitari WM, Hums E. Synthesis of hydroxy sodalite from coal fly ash using waste industrial brine solution. *J Environ Sci Health Part A*. 2011;46(14):1699–707.
19. Behin J, Bukhari SS, Dehnavi V, Kazemian H, Rohani S. Using Coal Fly Ash and Wastewater for Microwave Synthesis of LTA Zeolite. *Chem Eng Technol*. 2014;37(9):1532–40. Doi: 10.1002/ceat.201400225.
20. Dehnavi V, Luan BL, Shoesmith DW, Liu XY, Rohani S. Effect of duty cycle and applied current frequency on plasma electrolytic oxidation (PEO) coating growth behavior. *Surf Coat Technol*. 2013;226:100–7.
21. Senior E. *Microbiology of Landfill Sites*. Second. Boca Raton: Lewis Publishers; 1995.
22. Rivas FJ, Beltrán F, Carvalho F, Acedo B, Gimeno O. Stabilized leachates: sequential coagulation–flocculation + chemical oxidation process. *J Hazard Mater*. 2004;116(1–2):95–102. Doi: 10.1016/j.jhazmat.2004.07.022.
23. Ghafari S, Aziz HA, Isa MH, Zinatizadeh AA. Application of response surface methodology (RSM) to optimize coagulation–flocculation treatment of leachate using poly-aluminum chloride (PAC) and alum. *J Hazard Mater*. 2009;163(2–3):650–6. Doi: 10.1016/j.jhazmat.2008.07.090.
24. Turan NG, Ergun ON. Removal of Cu(II) from leachate using natural zeolite as a landfill liner material. *J Hazard Mater*. 2009;167(1-3):696–700.
25. Foo KY, Hameed BH. An overview of landfill leachate treatment via activated carbon adsorption process. *J Hazard Mater*. 2009;171(1–3):54–60. Doi: 10.1016/j.jhazmat.2009.06.038.

26. Wiszniowski J, Robert D, Surmacz-Gorska J, Miksch K, Weber JV. Landfill leachate treatment methods: A review. *Environ Chem Lett*. 2006;4(1):51–61. Doi: 10.1007/s10311-005-0016-z.
27. Renou S, Givaudan JG, Poulain S, Dirassouyan F, Moulin P. Landfill leachate treatment: Review and opportunity. *J Hazard Mater*. 2008;150(3):468–93. Doi: 10.1016/j.jhazmat.2007.09.077.
28. Omar H, Rohani S. Treatment of landfill waste, leachate and landfill gas: A review. *Front Chem Sci Eng*. 2015;9(1):15–32. Doi: 10.1007/s11705-015-1501-y.
29. Morschhäuser R, Krull M, Kayser C, Boberski C, Bierbaum R, P. A. Püschner, T. Glasnov, K.C. Oliver. Microwave-assisted continuous flow synthesis on industrial scale. *Green Process Synth*. 2012;1(3):281–90.
30. Treacy MMJ, Higgins JB. Collection of simulated XRD powder patterns for zeolites. Amsterdam, The Netherlands: Elsevier; 2007.
31. Bain DC, Smith BFL. Chemical analysis. Handbook of determinative methods in clay mineralogy. Glasgow: Blackie; 1987. p. 248–74.
32. Miller EK, Blum JD, Friedland AJ. Determination of soil exchangeable-cation loss and weathering rates using Sr isotopes. *Nature*. 1993;362(6419):438–41. Doi: 10.1038/362438a0.
33. Kjeldsen P, Barlaz MA, Rooker AP, Baun A, Ledin A, Christensen TH. Present and Long-Term Composition of MSW Landfill Leachate: A Review. *Crit Rev Environ Sci Technol*. 2002;32(4):297–336. Doi: 10.1080/10643380290813462.
34. Inada M, Tsujimoto H, Eguchi Y, Enomoto N, Hojo J. Microwave-assisted zeolite synthesis from coal fly ash in hydrothermal process. *Fuel*. 2005;84(12):1482–6.

35. Bukhari SS, Behin J, Kazemian H, Rohani S. A comparative study using direct hydrothermal and indirect fusion methods to produce zeolites from coal fly ash utilizing single-mode microwave energy. *J Mater Sci.* 2014;49(24):8261–71.
36. Khodabandeh S. *Synthesis of Alkaline-Earth Zeolites.* California Institute of Technology, Pasadena, California, 1997.
37. Baerlocher, Ch., McCusker, L.B., Olson, D.H. *Atlas of Zeolite Framework types.* 6th ed. New York, NY, USA: Elsevier Science; 2007.
38. Hums E, Musyoka NM, Baser H, Inayat A, Schwieger W. In-situ ultrasound study of the kinetics of formation of zeolites Na-A and Na-X from coal fly ash. *Ultrasonics.* 2014;54(2):537–43.
39. Bukhari SS, Behin J, Kazemian H, Rohani S. Synthesis of zeolite NA-A using single mode microwave irradiation at atmospheric pressure: The effect of microwave power. *Can J Chem Eng.* 2015;93(6):1081–90.
40. Tanaka H, Fujii A, Fujimoto S, Tanaka Y. Microwave-Assisted Two-Step Process for the Synthesis of a Single-Phase Na-A Zeolite from Coal Fly Ash. *Adv Powder Technol.* 2008;19(1):83–94. Doi: 10.1163/156855208X291783.
41. Kazemian H, Ghaffari Kashani T, Noorian M. Synthesis and characterization of Zeolite A, using fly ash of the Iran ferrosilice company and investigating its ion-exchange properties. *Iran J Crystallogr Mineral.* 2005;13(2):329–36.
42. Derkowski A, Franus W, Waniak-Nowicka H, Czimerova A. Textural properties vs. CEC and EGME retention of Na-X zeolite prepared from fly ash at room temperature. *Int J Miner Process.* n.d.;82(2):57–68. Doi: 10.1016/j.minpro.2006.10.001.

Curriculum Vitae

Name: Hecham Omar

Post-secondary Education and Degrees: The University of Western Ontario
London, Ontario, Canada
2010-2014 B.E.Sc.

Honours and Awards: Mitacs Accelerate Industrial Internship, The University of Western Ontario/ SALT Canada Inc., London, Ontario Canada
2014-2015

Ontario Graduate Scholarship (OGS), The University of Western Ontario, London, Ontario, Canada
2015-2016

Related Work Experience: Teaching Assistant
The University of Western Ontario
2014-2015

Publications:

Hecham Omar & Sohrab Rohani. (2015). Treatment of landfill waste, leachate and landfill gas: A review. *Frontiers of Chemical Science and Engineering*, 9, 15-32.

Hecham Omar & Sohrab Rohani. (2015). Transport Phenomena in the Conversion of an Anaerobic Landfill into an Aerobic Landfill. *Proceedings of the 2015 COMSOL Conference in Boston*.

Hecham Omar & Sohrab Rohani. (Submitted). The mathematical model of the conversion of a landfill operation from anaerobic to aerobic. Submitted to *Applied Mathematical Modelling*.

Syed Salman Bukhari, **Hecham Omar** & Sohrab Rohani. (Submitted). Effect of heavy metal concentration on microwave assisted zeolitization of coal fly ash. Submitted to *Journal of Hazardous Materials*.

Hecham Omar & Sohrab Rohani. (In Progress). Removal of CO₂ from landfill gas with landfill leachate using hybrid sorption. Eventual submission to *Journal of Environmental Chemical Engineering*.

Syed Salman Bukhari, **Hecham Omar** & Sohrab Rohani. (In Progress). Comparison of cation exchange capacity of zeolites using Kjeldahl method, UV-VIS spectroscopy and ion chromatography. Eventual submission to Microporous and Mesoporous Materials.

Conference Presentations:

Hecham Omar & Sohrab Rohani. (2015). Transport Phenomena in the Conversion of an Anaerobic Landfill into an Aerobic Landfill. 2015 COMSOL Conference Boston.